12-2013

SYNTHESIS AND CHARACTERIZATION OF POLYMER LAYERS FOR CONTROL OF FLUID TRANSPORT

Fehime Vatansever
Clemson University, fvatans@g.clemson.edu

SYNTHESIS AND CHARACTERIZATION OF POLYMER LAYERS FOR CONTROL OF FLUID TRANSPORT

A Dissertation
Presented to
the Graduate School of
Clemson University

In Partial Fulfillment
of the Requirements for the Degree
Doctor of Philosophy
Materials Science and Engineering

---

by
Fehime Vatansever
December 2013

Dr. Igor Luzinov, Committee Chair
Dr. Konstantin Kornev
Dr. Thompson Mefford
Dr. Douglas Hirt
Dr. Bogdan Zdyrko

ABSTRACT

The level of wetting of fiber surface with liquids is an important characteristic of fibrous materials. It is related to fiber surface energy and the structure of the material. Surface energy can be changed by surface modification via the grafting methodologies that have been reported for introducing new and stable functionality to fibrous substrates without changing bulk properties.

Present work is dedicated to synthesis and characterization of macromolecular layers grafted to fiber surface in order to achieve directional liquid transport for the modified fabric. Modification technique used here is based on formation of stable polymer layer on fabric surface using ``grafting to`` technique.

Specifically, modification of fabric with wettability gradient for facilitated one way-liquid transport, and pointed modification of yarn-based channels on textile microfluidic device for directional liquid transport are reported here. First, fabric was activated with alkali (NaOH) solution. Second, poly (glycidyl methacrylate) (PGMA) was deposited on fabric as an anchoring layer. Finally, polymers of interest were grafted to surface through the epoxy functionality of PGMA.

Effect of polymer grafting on the wicking property of the fabric has been evaluated by vertical wicking technique at the each step of surface modification. The results shows that wicking performance of fabric can be altered by grafting of a thin nanoscale polymeric film.

For the facilitated liquid transport, the gradient polymer coating was created using ``grafting to`` technique and its dependence on the grafting temperature. Wettability

gradient from hydrophilic to hydrophobic (change in water contact angle from 0 to 140 degrees on fabric) was achieved by grafting of polystyrene (PS) and polyacrylic acid (PAA) sequentially with concentration gradient. This study proposes that fabric with wettability gradient property can be used to transfer sweat from skin and support moisture management when it is used in a laminated garment structure. For cooling performance evaluation, modified fabrics were tested with surface differential scanning calorimeter, and improved cooling effect was found with the fabric that has wettability gradient.

Directional liquid transport can be achieved on amphiphilic fabric. To this end, fabric consisting of PET and PP yarn is fabricated. Activation and PGMA deposition yields an array of highly reactive PET channels that are constrained by hydrophobic PP boundaries. Aqueous solutions are transported in the channels by capillary forces where the direction of the liquid transport is defined by pH-response of the grafted polymers. The system of pH-selective channels in the developed textile based microfluidic chip could find analytical applications and can be used for smart cloth.

.

DEDICATION

I dedicate this dissertation to my parents Ramis and Fatma Vatansever, my sister and brother in-law Kadriye and Hakan Dugencioglu who always has been there for me, and believe in me. Their support encouragement, constant and unconditional love have sustained me throughout my life. I would also like to dedicate this to my fiancée Hakan Ozaltun, who was always supportive and never let me feel alone during this journey.

ACKNOWLEDGMENTS

First and foremost, I would like to thank my advisor Dr. Igor Luzinov, for providing me this wonderful opportunity, and also for his guidance and support during the course of this work.

I would like to thank to Dr Bogdan Zdyrko, Dr. Konstantin Kornev, Dr Douglas Hirt, Dr.O. Thompson Mefford for agreeing to be on my committee. I appreciate the guidance and help of these distinguished educators.

I am thankful to Dr. Ruslan Burtovyy for his patience and willingness to teach throughout my five years study. I appreciate his time and fruitful suggestions during the writing progression. I also thank to Dr. Chen-Chih Tsai for all the help and valuable discussion on wicking study.

I would also like to thank my current and past group members for maintaining a great work atmosphere at the lab: Dr. Olha Hoy and her husband Dr.Taras Andrukh, Dr. Suraj Sharma, Dr.Oleksandr Burtovyy, Yuriy Galabura, Dr.James Giammarco, Jake Townsend, AP Soliani, Tugba Demir, Bernice Nizioki, Dr. Marius Chyasnavichyus, Dr. Michael Seeber.

I would like to acknowledge Kimberly Ivey, who was always there for a great conversation, as well as to teach and educate me on all her instruments. She was always willing to discuss and help me no matter how busy she was.

Special thanks to my friends for making Clemson feel more like home; Tugba Demir, Ayse Korucu, Dr.Sine Kontbay, M.Oguz Kesimci, Mustafa Bahar, Dr.Begum Aybar Damali, Dr.Uzay Damali, Dr.Halil Levent Tekinalp, Semra Bakkaloglu.

Above all, my thanks go to Hakan Ozaltun for his patience, understanding and support. Last, but not least, I would like to thank my parents, my sister and my brother in law for their support, love and encouragement.

TABLE OF CONTENTS

LIST OF FIGURES

List of Figures (Continued)

List of Figures (Continued)

List of Figures (Continued)

List of Figures (Continued)

List of Figures (Continued)

List of Figures (Continued)

LIST OF TABLES

CHAPTER ONE

INTRODUCTION

The ultimate goal of this study was to synthesize and characterize polymeric layers grafted to fibrous surfaces that could be used to control the direction of fluid movement. In the pursuit of this, two different strategies were employed for specific applications. First, a polymer layer with gradients in concentration of the components was formed to achieve a wettability gradient on a fabric which served as a platform to control fluid movement towards one direction. Second, the surface of the fabric was designed and modified to obtain so-called microfluidic fibrous channels. The modified channels were used to control the movement of fluid, selectively, in a certain direction.

Chapter 2 of this dissertation provides an overview of polymer grafting methods, gradient polymer coatings, and recent developments in research towards fiber based microfluidics. The moisture management approach in textile materials is also introduced.

Chapter 3 provides descriptions of the experimental techniques used in this work.

Chapter 4 focuses on the fabrication of a polyester (PET) model film, and modification of the film surface with macromolecules via a poly(glycidyl methacrylate) (PGMA) anchoring layer. A thin film on a silicon wafer was deposited by dip coating, and the properties of the surface after various surface modifications were evaluated to develop a model approach for the surface modification of PET fibrous materials. The surface activation of the PET film with alkali and plasma treatments was studied, and the

influence of the treatment times on the surface wettability and thickness was also evaluated.

The PGMA layer was then anchored to the PET surface to introduce epoxy groups, which are known for being very reactive towards various functionalities. The polymers with different functionalities were then grafted to the surface using the "grafting to" methodology.

Chapter 5 deals with the surface modification of the PET fabric. The methodology used for the polymer grafting on the PET film was successfully applied to graft a number of polymers to the PET fiber surface. Fluorescence imaging and wettability of the surface (with water) were used to evaluate the surface activation of the PET fabric. Additionally, the effects of the surface coating on the porosity/permeability of the fabric were evaluated, since they influence the wicking (transport) performance of the fabric. Wicking is a critical parameter for us since this dissertation specifically focuses on changing the fluid transport ability of the fabric to use it in microfluidics, or as a moisture management fabric. Thus, the wicking rate of a liquid on the non-treated and treated fabrics is experimentally determined using a vertical wicking experimental set up.

Chapter 6 describes the synthesis of gradient polymer layers and fabrication of the wettability gradient on the PET fabric surface. Initially, the grafting kinetics for hydrophobic and hydrophilic polymers was studied for the model PET film. Next, the uniform-mixed polymer brush was formed under static conditions by first grafting the hydrophobic polymer (polystyrene, PS) onto the PGMA layer, and then backfilling the surface layer with a grafting of the hydrophilic polymer (polyacrylic acid, PAA).

Hydrophobic polymer layers with different grafting densities were used to achieve different polymer concentrations on the uniform-mixed polymer brush grafted layer. In order to form a gradient polymer coating on the fabric (for the wettability gradient) a controlled immersion technique was applied.

The feasibility of using such a ``gradient fabric`` in a laminated clothing structure, for the moisture management of a body armor garment, was evaluated by testing the cooling efficiency of the fabric with a custom-made surface differential scanning calorimeter.

In **Chapter 7**, the surface modification of a fabric containing PET and polypropylene fibers is reported. The fabric was designed and manufactured in our laboratory. The main target of the study was to fabricate yarn-based channels that have different functionalities. Modification of the channels with different polymers was demonstrated and the directional movement of water within the channels based on the pH values was investigated.

CHAPTER TWO

LITERATURE REVIEW

Present research is devoted to the preparation and the characterization of polymer-grafted layers for effective and selective liquid transport in PET-based fabric. Therefore, it is essential to understand principles and characterization of polymer layer fabrication. Throughout this research, PET fabric was used; thus, understanding the basics of interaction of liquid with the fabric material is also crucial.

This chapter attempts to provide a brief overview of grafted-polymer layer preparation, layer behavior, and gradient polymer layers. In addition, significance of moisture management for fabric, different approaches for developing fabric with a moisture management property, and current technology regarding the paper and fiber based micro fluidics are reviewed.

2.1. Introduction to polymer brushes

A "polymer brush" is generally defined as an array of macromolecular chains covalently grafted to a surface in close proximity so that polymer chains overlap.[1, 2] Therefore, individual polymer chains adapt new conformational dimension to avoid unfavorable interactions when exposed to a good solvent. Studies revealed that tethered polymer chain conformation on a surface strongly depends on the grafting density.[3-6] Two different conformational regimes are defined for the brushes: mushroom and brush regimes.[1] **Figure 2.1**[7] illustrates the relationship between brush height and grafting density. At low grafting densities, the distance between grafting sites (D) is higher than

size of macro molecule, and a polymer chain forms a coil-like conformation (mushroom regime). At high grafting densities, the grafting distance is smaller than the size of polymer coil. Thus, chains extend themselves, due to the excluded volume effect, and form a brush structure, resulting in the brush regime. The boundary for transition from the mushroom regime to the brush regime is suggested as the reduced tethered density ($\Sigma=\sigma\pi R^2_g$), where R_g is the radius of gyration for the free polymer chain and σ is the grafting density.[1]

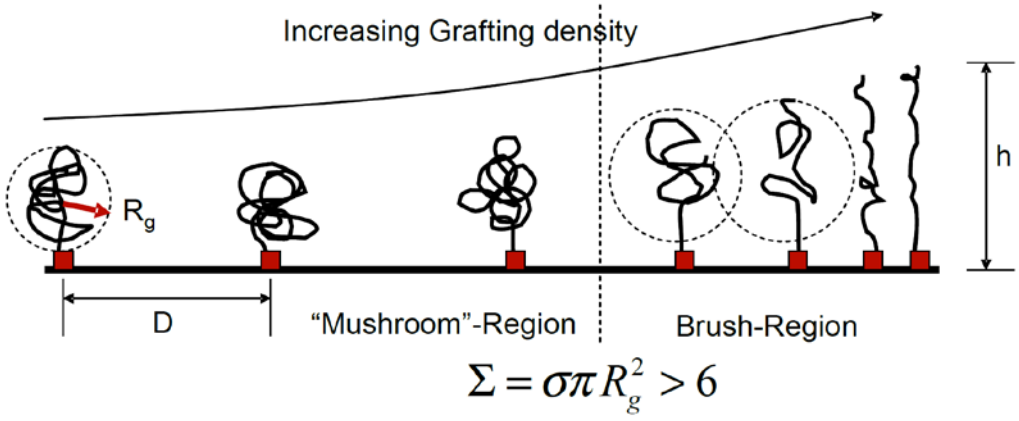

Figure 2.1. Polymer chain conformations on surface versus grafting density.

Some macromolecules, unlike the classical end grafted brush, can form multiple connections with substrates since they have multiple active sites on the chain. This type of brush is known as a ``Guiselin brush``[8] **(Figure 2.2)**.

The average pseudotail/tail size (number of monomeric units) of the Guiselin brush can be estimated by the following equation, where *N* is the degree of polymerization of the adsorbed polymer, *p* is fraction of the monomeric unit in the train,

and n is the number of monomeric units involved in one train section of the adsorbed macromolecule.

$$Size = N(1-p)/2(\mathrm{N}\,p/n) = (1-p)n/(2p) \qquad \textbf{E.2.1}$$

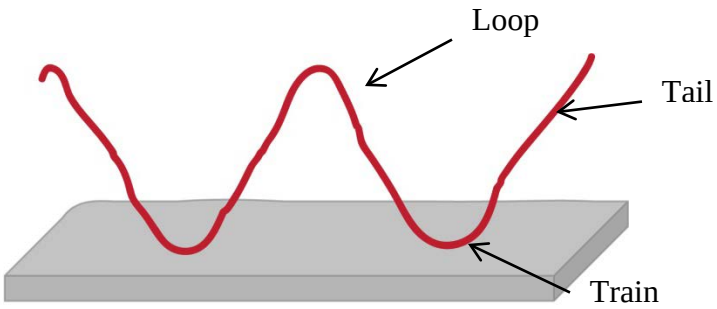

Figure 2.2. Concept of ``Guiselin brush``.

2.2. Synthesis of polymer brushes

Polymer brushes can be fabricated in two ways, physisorption and covalent attachment. In the case of physisorption, functionalized polymer or block copolymer adsorbs to a surface through interaction of the surface with functional group or one of the blocks that has high affinity to the surface. The other block extends itself away from the surface and forms a brush in the solution. A main drawback of the method is instability of the adsorbed polymer layer. Due to the weak interaction of the polymer with the substrate surface, the polymer can be desorbed in the presence of a good solvent and/or at an elevated temperature.[1] An irreversibly anchored polymer brush can be obtained by the ``grafting-to`` or ``grating-from`` techniques.[3, 9] The ``grafting-to`` approach is based on the reaction between a preformed (end-) functionalized polymer chain and a complementary group on the substrate surface. The ``grafting-from`` approach is based

on the polymerization reaction on the surface where the initiator is immobilized. All above brush formation techniques are illustrated in **Figure 2.3**.[1]

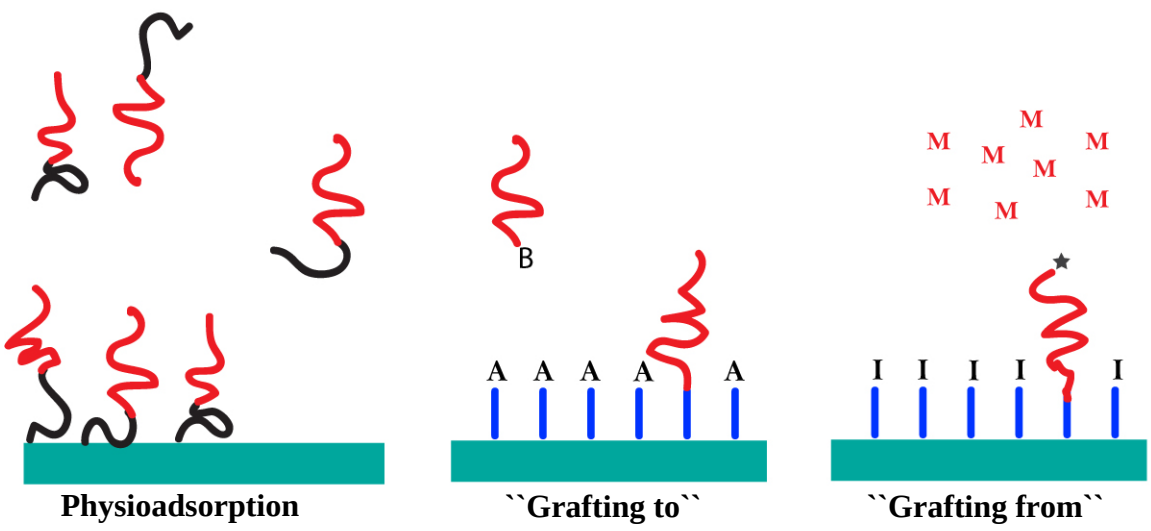

Figure 2.3. Schematics of three different methods to obtain polymer brushes. *Redrawn from reference.*[1]

2.2.1.Physisorption

Physisorption is the self-assembly of (end) functionalized polymers or block copolymers on a substrate through physical forces and is achieved in the presence of a selective solvent or selective surface.[10] The morphology of the physisorbed brush depends on the (co)polymer nature and the affinity of the solvent/surface to the blocks` functional groups. In the case of a selective solvent, the solvent should be ``ideal``for one part of the block and good for the other block to form an anchor layer and brush.[11] The polymer block for which the selected solvent is ideal (theta) readily adsorbs on the surface. In the case of a selective surface, one block preferentially adsorbs to the surface due to its higher affinity, and the other block forms a polymer brush in the solution.[12, 13]

Parsonage et al.[11] studied the effect of molecular weight and block composition on the adsorbed amount of polystyrene-b-poly(2-vinyl pyridine) block copolymer(PS-b-P2VP) from a toluene solution on a mica and silicon wafer. They observed that the size of each block influences the adsorption amount. Different regimes of adsorption based on symmetry of the blocks were observed. For the block copolymer of high asymmetry, the surface density is determined by the size of a well-solvated block that is PS. When block asymmetry is moderate or low, the size of the anchoring block, which is P2VP, determines the surface density.

Physisorption is a relatively straightforward technique. However, synthesis of a block copolymer that can display desirable surface properties and is suitable for physisorption may be challenging.[14] Moreover, the interaction between substrate and block copolymers usually is via van der Waals forces or hydrogen bonding. Thus, the polymer brush formed by physisorption can be desorbed upon changes in thermodynamic parameters, such as temperature.[15, 16] For instance, an elevated temperature may result in polymer desorption. Additionally, other molecules whose affinity to the substrate is thermodynamically higher can displace the adsorbed polymers.[14] Exposing the surface to another good solvent also can cause desorption.

The covalent attachment of polymer chains to the substrate is the most widely adapted technique to overcome the drawbacks of physisorption. ``Grafting to`` and ``grafting from`` are the generally used approaches for the covalent bonding of macromolecules to substrates.

2.2.2. ``Grafting-to`` approach

A covalently attached polymer brush can be readily created with the ``grafting-to`` technique. In the ``grafting-to`` method, a reactive polymer interacts with a surface containing complementary functional groups.[17] Covalent attachment provides a stable brush over a wide range of chemical and thermal conditions.

The main advantages of the technique are a chemically uncomplicated synthesis, accurate characterization of the grafted polymers, and narrow molecular weight distribution.[1] The polymer to be grafted can be synthesized with low molecular weight distribution for a particular application and can be designed to have the necessary active groups to react with the substrate. However, diffusion is an important hindering process for the formation of thicker polymer brushes by the ``grafting-to`` approach. Polymer chains must diffuse through an already grafted polymer layer to react with the surface's active site. As film thickness increases, the diffusion barrier becomes more pronounced.[3]

Previous studies show that there are different regimes of attachment in a good solvent. For instance, Ligoure and Leibler[18] observed two regimes during the grafting. The first regime is defined by fast tethering kinetics in which the adsorption rate is controlled by the Brownian motion of the chains in the solution. The second regime is diffusion controlled since the polymer chains should overcome the barrier of tethered polymer chains to reach the surface. Rate of diffusion in the second regime would get progressively lower as the thickness of the anchored layer increases. It is proposed that, during the first regime, relaxed polymer coils form a non-overlapping mushroom conformation on the surface, and the second regime corresponds to the brush formation.

In essence, as more polymers attach to the surface with one end, the chains gradually stretch away from the surface to avoid overlapping.

Huang et al.[19] studied the tethering kinetics of monodisperse amine-ended polystyrene. Like the previous researchers[18], they also observed slow and fast regimes in which mushroom-like conformation and brush formation, respectively were observed. Moreover, their results indicate the existence of a third regime in which the transition from a mushroom to a brush regime is complete **(Figure 2.4)**. Hypothesis of this research is supported with AFM analysis of a surface at different stages of tethering.

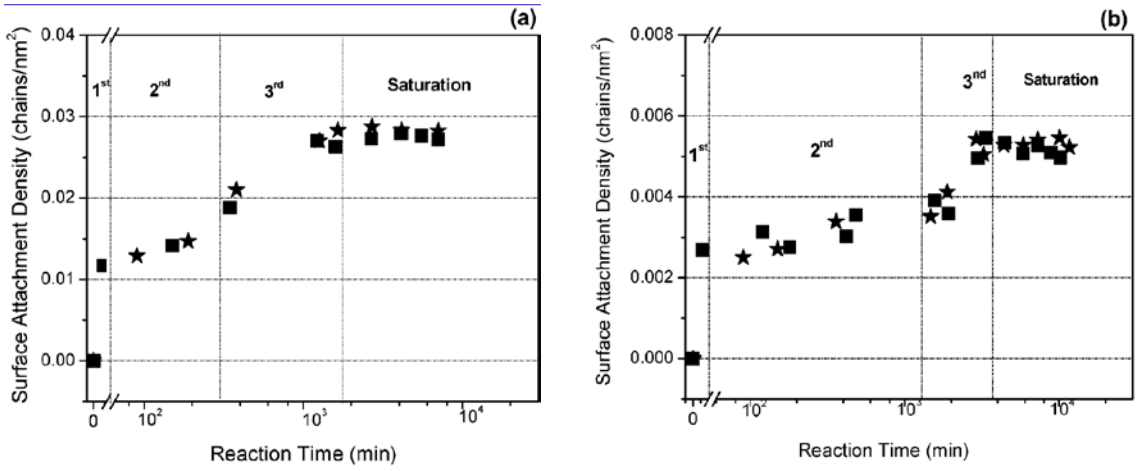

Figure 2.4. Typical profile for the tethering kinetics of monodisperse, chain-end-functionalized polymers. The surface attachment density is plotted versus time for the tethering of monodisperse, amine-ended polystyrene, (a) Mn = 15 000 g/mol and (b) Mn = 44 000 g/mol, from toluene to epoxide-derivatized silicate glass. The x-axis for the first regime is linear, while for the remainder it is logarithmic. For each molecular weight, twin reactions were conducted side by side to check for reproducibility; the squares are for one twin, and the circles are for the other.[19] *Reprinted with permission from ref 19. Copyright (2004) American Chemical Society.*

2.2.3. ``Grafting-from`` approach

The ``grafting-from`` technique involves in-situ surface-initiated polymerization to generate tethered polymers on a surface functionalized by an anchored initiator.[3] Immobilization of the initiator on a substrate can be done by forming initiator-containing self-assembled monolayers (SAMs), treating the surface with plasma or glow discharge in the presence of gas, or thin reactive polymer film[20]. A polymer brush with the ``grafting-from`` approach can be obtained through free radical polymerization[21], ring opening polymerization[22], cationic polymerization[23], anionic polymerization[24], plasma polymerization[25], photochemical polymerizations[26], electrochemical polymerization[27], and living polymerization.[28-30]

In the ``grafting-from`` technique, the grafted layer is swollen by the monomer solution that feeds the growing chains. Hence, contrary to the ``grafting-to`` approach, the growth of chains is not limited by diffusion unless a very high grafting density is approached. Therefore, brushes with very high thickness can be achieved. Conversely, ``grafting-from`` polymerization may produce layers with broader molecular mass distribution due to the limitation of initiator surface coverage, initiator efficiency, and the rate of monomer diffusion to active polymerization sites.[1] Moreover, the effect of side reactions (such as chain transfer to polymer) may be more important compared to bulk polymerization.

2.3. Gradient polymer layers

Gradient polymer layers vary directionally in molecular weight, chemical composition, grafting density, or number of nanoparticles, nanostructures, or functional groups. Surfaces with gradually changing properties have found an application in combinatorial studies. For example, they were used in the design, discovery, and development of a catalyst, drugs[31, 32], and analytical approaches and measurement tools. [33, 34]

Like the regular brush formation, gradient brush surfaces can be fabricated using grafting techniques. Temperature, time, initiator concentration on the surface, or monomer concentration in the solution are the parameters in controlling final brush density. To vary these parameters, different techniques have been developed. Genzer and Bhat classified all techniques in two major categories: ``bottom up`` and ``top down``[35]. In the ``bottom-up`` approach, building blocks of the gradients are deposited on a substrate in gradient manner using either manmade or natural deposition methods. Manmade deposition methods are control immersion of sample into a solution, and deposition dependent evaporation. Natural deposition methods are diffusion, propagating methods. In the ``top-down`` approach, a flat substrate is progressively modified.

Ionov and coworkers[36] reported the preparation of ultrathin tethered polymer (hydrophilic and hydrophobic) layers with a gradually changing thickness **(Figure 2.5)**. The polymers were attached to an epoxy functionalized surface using the ``grafting-to`` method. Grafting was induced by a temperature gradient stage in which temperatures from 50°C to 130°C can be achieved. It has been demonstrated that the approach is

suitable for the grafting of both hydrophilic and hydrophobic polymers in a gradient manner. Researchers observed gradual changes in wetting properties and a morphology transition from pinned micelles to a brush regime for the PS layer and a progressive increase of surface crystals for the PEG-grafted-layer along the substrate.

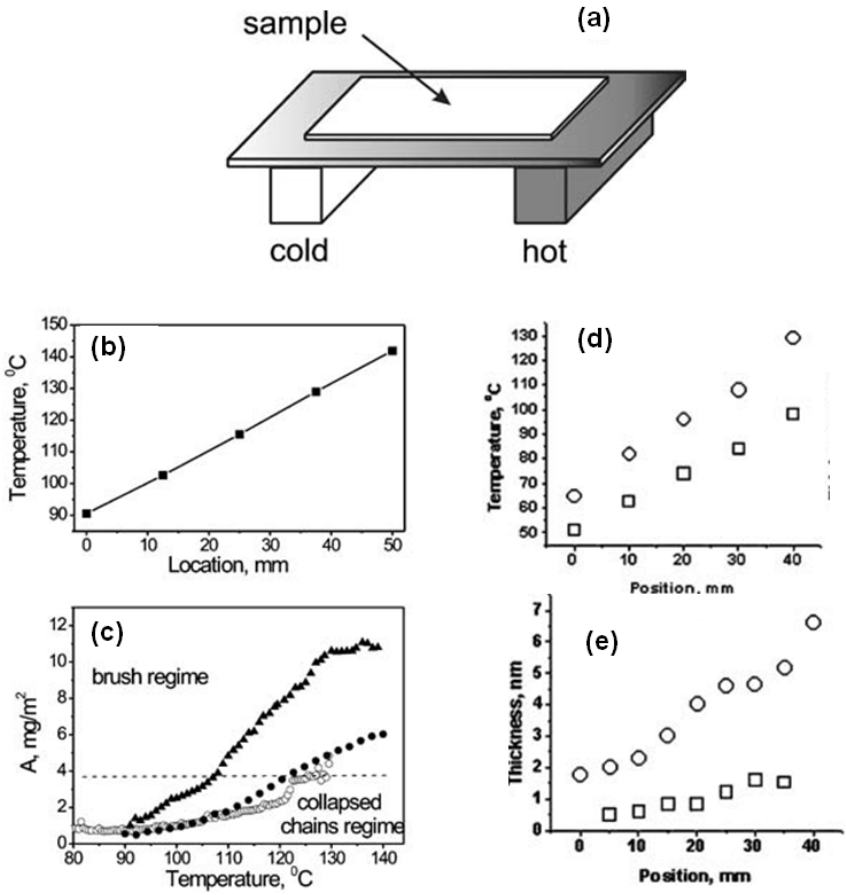

Figure 2.5. (a) Principal scheme of temperature gradient stage. (b) Example of temperature gradient created. The data were obtained with thermocouples. (c) Thickness profile of PS-COOH film grafted through (open circles) GPS (4 h.), (filled circles) PGMA (4 h.) and (filled triangles) PGMA (12 h.) anchoring layers. (d) Temperature gradients used for PEG grafting. Length–40 mm. (e) PEG brush thickness profiles. Circle–grafting time 4 h., temperature 65°C –129°C; square–grafting time 1 h., temperature 51°C –98°C.[36] *Reprinted with permission from Wiley.*

Lee et al.[37] fabricated a gradient in the chain density of comb-like polyethylene oxide (PEO) layer on low-density polyethylene (PE) surface **(Figure 2.6)**. The surface of PE was activated by a corona discharge, where power was gradually changed to form a concentration gradient of the active compound. Then poly (ethylene glycol) monomethacrylate macromeres (PEO-MA) were copolymerized using a graft copolymerization technique. Because polymerization was done on a surface that already has a concentration gradient of the active compound, the grafted polymer layer also has a gradient nature. **Figure 2.7a** shows that a wettability gradient was formed on the PE surface after a corona treatment. The grafting density of PEO-MA on the PE surface increased with the increased wettability of the PE surface due to a gradual increase in peroxide concentration on the surface after corona treatment **(Figure 2.7b)**. Plasma protein adsorption and platelet adhesion on the PEO gradient surfaces decreased with increasing PEO chain length and surface density.

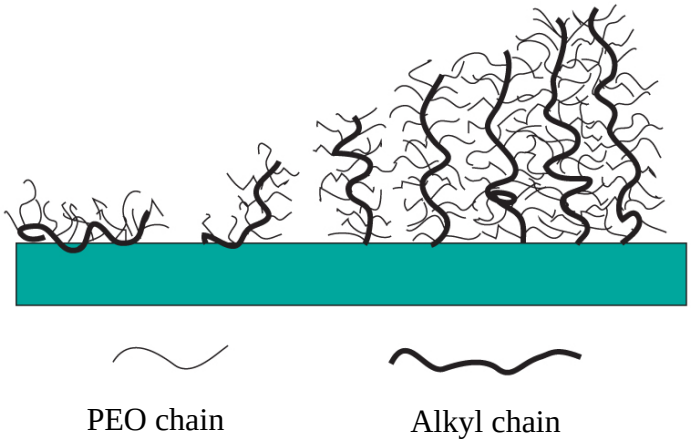

Figure 2.6. Schematic diagram showing a comb-like PEO gradient produced on polymer surfaces. *Redrawn after reference.*[37]

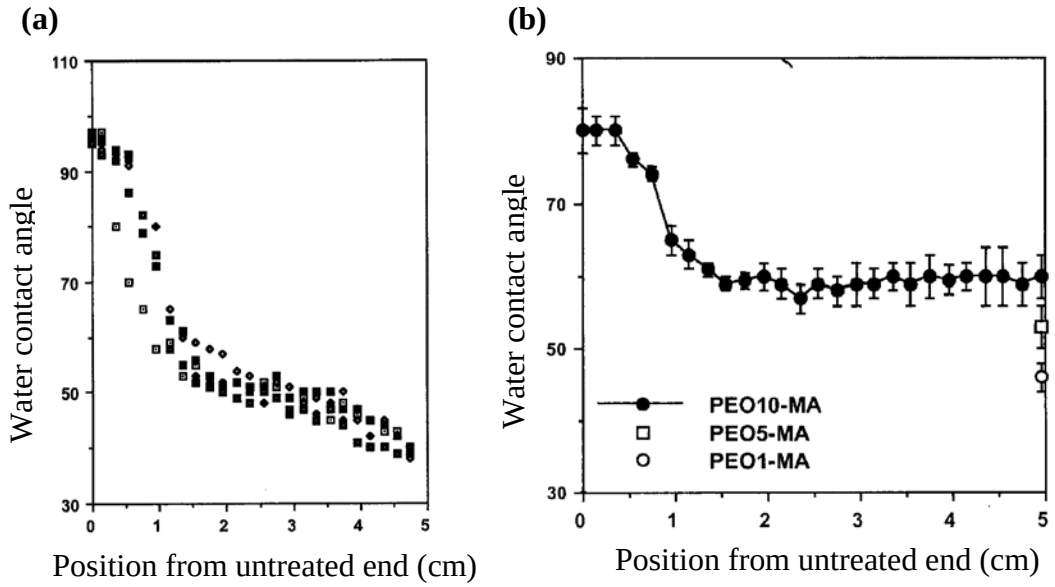

Figure 2.7. Changes in water contact angle along the sample length; (a) corona-treated PE surface, (b) PEO-MA grafted PE surface.[37] *Reprinted with permission from Wiley.*

Yu and coworkers[38] have fabricated a surface with a wettability gradient demonstrating a change from super-hydrophobicity to super-hydrophilicity. The wettability gradient was achieved by self-assembling thiol molecules on a gold surface in which molecule densities were controlled by varying immersion times **(Figure 2.8b)**. As solution was added to the bath, immersion time for the bottom part of the sample increased as compared to the top part. It was observed that the water contact angle changed with immersion **(Figure 2.8a)** and the sharpness of the gradient was changed by altering the solution's concentration.

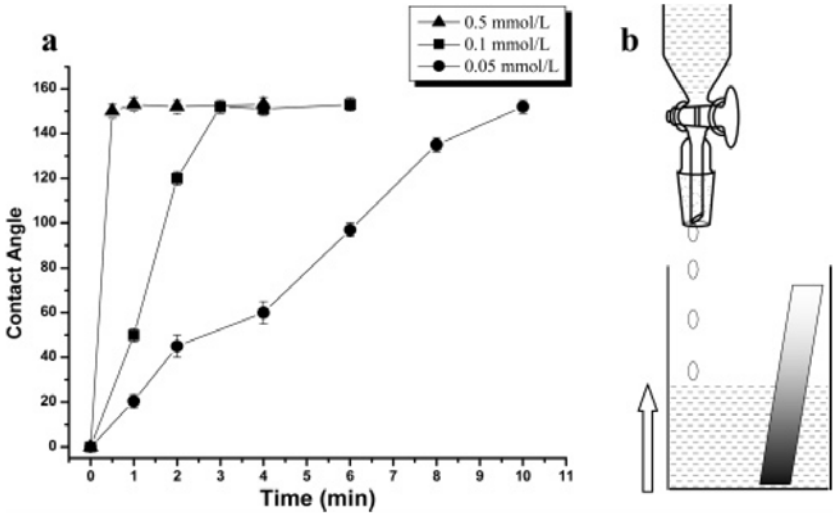

Figure 2.8. (a) Contact angle of the rough surface after being modified with an HS(CH2)11CH3 solution at different concentrations and different immersion times. All measurements are conducted after the substrates are further modified with HS9(CH2)10CH2OH solution for 10 min. (b) Scheme of the preparation process of the gradient surface.[38] *Reprinted with permission from ref 38. Copyright (2006) American Chemical Society.*

2.4. Microfluidics

Microfluidics is the handling and analyzing of fluids in micrometer scale structures.[39] By using micro-sized channels in which fluid can be moved and collected at the desired area, one can do various analytical and chemical reactions using a small amount of reagent in a considerably short time. Using capillary action, the energy needed to carry liquid in the microchannels can be eliminated.[40]

Many methods are used to fabricate microfluidics devices: micromachining, soft lithography, and micro molding.[41] Early microfluidic devices were fabricated via wet etching and laser ablation.[42] The wet etching method involves using photoresist and mask

with a desired pattern. Part of the photoresist defined by mask is cured upon exposure to light. Uncured photoresist is removed, and the substrate is partially covered with cured photoresist. Microchannels are formed on this surface after exposing it to a chemical bath. A substrate with microchannels is generally deposited on the glass or silicon wafer. This is one of the disadvantages of the technique, since it is unsuitable when flexible assembly is required. Moreover, the technique is costly, and it requires a specialized facility, equipment, and skilled labor. A more recently developed method, soft lithography on polydimethylsiloxane (PDMS), is a technique that is more practical than micromachining, since it is faster and less complicated.

Recent studies focus on replacing PDMS with more economical, flexible substrates. Specifically, fibrous materials like paper and threads are being considered for integration in microfluidic devices. Fluid distribution in fibrous material is capillary driven, thus eliminating the need for external pumping devices. Fabrication of paper-based microfluidics (μPADs) has been widely reported.[43-49] The advantages of paper for microfluidic applications are that it is lightweight, inexpensive, biodegradable, and easy to functionalize; moreover, paper is easily available and compatible with biological samples.[50] The most important characteristic of paper is its high wicking ability, and the disadvantage of paper is its lack of durability. Alternatively, scientists have used thread in microfluidics. Thread-based microfluidics is called μTADs. The types of yarns that can be used are cotton, nylon, polyester, silk, and polyvinylidene fluoride (PVDF).[51-55]

Li et al.[52] reported the fabrication of μTADs from cotton treated where it was sewn in other materials (e.g., polymer film or paper) to fabricate 3D and semi-

quantitative microfluidic devices. Reches et al. demonstrated three different designs for the μTAD: woven array, branching design, and sewn array design.[53] The function of thread-based microfluidic devices is demonstrated by testing five different colorimetric assays: detection of ketones, nitrite, protein, and glucose in artificial urine, and detection of alkaline phosphatase in artificial plasma **(Figure 2.9)**.

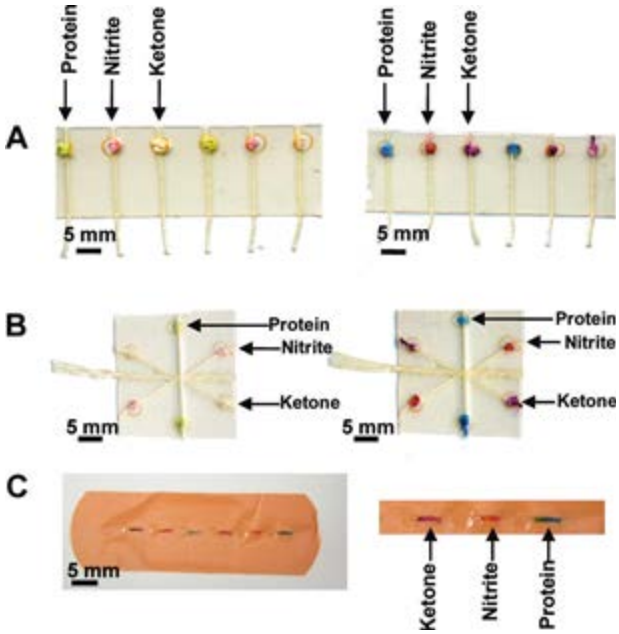

Figure 2.9. Colorimetric assays performed using the (A) woven array device, (B) branching device, (C) sewn array design.[53] *Reprinted with permission from ref 53. Copyright (2010) American Chemical Society.*

A conventional weaving technique was also recently utilized to fabricate a fabric-based microfluidic sensor.[55] Specifically, silk yarns with different wicking properties were used to form strips in fabric as transport and control units in fabric. Owens et al. utilized hydrophobic polypropylene (PP) and hydrophilic poly(ethylene terephthalate) (PET) yarns to systematically engineer woven textiles to create amphiphilic

microchannels with defined orientations and locations.[56] As a result, the microfluidic coflow of immiscible liquids (water and dodecane) within the textile structures was demonstrated.

2.5. Moisture management in textiles

Performance fabrics are said to be designed not only for fashion or as a passive skin cover, but also to have properties that improve (or at least do not impede) the wearer's comfort and performance.[57] It has been reported many times that maintaining the wearer's comfort is strongly related to effective moisture evaporation to keep the body`s core temperature constant. Therefore, the fabric should be designed to interact with the skin and environment, adjusting the skin's heat-regulating function as the environment interacts with it.[58] Moisture management in fabric can be defined as the controlled movement of water vapor or liquid water (perspiration) from the skin to the atmosphere through the fabric.

The human body produces heat and sweat in liquid or vapor form during physical activity. The heat is supposed to be emitted in order to keep the body's core temperature at a healthy level. Sweat production is the body's regulatory mechanism to keep its temperature at 37°C. If perspiration evaporates from the skin, the required heat is mostly extracted from the body. On the other hand, specifically during heavy exercise, sweat can penetrate into clothing and then evaporate, in which case heat is drawn from the surrounding air. When wet clothing touches the skin, comfort can be reduced, if

evaporation from the fabric is slow. That means it will extract heat from the body; this will cool the body but make the wearer tired and cause post-exercise chilling, which is associated with comfort loss.

Studies on developing a garment with moisture management properties focus on several characteristics: fiber development, fabric surface modification, fabric construction, fabric consisting of blended yarn[59], and composite garments.[7]

Natural fibers have great wicking properties and can absorb a large amount of liquid; however, they dry slowly. Moisture management on a fiber surface has mainly been achieved with two approaches, making the polymer itself hydrophilic[60] and rendering fiber surface to increase surface area of fibers[61, 62]. For example, there has been much effort to develop cross-shaped fibers to replicate natural fiber shapes. A hexa-channel cross section and scalloped oval cross section have been shown to improve water transport properties of fibers.[63, 64] Doi et al. reported that varying the cross-sectional shape of fibers one can obtain improved moisture-releasing and -absorbing properties with fabric.[65] Thus, researchers have developed circular, triangular, L-shaped, T-shaped, and Y-shaped hollow fibers **(Figure 2.10).** Lancaster[66] has developed fibers with open hallow cross-sections and reported that the wicking performance of a fabric made of open hallow fibers demonstrated improved wicking performance, compared to identically constructed fabric containing fibers with a circular cross section. Another approach is to add hydrophilic compounds to the fiber surface to provide hydrophilicity. To this end, acid and base treatments of polyester and hydrophilic polymer grafting to fiber surfaces

have been reported.[60, 67] Hydrotech fiber is one example of hydrophilic polyester commercialized by Delcron®.[68]

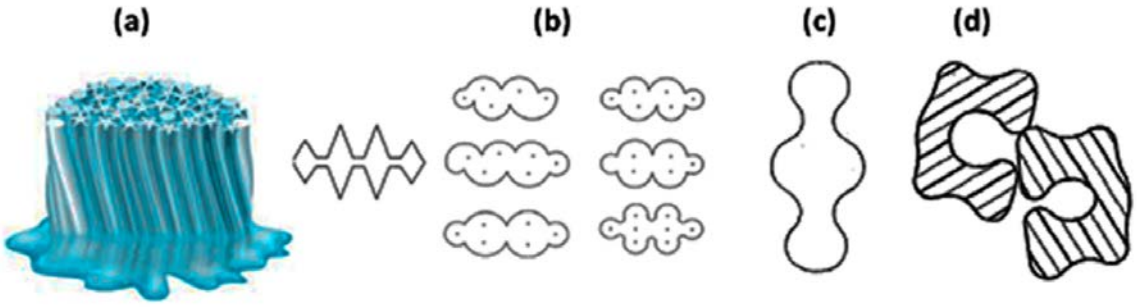

Figure 2.10. Demonstration of different cross sectional fiber shape.[69]

Other than fibers parameters, the yarn parameters (material and texture) have also been developed for better moisture transport in fabric. Core sheath yarn, textured yarn, crimped yarn, and composite yarns have shown improved moisture absorption and release properties.

Composite and core sheath yarns are composed of hydrophilic yarn located in the center and hydrophobic yarn at the outer layer **(Figure 2.11)**.[69] The whole structure has high permeability, which contributes to an improved wicking rate, and hydrophobic yarn provides low water retention. Polyester and cotton blended yarn has been chosen due to good wicking property of cotton and reduced water absorbent capacity of the polyester. Blended yarns with different deniers also exhibited increased wicking and drying rates.[70]

Another important factor is the swelling of fibers. According to Das et al.[71], the fiber type can change the yarn structure due to swelling, thus changing the fabric wicking

property and retention capacity. Swelling of the fibers can cause bottle-necking or closing of the capillaries, and then, flow may even stop.

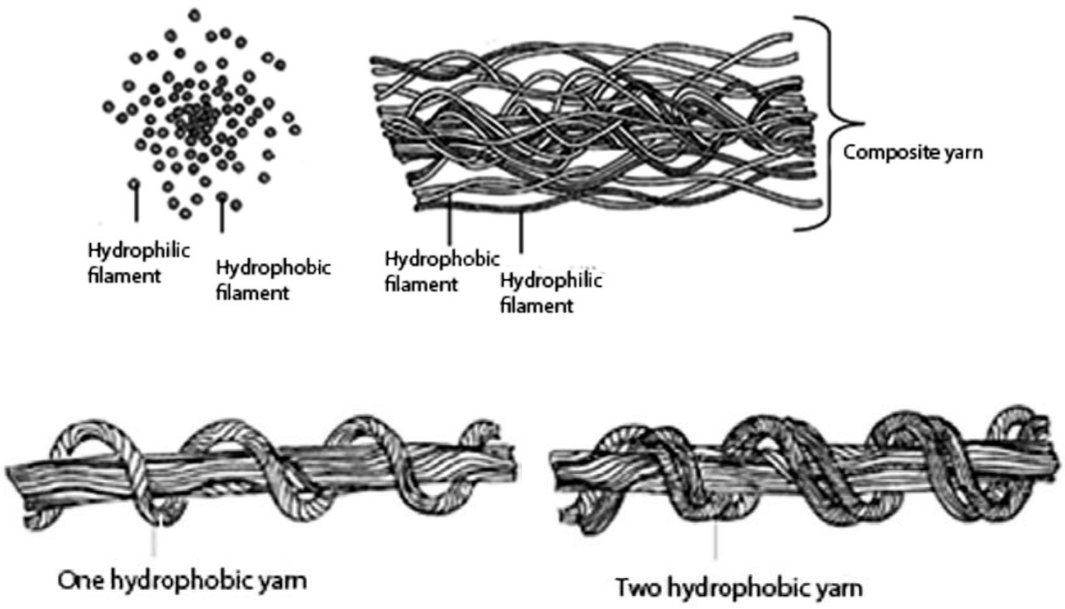

Figure 2.11. Core sheath, and composite yarns.[69]

Fabric parameters such as pore size, porosity, thickness, density, material, and construction have been reported to influence moisture management property of clothing.[69] Different weaves, knits, nonwoven structures, and laminated fabric constructions have been developed.[69, 72] In all the cases, less contact between the fabric and the skin is preferred for better air circulation to let the body breathe.

2.5.1. Multi-layered clothing for moisture management

Part of this dissertation focuses on developing fabric that can be used in multilayer protective garment construction to achieve improved moisture management.

Hence, in the current chapter, different single-layer fabric constructions will not be covered. It is important to note that even fabric construction (weave pattern) contributes to moisture management property of the fabric; increased moisture management property can be achieved by using hydrophilic and hydrophobic yarns in the structure, regardless of the weave pattern.

Multi-layered clothing constructions have also been developed.[73] Multilayered garments can be produced by bonding, laminating, coating, and stitching. A layered structure could be an advantageous and practical solution when several different functions are required—functions like thermal insulation, water permeability, and low or high water absorption. Specifically, in cold environments, multilayered clothing can perform more functions then single-layer fabrics.

Okada[74] and many others[73, 75] developed multilayered outwear to improve sweat absorbency. The general approach is to use at least two layers and form a structure with a hydrophobic to hydrophilic gradient in the cross section that can carry moisture to the outer layer. In the laminated garment design, hydrophobic fabric should face the skin. If hydrophilic fabric is first layer and in contact with the skin, it can absorb water and keep skin dry. However, during heavy sweating, the hydrophilic fabric structure can get saturated. In saturated fabric, water will block air spaces and decrease thermal insulation[76], making the body feel wet and cold. Air is a relatively poor conductor of heat as compared to water. It has been estimated that water cools the body 25 times faster than air.[57]

Figure 5.12[75] illustrates the construction of a three-layer outfit. Water and moisture-permeable fabric with low water absorbency (hydrophobic layer) is positioned on top of the skin; the intermediate layer helps carry liquid away from the surface to the outer layer where evaporation occurs. Outer layer is hydrophilic fabric. Zhang et al.[76] has studied liquid water transport in a two-layer system and demonstrated that more water can be transferred to the outer layer by capillary action when the inner layer is hydrophobic.

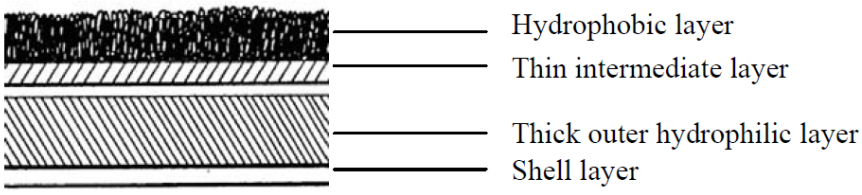

Figure 2.12. Cross-sectional view of three-layer moisture management fabric. [75]

2.6. Conclusion

This literature review indicates that PET surfaces have been used widely in everyday and industrial application. Also, it is an attractive candidate for smart materials, and sensor applications. Many approaches have been developed to modify PET surfaces, and wettability alterations of PET fabrics with surface modification has been extensively studied. However, much research is still needed for full understanding of the effect of polymer coating on the wicking property of fabric to develop textile surfaces for controlled fluid movement and to design smart textiles for everyday or sensorial use.

2.7. References

1. Brittain, W. J.; Minko, S., A structural definition of polymer brushes. *Journal of Polymer Science Part A: Polymer Chemistry* **2007,** *45* (16), 3505-3512.

2. Azzaroni, O., Polymer brushes here, there, and everywhere: Recent advances in their practical applications and emerging opportunities in multiple research fields. *Journal of Polymer Science Part A: Polymer Chemistry* **2012,** *50* (16), 3225-3258.

3. Zhao, B.; Brittain, W. J., Polymer brushes: Surface-immobilized macromolecules. *Progress in Polymer Science* **2000,** *25* (5), 677-710.

4. Nystrom, D.; Lindqvist, J.; Ostmark, E.; Hult, A.; Malmstrom, E., Superhydrophobic bio-fibre surfaces via tailored grafting architecture. *Chemical Communications* **2006,** *0* (34), 3594-3596.

5. Hollmann, O.; Gutberlet, T.; Czeslik, C., Structure and Protein Binding Capacity of a Planar PAA Brush. *Langmuir* **2006,** *23* (3), 1347-1353.

6. Wu, T.; Gong, P.; Szleifer, I.; Vlček, P.; Šubr, V.; Genzer, J., Behavior of Surface-Anchored Poly(acrylic acid) Brushes with Grafting Density Gradients on Solid Substrates: 1. Experiment. *Macromolecules* **2007,** *40* (24), 8756-8764.

7. Li, Z. Protein interactions with mixed poly(ethylene glycol)/polyacrylic acid brushes. M.S., Clemson University, United States -- South Carolina, 2008.

8. Guiselin, O., Irreversible adsorption of a concentrated polymer solution. *EPL (Europhysics Letters)* **1992,** *17* (3), 225.

9. Zdyrko, B.; Luzinov, I., Polymer brushes by the "grafting to" method. *Macromolecular Rapid Communications* **2011,** *32* (12), 859-869.

10. Bug, A.; Cates, M.; Safran, S.; Witten, T., Theory of size distribution of associating polymer aggregates. I. Spherical aggregates. *The Journal of chemical physics* **1987,** *87*, 1824.

11. Parsonage, E.; Tirrell, M.; Watanabe, H.; Nuzzo, R. G., Adsorption of poly(2-vinylpyridine)-poly (styrene) block copolymers from toluene solutions. *Macromolecules* **1991,** *24* (8), 1987-1995.

12. Marra, J.; Hair, M. L., Interactions between two adsorbed layers of poly(ethylene oxide)/polystyrene diblock copolymers in heptane—toluene mixtures. *Colloids and Surfaces* **1988,** *34* (3), 215-226.

13. Guzonas, D.; Boils, D.; Hair, M. L., Surface force measurements of polystyrene-block-poly(ethylene oxide) adsorbed from a nonselective solvent on mica. *Macromolecules* **1991,** *24* (11), 3383-3387.

14. G.J Fleer, M. A. C.-S., J.M.H Scheutjens, T Cosgrove, B Vincent *Polymers at interfacesChapman and Hall, London* **(1993)**.

15. Yerushalmi-Rozen, R.; Klein, J.; Fetters, L. J., Suppression of rupture in thin, nonwetting liquid films. *Science-AAAS-Weekly Paper Edition-including Guide to Scientific Information* **1994,** *263* (5148), 793-795.

16. Reiter, G.; Schultz, J.; Auroy, P.; Auvray, L., Improving adhesion via connector polymers to stabilize non-wetting liquid films. *EPL (Europhysics Letters)* **1996,** *33* (1), 29.

17. Zdyrko, B.; Varshney, S. K.; Luzinov, I., Effect of molecular weight on synthesis and surface morphology of high-density poly (ethylene glycol) grafted layers. *Langmuir* **2004,** *20* (16), 6727-6735.

18. Ligoure, C.; Leibler, L., Thermodynamics and kinetics of grafting end-functionalized polymers to an interface. *J. Phys. France* **1990,** *51* (12), 1313-1328.

19. Huang, H.; Rankin, S. E.; Penn, L. S.; Quirk, R. P.; Cheong, T. H., Transition from Mushroom to Brush during Formation of a Tethered Layer. *Langmuir* **2004,** *20* (14), 5770-5775.

20. Luzinov, I.; Minko, S.; Tsukruk, V. V., Responsive brush layers: from tailored gradients to reversibly assembled nanoparticles. *Soft Matter* **2008,** *4* (4), 714-725.

21. Prucker, O.; Rühe, J., Synthesis of Poly(styrene) Monolayers Attached to High Surface Area Silica Gels through Self-Assembled Monolayers of Azo Initiators. *Macromolecules* **1998,** *31* (3), 592-601.

22. Buchmeiser, M. R.; Sinner, F.; Mupa, M.; Wurst, K., Ring-Opening Metathesis Polymerization for the Preparation of Surface-Grafted Polymer Supports. *Macromolecules* **1999,** *33* (1), 32-39.

23. Kang, J. F.; Liao, S.; Jordan, R.; Ulman, A., Mixed Self-assembled Monolayers of Rigid Biphenyl Thiols: Impact of Solvent and Dipole Moment. *Journal of the American Chemical Society* **1998,** *120* (37), 9662-9667.

24. Jordan, R.; Ulman, A.; Kang, J. F.; Rafailovich, M. H.; Sokolov, J., Surface-Initiated Anionic Polymerization of Styrene by Means of Self-Assembled Monolayers. *Journal of the American Chemical Society* **1999,** *121* (5), 1016-1022.

25. Chen, W.; Fadeev, A. Y.; Hsieh, M. C.; Öner, D.; Youngblood, J.; McCarthy, T. J., Ultrahydrophobic and Ultralyophobic Surfaces: Some Comments and Examples. *Langmuir* **1999,** *15* (10), 3395-3399.

26. Prucker, O.; Naumann, C. A.; Rühe, J.; Knoll, W.; Frank, C. W., Photochemical Attachment of Polymer Films to Solid Surfaces via Monolayers of Benzophenone Derivatives. *Journal of the American Chemical Society* **1999,** *121* (38), 8766-8770.

27. Gurtner, C.; Wun, A. W.; Sailor, M. J., Surface Modification of Porous Silicon by Electrochemical Reduction of Organo Halides. *Angewandte Chemie International Edition* **1999,** *38* (13-14), 1966-1968.

28. Liu, Y.; Klep, V.; Luzinov, I., Segregated Polymer Brushes via "Grafting to" and ATRP "Grafting from" Chain Anchoring. In *Controlled/Living Radical Polymerization: Progress in ATRP*, American Chemical Society: 2009; Vol. 1023, pp 215-230.

29. Liu, Y.; Klep, V.; Luzinov, I., To Patterned Binary Polymer Brushes via Capillary Force Lithography and Surface-Initiated Polymerization. *Journal of the American Chemical Society* **2006,** *128* (25), 8106-8107.

30. Liu, Y.; Klep, V.; Zdyrko, B.; Luzinov, I., Synthesis of High-Density Grafted Polymer Layers with Thickness and Grafting Density Gradients. *Langmuir* **2005,** *21* (25), 11806-11813.

31. Fischer, D. A.; Efimenko, K.; Bhat, R. R.; Sambasivan, S.; Genzer, J., Mapping Surface Chemistry and Molecular Orientation with Combinatorial Near-Edge X-Ray Absorption Fine Structure Spectroscopy. *Macromolecular rapid communications* **2004,** *25* (1), 141-149.

32. Jandeleit, B.; Schaefer, D. J.; Powers, T. S.; Turner, H. W.; Weinberg, W. H., Combinatorial Materials Science and Catalysis. *Angewandte Chemie International Edition* **1999,** *38* (17), 2494-2532.

33. Genzer, J.; Fischer, D. A.; Efimenko, K., Combinatorial near-edge x-ray absorption fine structure: Simultaneous determination of molecular orientation and bond concentration on chemically heterogeneous surfaces. *Applied Physics Letters* **2003,** *82* (2), 266-268.

34. Julthongpiput, D.; Fasolka, M. J.; Zhang, W.; Nguyen, T.; Amis, E. J., Gradient Chemical Micropatterns:â€‰ A Reference Substrate for Surface Nanometrologyâ€ *Nano Letters* **2005,** *5* (8), 1535-1540.

35. Genzer, J.; Bhat, R. R., Surface-bound soft matter gradients. *Langmuir* **2008,** *24* (6), 2294-2317.

36. Ionov, L.; Zdyrko, B.; Sidorenko, A.; Minko, S.; Klep, V.; Luzinov, I.; Stamm, M., Gradient polymer layers by "grafting to" approach. *Macromolecular rapid communications* **2004,** *25* (1), 360-365.

37. Lee, J. H.; Jeong, B. J.; Lee, H. B., Plasma protein adsorption and platelet adhesion onto comb-like PEO gradient surfaces. *Journal of Biomedical Materials Research* **1997,** *34* (1), 105-114.

38. Yu, X.; Wang, Z.; Jiang, Y.; Zhang, X., Surface Gradient Material:â€‰ From Superhydrophobicity to Superhydrophilicity. *Langmuir* **2006,** *22* (10), 4483-4486.

39. Beebe, D. J.; Mensing, G. A.; Walker, G. M., Physics and applications of microfluidics in biology. *Annual Review of Biomedical Engineering* **2002,** *4*, 261-286.

40. Owens, T. L., Engineering amphiphilic fabrics for microfluidic applications. **2011**.

41. Whitesides, G. M., The origins and the future of microfluidics. *Nature* **2006,** *442* (7101), 368-373.

42. Whitesides, G. M.; Stroock, A. D., Flexible methods for microfluidics. *Physics today* **2001,** *54*, 42.

43. Martinez, A. W.; Phillips, S. T.; Wiley, B. J.; Gupta, M.; Whitesides, G. M., FLASH: A rapid method for prototyping paper-based microfluidic devices. *Lab on a Chip* **2008,** *8* (12), 2146-2150.

44. Khan, M. S.; Thouas, G.; Shen, W.; Whyte, G.; Garnier, G., Paper diagnostic for instantaneous blood typing. *Analytical Chemistry* **2010,** *82* (10), 4158-4164.

45. Martinez, A. W.; Phillips, S. T.; Butte, M. J.; Whitesides, G. M., Patterned paper as a platform for inexpensive, low-volume, portable bioassays. *Angewandte Chemie International Edition* **2007,** *46* (8), 1318-1320.

46. Abe, K.; Suzuki, K.; Citterio, D., Inkjet-printed microfluidic multianalyte chemical sensing paper. *Analytical Chemistry* **2008,** *80* (18), 6928-6934.

47. Li, X.; Tian, J.; Nguyen, T.; Shen, W., Paper-based microfluidic devices by plasma treatment. *Analytical Chemistry* **2008,** *80* (23), 9131-9134.

48. Martinez, A. W.; Phillips, S. T.; Whitesides, G. M., Three-dimensional microfluidic devices fabricated in layered paper and tape. *Proceedings of the National Academy of Sciences* **2008,** *105* (50), 19606-19611.

49. Callegari, G.; Tyomkin, I.; Kornev, K. G.; Neimark, A. V.; Hsieh, Y.-L., Absorption and transport properties of ultra-fine cellulose webs. *Journal of Colloid and Interface Science* **2011,** *353* (1), 290-293.

50. Martinez, A. W.; Phillips, S. T.; Whitesides, G. M.; Carrilho, E., Diagnostics for the developing world: Microfluidic paper-based analytical devices. *Analytical Chemistry* **2009,** *82* (1), 3-10.

51. Tsai, C.-C.; Mikes, P.; Andrukh, T.; White, E.; Monaenkova, D.; Burtovyy, O.; Burtovyy, R.; Rubin, B.; Lukas, D.; Luzinov, I.; Owens, J. R.; Kornev, K. G., Nanoporous artificial proboscis for probing minute amount of liquids. *Nanoscale* **2011,** *3* (11), 4685-4695.

52. Li, X.; Tian, J.; Shen, W., Thread as a Versatile Material for Low-Cost Microfluidic Diagnostics. *ACS Applied Materials & Interfaces* **2009,** *2* (1), 1-6.

53. Reches, M.; Mirica, K. A.; Dasgupta, R.; Dickey, M. D.; Butte, M. J.; Whitesides, G. M., Thread as a matrix for biomedical assays. *ACS Applied Materials & Interfaces* **2010,** *2* (6), 1722-1728.

54. Ballerini, D. R.; Li, X.; Shen, W., Flow control concepts for thread-based microfluidic devices. *Biomicrofluidics* **2011,** *5* (1), 014105-13.

55. Bhandari, P.; Narahari, T.; Dendukuri, D., 'Fab-Chips': a versatile, fabric-based platform for low-cost, rapid and multiplexed diagnostics. *Lab on a Chip* **2011,** *11* (15), 2493-2499.

56. Owens, T. L.; Leisen, J.; Beckham, H. W.; Breedveld, V., Control of microfluidic flow in amphiphilic fabrics. *ACS Applied Materials & Interfaces* **2011,** *3* (10), 3796-3803.

57. Simile, C. B., Critical evaluation of wicking in performance fabrics. **2004**.

58. Zhang, P.; Gong, R.; Yanai, Y.; Tokura, H., Effects of clothing material on thermoregulatory responses. *Textile Research Journal* **2002,** *72* (1), 83-89.

59. Piehler, J.; Brecht, A.; Valiokas, R.; Liedberg, B.; Gauglitz, G., A high-density poly(ethylene glycol) polymer brush for immobilization on glass-type surfaces. *Biosensors and Bioelectronics* **2000,** *15* (9–10), 473-481.

60. Yoo, S.; Barker, R. L., Moisture management properties of heat-resistant workwear fabrics— Effects of hydrophilic finishes and hygroscopic fiber blends. *Textile Research Journal* **2004,** *74* (11), 995-1000.

61. Sampath, M.; Mani, S.; Nalankilli, G., Effect of filament fineness on comfort characteristics of moisture management finished polyester knitted fabrics. *Journal of Industrial Textiles* **2011,** *41* (2), 160-173.

62. Guimond, S.; Hanselmann, B.; Amberg, M.; Hegemann, D., Plasma functionalization of textiles: specifics and possibilities. *Pure and Applied Chemistry* **2010,** *82* (6), 1239-1245.

63. Aneja, A. P., Improving comfort by mixing deniers. EP Patent 1,068,379: 2003.

64. Aneja, A. P., Comfort by mixing deniers. Google Patents: 2000.

65. Doi, M.; Sugaya, T.; Ohashi, S., Moisture-absorbing/releasing synthetic fiber and fabric using the same. Google Patents: 2002.

66. LANCASTER, P., Polymer filaments having profiled cross-section. WO Patent 2,002,004,720: 2002.

67. Gowri, S.; Almeida, L.; Amorim, T.; Carneiro, N.; Pedro Souto, A.; Fátima Esteves, M., Polymer Nanocomposites for Multifunctional Finishing of Textiles - a Review. *Textile Research Journal* **2010,** *80* (13), 1290-1306.

68. Delcron® Hydrotec fiber. http://www.dakamericas.com/us-en/products/fibers_delcron_hydrotec.php (accessed 06.30.2013).

69. Chen, Q., Development of plant structured knitted fabrics. **2011**.

70. Yeh, P., Composite textile fabric having moisture management. Google Patents: 2002.

71. Das, A.; Kothari, V. K.; Sadachar, A., Comfort characteristics of fabrics made of compact yarns. *Fibers and Polymers* **2007,** *8* (1), 116-122.

72. Bedek, G.; SalaÃ¼n, F.; Martinkovska, Z.; Devaux, E.; Dupont, D., Evaluation of thermal and moisture management properties on knitted fabrics and comparison with a physiological model in warm conditions. *Applied Ergonomics* **2011,** *42* (6), 792-800.

73. Hall, M. R., Multilayer moisture management fabric. Google Patents: 2009.

74. Okada, H., Sweat-absorbent textile fabric. Google Patents: 1985.

75. Moretz, H. L.; Brier, D. L., Multi-layer moisture management fabric and garments incorporating a moisture management panel. Google Patents: 1994.

76. Zhang, W.; Li, J.; Chen, W.; Long, S., Wetness comfort of fine-polypropylene-fibre fabrics. *Journal of The Textile Institute* **1999,** *90* (2), 252-263.

CHAPTER THREE

EXPERIMENTAL

3.1. Chemical reagent used

Hydrogen peroxide:

Company Identification: Acros Organics

MSDS Name: Hydrogen peroxide (30% in Water) (without stabilizer), Reagent ACS

CAS Number: 7722-84-1

Sulfuric acid 98%:

Company Identification: Acros Organics

MSDS Name: Sulfuric acid, Reagent ACS

CAS Number: 7664-93-9

Toluene:

Company Identification: Acros Organics

MSDS Name: Toluene, Reagent ACS

CAS Number: 108-88-3

Methyl ethyl ketone (MEK):

Company Identification: Acros Organics

MSDS Name: 2-Butanone, 99+%

CAS Number: 78-93-3

Ethanol:

Company Identification: Mallinckrodt Baker, Inc.

MSDS Name: Reagent alcohol, ACS

CAS Number: 64-17-5

Methanol:

Company Identification: VWR International, LLC

MSDS Name: Methanol, ACS

CAS Number: 67-56-1

Acetone:

Company Identification: VWR International, LLC

MSDS Name: Acetone, ACS

CAS Number: 67-64-1

Tetrahydrofuran (THF):

Company Identification: Alfa Aesar

MSDS Name: Tetrahydrofuran, 99.8%

CAS Number: 109-99-9

3.2. Polymers used for surface modification

Poly(glycidyl methacrylate) (PGMA) (S.3.1)

PGMA with two different number average molecular weights were used:

1. Mn=63,000 g/mol with PDI= 1.9, before RhB attachment

   Mn=80,000 g/mol with PDI= 2.57, after RhB attachment

2. Mn=176,000 g/mol with PDI= 2.7

PGMA was synthesized by solution radical polymerization and purified using multiple precipitations by Yuriy Galabura according to the procedure reported elsewhere.[1] Fluorescent labeling of the PGMA (Mn=63,000 g/mol) was performed according to the previously developed procedure.[2]

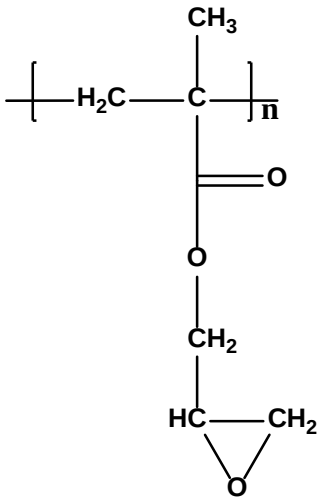

S 3.1

Carboxy terminated polystyrene (PS) (S.3.2)

Carboxy terminated polystyrene (Mn=48,000 g/mol, PDI=1.05) was obtained from Polymer Source Inc., Canada.

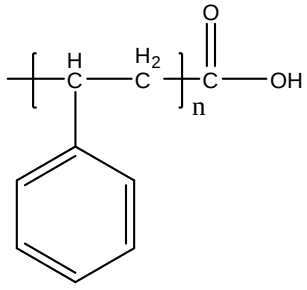

S 3.2

Carboxy terminated poly(2-vinyl pyridine) (PVP) (S.3.3)

Carboxy terminated poly(2-vinyl pyridine) (Mn=53,000 g/mol, PDI=1.06) was obtained from Polymer Source Inc., Canada.

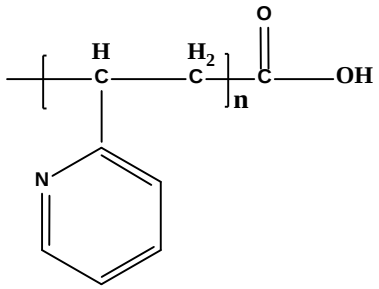

S 3.3

Carboxy terminated polyethylene glycol (PEG) (S.3.4)

Poly(ethylene glycol) mono-methyl ether (Mn=5,000) was obtained from Sigma-Aldrich and modified with succinic anhydride to form a carboxy terminated derivative by Dr. B. Zdyrko according to the procedure reported elsewhere.[3]

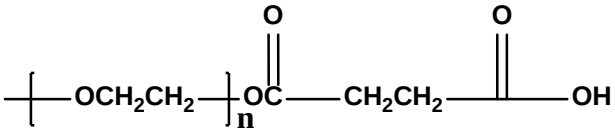

S 3.4

Poly acrylic acid (PAA) (S.3.5)

PAA (Mw=100,000 g/mol) was obtained from VWR International. It was precipitated from water solution with acetone, dried in vacuum and dissolved in methanol to prepare solution to be used for deposition.

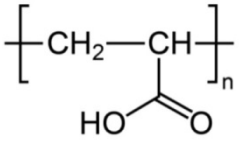

S 3.5

Poly(styrene-alt-maleic anhydride) (PSMA) (S.3.6)

Poly(styrene-alt-maleic anhydride) (Mw=350,000) was obtained from Sigma-Aldrich (CAS: 477699). The PSMA was subjected to base-catalyzed hydrolysis of the anhydride groups to form polymer PSMA according to the published procedure.[4] Briefly, 1.5 g of PSMA was added to 20 mL of a 2.2 M NaOH solution and stirred for 5 h at room temperature. The copolymer was recovered from the NaOH solution by acid precipitation using 1 N HCl. The solution was then centrifuged and the precipitated copolymer was rinsed with DI water, and then dried in vacuum. Dried copolymer was dissolved in methanol to prepare solution to be used for deposition.

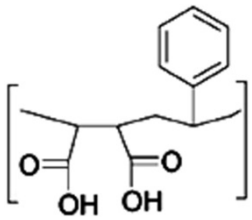

S 3.6

3.3. Principles of experimental and characterization techniques

3.3.1. Dip coating

Dip coating technique **(Figure 3.1)** can be described as a process where the substrate is immersed in a solution and then withdrawn with a well-defined constant speed, under controlled temperature and atmospheric conditions. The coating thickness is determined by the withdrawal speed, and concentration[5]. To achieve a contaminant free surface, the dip coating should be done in a clean room environment. If there is no evaporation, the thickness of the obtained film can be estimated as **(E.3.1):**[6]

$$h = 0.944.\left(\frac{\eta v}{\rho g}\right)^{1/2}.\left(\frac{\eta v}{\sigma}\right)^{1/6} \qquad \textbf{E.3.1}$$

Where η is the dynamic viscosity of the solvent, v is the withdrawal speed, ρ is the liquid density, g is the acceleration of gravity, and σ is the liquid surface tension. The dip coating was performed in a clean room environment using the Mayer Fientechnik D-3400 dip coater. The withdrawal speed was adjusted to 4 mm/sec for the polymer coating, and 1mm/sec for the PET film deposition.

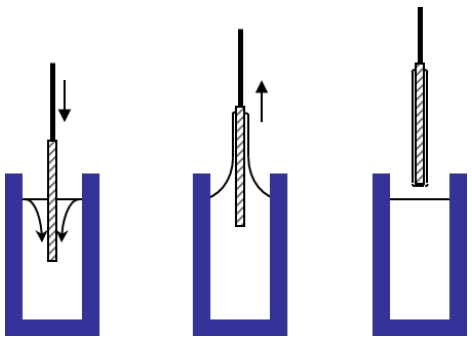

Figure 3.1. Procedure for coating substrate with dip-coating apparatus.

3.3.2. Ellipsometry

Ellipsometry measures the change in the polarization state of light reflected from the surface of a sample.[7] The measured values are expressed as Ψ and Δ, which are related to the ratio of the Fresnel reflection coefficients, R_p and R_s for *p* and *s*-polarized light, respectively.

$$\tan(\Psi)e^{i\Delta} = R_p / R_s \qquad \textbf{E.3.2}$$

Because ellipsometry measures the ratio of two values, it can be highly accurate and very reproducible. From **E.3.2**, the ratio is seen to be a complex number, thus it contains "phase" information contained in Δ, which makes the measurement very sensitive. A linearly polarized input beam is converted to an elliptically polarized reflected beam. For any angle of incidence greater than 0° and less than 90°, *p*-polarized and s-polarized light will be reflected differently.

The coordinate system used to describe the ellipse of polarization is the *p*-*s* coordinate system. The s-direction is taken perpendicular to the direction of propagation and parallel to the sample surface, and the *p*-direction is taken perpendicular to the direction of propagation and contained in the plane of incidence.

Ellipsometry was performed using a COMPEL automatic ellipsometer (InOmTech, Inc.) at an angle of incidence of 70^o. For all of the experiments in the current research, it was decided to keep the compensator on for thickness values of less than 11 nm and removed for thicknesses greater than 14 nm. For thickness values between 11 nm

and 14 nm (both limits included), the average value of the thickness with and without the compensator was used.

3.3.3. Atomic force microscopy (AFM)

Atomic force microscopy (AFM) is in the family of scanning probe microscopy. The fundamental components and basic concept of the AFM are represented in the schematic illustration in **Figure 3.3**.

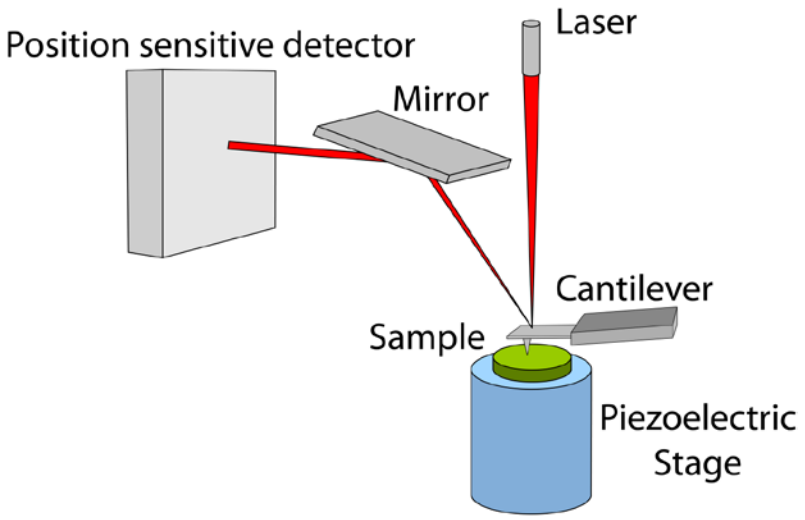

Figure 3.2. AFM schematics.

In AFM, a cantilever with a sharp tip is brought into interaction with the sample to scan the surface. The cantilever is typically made from silicon or silicon nitride. V-shaped cantilevers are common since they provide low mechanical resistance to vertical deflection and high resistance to lateral torsion. The AFM can be operated in two scanning modes: contact mode and tapping mode. When the tip is in the vicinity of the surface, the attractive and repulsive forces rise and lead to a deflection of the cantilever.

This deflection is measured using laser spot reflection from the top surface of the cantilever, which is detected by photodiodes.

All AFM studies were performed on a Dimension 3100 (Digital Instruments, Inc.) microscope. The tapping mode was used to study the surface morphology of the samples in ambient air. Silicon tips with spring constants of 50 N/m were used to scan the surfaces with a 1 Hz scanning rate.

3.3.4. Plasma generator

Plasma is composed of highly excited atomic, molecular, ionic, and radical species, and considered to be the fourth state of matter.[8] The plasma state is generated when a gas is exposed to a high energy environment which is sufficient to break down its molecular integrity and cause it to dissociate.[9]

Plasma surface modification is based on the interaction of excited plasma species with the surface. Depending on the nature of the material, and the desired surface properties, different gases can be employed during plasma treatment: oxygen, nitrogen, hydrogen, ammonia, and argon. Different plasmas generate different chemical activity and lead to a physical modification of the surface. Plasma surface modification has been used extensively for the modification and/or activation of polymeric material.

A plasma generator was obtained from Harrick Scientific Corporation (Model PDC-32G). The plasma cleaner/sterilizer used in the current study is a compact, table model, electrode-less, radio frequency glow discharge apparatus.[10] It has a 3" diameter by

7" long chamber and a removable cover. The chamber has two hoses for connection to the vacuum source, and introducing the required gas for the sample treatments.

3.3.5. Contact angle

The contact angle is a quantitative measurement of a liquid`s ability to spread on a surface. It is a consequence of the surface tension between phases. When a drop of liquid is placed on a surface, it may either spread over the surface or remain as a drop. The spreading conditions for a drop are given by **E.3.3**, where Υ is the interfacial tension between phases and the subscripts *S*, *L*, and *V* refer to solid, liquid, and vapor, respectively. When spreading conditions **(E.3.3)** are not satisfied, an equilibrium contact angle (θ_E) exists, which is governed by the force balance at the three phase-boundaries **(Figure 3.4)** as defined by Young's equation **(E.3.4)**.

$$\Upsilon_{sv} - \Upsilon_{sl} > \Upsilon_{lv} \qquad \textbf{E.3.3}$$

$$\Upsilon_{sv} - \Upsilon_{sl} = \Upsilon_{lv} \cos\theta_E \qquad \textbf{E.3.4}$$

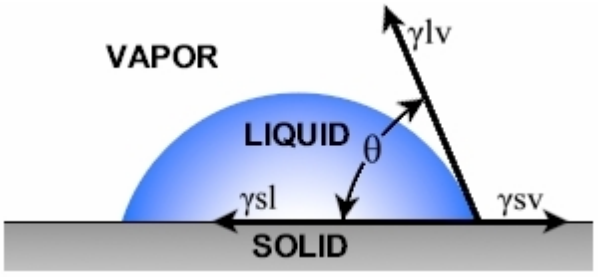

Figure 3.3. Representation of the equilibrium contact angle at the three phase boundaries.[11]

The contact angle is very sensitive to the chemical composition of the top layer of a surface, and is an inexpensive, relatively simple, and reliable technique for polymer surface characterization. Experiments in this dissertation were performed using a sessile drop technique, and the static contact angle measurements were taken using a contact angle goniometer (Kruss, Model DSA10). The contact angle measurements were taken with the liquid at a static time of 30 s before angle recording.

3.3.6. Fluorescent microscopy

A fluorescent microscope is an optical microscope with added features, such as a high intensity light source, with excitation and emission filters that are specific to certain wavelengths. The features and basic principles of fluorescent microscopy are schematically presented in **Figure 3.5**. In this work, fluorescence imaging was conducted using an SZXILL100 microscope (Olympus Optical Co. Ltd., Japan).

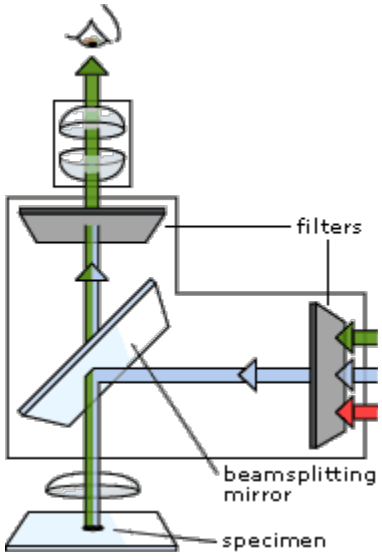

Figure 3.4. Fluorescent microscopy schematics.[12]

3.3.7. Scanning electron microscopy (SEM)

An SEM is a type of electron microscope which uses focused high energy electrons to bombard the surface of the sample. These electrons and sample interactions produce a number of useful signals which can be detected by a detector, including secondary electrons, backscatter electrons, and X-rays.

The FESEM Hitachi S4800 and S3500N, present in the Advanced Materials Research Laboratory (AMRL) (Research Park, Clemson University), were used for scanning purposes. The S4800 offers field emission for high resolution microscopy and the S3500 is designed for conventional and variable pressure microscopy. Prior to scanning, all of the samples were coated with platinum using a Hummer 6.2 sputtering system for approximately 2 minutes with the pressure and voltage set to 70 millitorr and 15 milliamperes, respectively. This was done to reduce the specimen charging.

3.4. Characterization of polymer films

For the characterization of the polymer layers, several parameters were evaluated,[13] such as surface coverage (Γ), grafting density (Σ), and the distance between grafting sites. The surface coverage is the measurement of the amount of the polymer grafted per unit area in mg/m^2, and was calculated from the ellipsometry thickness (h, nm) and density (ρ, g/cm^3) of the polymer using the following equation:

$$\Gamma = h * \rho \qquad \textbf{E.3.5}$$

The density data for the PEG (1.09 g/cm^3), PAA (1.14 g/cm^3), PS (1.05 g/cm^3), P2VP (1.17 g/cm^3), and PSMA (1.27 g/cm^3) were provided by supplier. The density of

the PGMA (1.08 g/cm^3) was assumed to be the same as for the poly(propyl methacrylate).[14]

The chain density, Σ (chain/nm^2), is the inverse of the average area per adsorbed chain. This was determined by the following equation, where N_A is Avogadro's number and M_n (g/mol) is the number average molar mass of the grafted polymer:

$$\Sigma=\Gamma*N_A*10^{-21}/M_n= (6.023*\Gamma*100)/M_n \quad \textbf{E.3.6}$$

The distance between grafting sites, D (nm), was calculated using following equation:

$$D= (4/\pi\Sigma)^{1/2} \quad \textbf{E.3.7}$$

E.3.7 assumes even distribution of attached polymer chains. The end-to-end distance ($<r^2>^{1/2}$) for the macromolecules in the bulk was estimated by the following equation:[15, 16]

$$<r^2>^{0.5}=aN^{0.5} \quad \textbf{E.3.8}$$

The root-mean-square roughness (RMSR) of the samples was computed from the topographical AFM images recorded in the tapping mode using NanoScope version 5.3.0r3.sr3 software (Veeco Instruments Inc.). The RMSR is the standard deviation of the feature height (*Z*) values within a given area. The formula used to calculate the RMSR is:[17]

$$Roughness(RMSR) = \sqrt{\frac{\sum_{i=1}^{N}(Z_i - Z_{ave})^2}{N}} \quad \textbf{E.3.9}$$

Where Z_{ave} is the average Z value within the given area, Z_i is the current Z value, and N is the number of points within a given area.

3.5. Substrate preparation procedure

3.5.1. Model film preparation

Highly polished single-crystal silicon wafers (Semiconductor Processing Co.) were used as model flat substrates. The silicon wafers were initially cleaned with de-ionized (DI) water in an ultrasonic bath for 30 min; then the wafers were placed in piranha solution (3:1 concentrated sulfuric acid/30% hydrogen peroxide) for approximately 1 hour at 80°C and rinsed several times with DI water. After rinsing, the substrates were dried under a stream of nitrogen in class 100 clean room conditions.

To obtain thin polyester films, PET chips were dissolved in 1,1,1,3,3,3-hexafluoro-2-propanol (HFIP), and the film was dip coated onto the clean silicon substrate from a 1 wt/vol % solution. The specimens were placed in a vacuum oven at 140°C for ~3 h to ensure a complete removal of the solvent and a crystallization of the polymer constituting the film.

3.5.2. Fabric preparation

Polyester fabric poly(ethylene terephthalate) (PET) (Dacron type heat set 122 g m^{-2}) was obtained from Test Fabrics (style #777H). PET multifilament yarn (500/70 Denier-3Ztwist) was provided by Middleburg Yarn Processing Co Inc. PP multifilament yarn (100/40 Denier) was provided by Fiber Visions, Inc. and was twisted (4Z) with

Saurer Allma Assembly Twisting Machines to achieve required mechanical properties for weaving.

The fabric preparation and activation were accomplished according to the procedure published elsewhere.[18] In order to remove any finishes or contaminants, each fabric was rinsed sequentially with DI water, acetone, toluene, ethanol, and once again with DI water. The clean fabrics were then treated with a 40% sodium hydroxide solution (40/30/30 wt % NaOH/methanol/DI water; alcohol was added to improve wettability) for 2 min at room temperature. An alkali treatment is a generally accepted hydrolysis procedure for textiles, and creates active groups (carboxylic and hydroxyl) on the PET fiber surface, making the fibers relatively more reactive for further modification.[19-21] After the hydrolysis, the fabrics were rinsed with DI water, then with diluted HCL(in DI water), and again with DI water until all the residues were removed. The samples were dried at 80°C in an oven until constant mass was achieved.

3.6. References

1. Zdyrko, B.; Swaminatha Iyer, K.; Luzinov, I., Macromolecular anchoring layers for polymer grafting: comparative study. *Polymer* **2006,** *47* (1), 272-279.

2. Tsyalkovsky, V.; Burtovyy, R.; Klep, V.; Lupitskyy, R.; Motornov, M.; Minko, S.; Luzinov, I., Fluorescent nanoparticles stabilized by poly(ethylene glycol) containing shell for pH-triggered tunable aggregation in aqueous environment. *Langmuir* **2010,** *26* (13), 10684-10692.

3. Zdyrko, B.; Klep, V.; Luzinov, I., Synthesis and surface morphology of high-density poly (ethylene glycol) grafted layers. *Langmuir* **2003,** *19* (24), 10179-10187.

4. Henry, S. M.; El-Sayed, M. E. H.; Pirie, C. M.; Hoffman, A. S.; Stayton, P. S., pH-Responsive poly(styrene-alt-maleic anhydride) alkylamide copolymers for intracellular drug delivery. *Biomacromolecules* **2006,** *7* (8), 2407-2414.

5. L. Landau, B. L.; Acta Phys. Chim. USSR, Entrainment of fluid by the driven plate. *Acta Phys.-Chim* **1942,** *17* 42.

6. Crawford, L. J.; Edmonds, N. R., Calculation of film thickness for dip coated antireflective films. *Thin Solid Films* **2006,** *515* (3), 907-910.

7. Fujiwara, H., *Spectroscopic ellipsometry: principles and applications*. John Wiley & Sons: 2007.

8. Chu, P. K.; Chen, J. Y.; Wang, L. P.; Huang, N., Plasma-surface modification of biomaterials. *Materials Science and Engineering: R: Reports* **2002,** *36* (5–6), 143-206.

9. James D. Getty, M. P. S., Concord, Calif. *How plasma-enhanced surface modification improves the production of microelectronics and optoelectronics*.

10. http://www.harrricksci.com.

11. http://www.ramehart.com/contactangle.htm.

12. http://www.nobelprize.org/educational/physics/microscopes/fluorescence/.

13. Henn, G.; Bucknall, D. G.; Stamm, M.; Vanhoorne, P.; Jérôme, R., Chain end effects and dewetting in thin polymer films. *Macromolecules* **1996,** *29* (12), 4305-4313.

14. Krevelen, D. W. v.; Nijenhuis, K. t. Properties of polymers their correlation with chemical structure ; their numerical estimation and prediction from additive group contributions. http://site.ebrary.com/id/10305619.

15. Siqueira, D. F.; Kohler, K.; Stamm, M., *Langmuir* **1995,** *11* (null), 3092.

16. Sperling, L. H., *Introduction to physical polymer science*. Wiley. com: 2005.

17. Scanning Probe Microscopy: Training Notebook, D. I., Veeco Metrology Group, 2000, p.40.

18. Ramaratnam, K.; Tsyalkovsky, V.; Klep, V.; Luzinov, I., Ultrahydrophobic textile surface via decorating fibers with monolayer of reactive nanoparticles and non-fluorinated polymer. *Chemical Communications* **2007,** *0* (43), 4510-4512.

19. Heywood, a. D., Textile Finishing. *Society of Dyers and Colourists, UK* **2003**, p. 329.

20. Hsieh, Y.-L.; Miller, A.; Thompson, J., Wetting, pore structure, and liquid retention of hydrolyzed polyester fabrics. *Textile Research Journal* **1996,** *66* (1), 1-10.

21. Voncina, B., Vivod, V., *Application of cyclodextrins in textile dyeing.* In: Hauser PJ ed.; Rijeka:InTech, 2011.

CHAPTER FOUR

MODIFICATION OF THIN PET FILM WITH POLYMER LAYER VIA THE "GRAFTING TO" APPROACH

4.1. Introduction

Polyester (PET) has a widespread range of uses in many applications such as apparel, home furnishing, interior textiles, and medical textiles. It has outstanding chemical, physical and mechanical properties; however, some intrinsic properties (relative hydrophobicity and inertness) have been disadvantages and limiting factors for some applications.[1, 2] Thus, extensive studies have been conducted to obtain PET surfaces with increased wettability,[3, 4] moisture regain and antistatic properties,[4-6] dyeability,[7, 8] adhesivity,[9, 10] conductivity,[11] and biocompatibility.[12, 13] For many applications, it is vital to keep bulk PET material properties intact while adding functional properties to the surface. Such effect can be obtained by surface modification.

The surface properties of PET can be altered by physical or chemical treatments. For example, etching is one commonly used surface modification technique for polyester. Specifically for textile applications, hydrolytic etching with sodium hydroxide has been widely investigated, and applied at industrial levels to increase wettability, dyeability, and adhesivity.[5, 14-16] The effects of alkali treatment parameters (concentration, time, temperature, or presence of organic solvent) on material have been studied, and changes in surface chemistry have been reported.[15, 17, 18]

Alkali hydrolysis creates polar functional groups on the PET surface through a chain scission mechanism.[19] One consequence of the alkali treatment is weight loss of material due to the etching process, which may lead to the formation of surface cracks and voids.[20, 21]

Another broadly used technique for surface modification is plasma treatment.[22, 23] Plasma gas is composed of charged particles, radicals, and photons, and the interaction of these active species with the surface will modify only the upper layer, while leaving the bulk material properties unchanged.[24, 25] Similar to alkali treatment, plasma modification generates polar functional groups on PET surfaces by chain scission.[22, 23] Excessive chain scission can change the mechanical properties due to the formation of surface defects (voids and cracks) and increased roughness. Sometimes surface defects can be a desirable feature in various applications. For instance, the formation of micro roughness on ultra-high molecular weight poly ethylene (UHMWPE) fibers results in better mechanical interlocking of the fiber surface with the resin matrix.[26] Even though the surface defects can be an assistive feature for some applications, the process must be monitored and controlled since it may lead to deterioration of the mechanical properties.[27-29]

Having added features, such as super hydrophilicity–hydrophobicity, moisture management, and self-cleaning properties, requires the existence of different functionalities on the surface. Surface treatments (alkali and plasma) of PET introduce reactive functionality to the surface that can be utilized to tune the surface chemistry for the targeted application. An effective method for surface modification is the “grafting to” technique,[30, 31] which involves the covalent reaction between pre-synthesized, end-

functionalized polymer chains and the complementary surface functionality.[32] The chemical reaction between the surface and the polymer provides a stable coating (and properties) over a wide range of chemical, thermal, and environmental conditions. [33]

Abundant functionality and high reactivity of the surface towards various functional groups increases the number of polymers that could be grafted to the PET surface. To this end, epoxy containing polymer, poly(glycidyl methacrylate) (PGMA), was used as an anchoring layer in this study. The polymer demonstrated a high efficiency in grafting reactions due to the mobility of the epoxy units in the PGMA layer.[34-36] For example, Burtovyy et al. studied polymer grafting via the PGMA anchoring layer to a plasma activated PET film surface.[37, 38] Studies proved that the PGMA layer could be anchored to the PET film, and be utilized to graft hydrophobic and hydrophilic macromolecules to the PET surface.

Several surface analysis techniques can be used to study and understand the surface properties of polymer grafted substrates. For example, atomic force microscopy (AFM),[39, 40] contact angle measurement,[41] Fourier transform infrared spectroscopy (FTIR), and X-ray photoelectron spectroscopy (XPS)[42, 43] are used to understand the effect of the modification on the surface morphology, surface energy, and chemical composition, respectively. These techniques have been used for the surface analysis of textiles; however, in general, they are challenging and not practical for the systematic fundamental study of surface modification of textile materials due to possible manufacturing defects of textile substrates. To overcome the aforementioned challenges, researchers have developed model systems (typically flat and uniform polymer films) to

study the modification of textile materials.[35, 37, 44] Generally, the approach is to form a polymer film on a flat substrate, for instance, on a silicon wafer.[37] If a uniform and reproducible film can be generated on a flat surface, then the surface morphology and thickness of the grafted layers can be straightforwardly followed by AFM and ellipsometry, respectively.[45] For example, AFM and ellipsometry have been used for the thickness analysis of polymer films on silicon wafers.[45, 46] Many film characteristics (roughness, grafting density, and distance between grafting sites) can be calculated from the measured values.[37]

Burtovvy et al.[38, 47] have studied the modification of PET and nylon substrates with hydrophobic and hydrophilic polymers using model films deposited on silicon wafers. The coating approach developed for the film was applied to real materials: membranes and fabrics.[37, 38, 47] Iyer and coworkers conducted a study to evaluate grafting of anchoring polymer (PGMA) layer on silicon substrates, and demonstrated that the anchoring PGMA layer technique can be transferred to polymer surfaces, such as extruded PET films, to tune surface properties.[35] Motornov et al.[48] have studied the modification of polyamide substrates with polymer grafting on a model nylon film deposited on a silicon wafer. The study was then extended to a nylon textile material, and good agreement of wetting behavior between the modified film and fabric was demonstrated.

In this dissertation, model surface modification studies have been performed on PET films to be transferred later to the surface modification of the material of interest. Particularly, in this chapter, PET thin film formation on silicon wafers, surface activation

of the PET film, PGMA anchoring layer deposition, and surface modification of the PET film surface by grafting of a number of polymers are reported.

4.2. Experimental

Model film preparation was explained in **Section 3.5.1**. The crystalized PET film was treated to increase surface functionalities and enhance anchoring polymer adsorption and grafting onto the surface, in order to provide greater functionality. Two different treatment methods were applied in this study: alkali treatment and air plasma treatment.

Plasma activation was done at a low intensity level (6.8W). The exposure time was varied from 10 seconds to 70 seconds, and after the plasma, the treated samples were washed in methanol for approximately 10 minutes to remove residuals and ensure a clean surface. These experiments have been designed and followed to evaluate the effects of plasma exposure time on the PET film.

For the alkali treatment, the PET film was subjected to a 40 wt/vol % NaOH solution at room temperature to generate hydroxyl and carboxyl end groups. To evaluate the influence of the alkali treatment time, exposure time was varied from 30 seconds to 6 minutes, and to avoid film delamination, the alkali solution was placed dropwise in the middle of the film, avoiding the edges of the sample. After the alkali treatment, the samples were thoroughly washed with DI water to neutralize the surface and remove low molecular weight oligomers from the substrate.

Both the plasma and alkali treated surfaces were coated with an anchoring PGMA layer. The PGMA film was deposited on the plasma treated surface by dip coating from a

1 wt/vol % PGMA/MEK solution (PGMA, Mn ≈ 176,000 g/mol) and attachment was carried out at 60°C in a vacuum oven for 3 hours.

A Rhodamine B (RhB) labeled PGMA anchoring layer was also deposited on the hydrolyzed PET surface from a 0.5 wt/vol % PGMA-RhB (Mn ≈ 80,000 g/mol) solution in MEK by adsorption at 50°C for 3 h. The unattached polymer was rinsed with fresh MEK.

PAA (VWR, 1 wt/vol % in methanol), P2VP-COOH (Polymer Source Inc., 1 wt/vol % in THF), PEG-COOH (Sigma-Aldrich, 1 wt/vol % in methanol), PS-COOH (Polymer Source Inc., 1 wt/vol % in Toluene), and PSMA-h (Sigma-Aldrich, 1 wt/vol % in methanol) were deposited on the PGMA layer by drop casting, followed by annealing at 120°C for 1 h, 120°C for 2 h, 120°C for 3 h, 150°C for 100 min, and 120°C for 1 h, respectively. To avoid dewetting during the annealing, 0.1% ultrahigh-molecular nonreactive PEO (Sigma-Aldrich, Mn 1000000) was added to the PEG-COOH solution.

Water contact angle and thickness measurements were performed to confirm surface activation as well as effect of polymer coating on the wetting characteristics of the PET film, and determine the influence of the plasma exposure or alkali activation time on the film thickness. AFM studies were carried out to evaluate morphological changes on the surface after the treatment. For ellipsometric measurements, the refractive index for the polymer layers was set to 1.5.

4.3. Results and discussion

4.3.1. Fabrication of model PET film

In order to develop a methodology for fabric coating, experiments have been conducted on a model thin PET film that was deposited on a silicon wafer. This model film enables us to measure grafted polymer layer thicknesses and morphology. The silicon wafer has been particularly selected (over the glass slide) as a supportive substrate for the model thin PET film, since it has the reflective surface that is required for ellipsometric studies. In addition, the wafer has very low surface roughness, less than 0.1 nm, so it is possible to follow changes in the surface roughness after modification with polymer layers.

The dip coating technique has been used for the formation of a uniform PET layer on a silicon wafer, and PET films with ~69 nm and ~43 nm thicknesses were obtained. The RMS roughness of the deposited films was 0.3 nm for both the 10x10 and 1x1 micron area images. An AFM analysis of the deposited PET film **(Figure 4.1)** indicated uniform surface coverage on both the nano and micro scale. Homogeneity of the film is important, since it influences the overall surface properties, such as roughness and wettability.

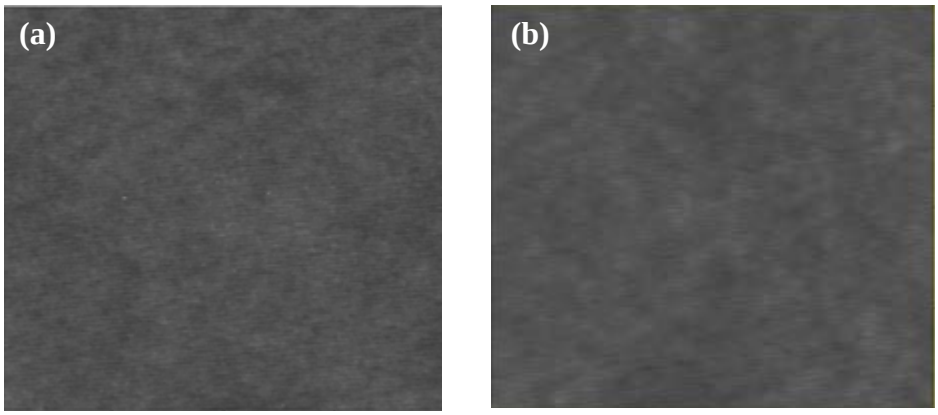

Figure 4.1. Topographical AFM images of the PET films (69 nm) deposited on the silicon substrate using the dip coating technique. (a) and (b) 10x10 and 1x1 micron images, respectively. The vertical scale is 10 nm.

AFM morphology **(Figure 4.1)** of the deposited PET film revealed that when the film was formed by dip coating from solution, smooth and homogenous surfaces were obtained without any crystal formation. However, it is well known that PET is a semi-crystalline material.[37, 49, 50] In fact, PET textiles are made of fibers that are crystallized upon cooling during the manufacturing process that involves extrusion, spinning, and drawing.[49, 51] Since the PET film here is formed to represent a real PET fibrous material, it is necessary to form a crystal structure in the film for the best representation of the PET fabric. The importance of using semi-crystalline film for this study comes from the fact that surface activation will occur at a different rate in amorphous regions than in crystal regions. In fact, the PET surface activation techniques are based on the etching of the surface. Etching is a kinetic process and was reported to occur at a slower rate in the crystalline part than in the amorphous part of the PET material.[35, 52-54] Thus, it is apparent that PET surface activation can result in not only the formation of pits, cracks, and voids,

but also change the roughness and morphology at nano scale.[35, 37] Consequently, it will influence the wettability of the grafted layer. Therefore, a model film of a semi-crystalline nature should be used in our model studies for a better understanding of the effects of the coatings.

In order to form a crystal structure, the film had to be heated above the glass transition temperature to allow the polymer chains to rearrange themselves and form crystals. Therefore, the thermal transitions for the PET material should be known. The thermal transitions of the PET chips used in this study were determined by differential scanning calorimetry (DCS). PET has a glass transition at ~65^{o}C, a melting point at ~235^{o}C, and a crystallization temperature of 120^{o}C **(Figure 4.2)**. The glass transition region of the PET film on a silicon wafer has been reported previously to be between 70^{o}C and 90^{o}C as measured by AFM analysis.[37] Hence, the PET film was annealed in a vacuum oven at 140^{o}C, above its glass transition temperature, for 3 hours. AFM analysis confirmed crystal formation on the film surface after the annealing **(Figure 4.3)**.

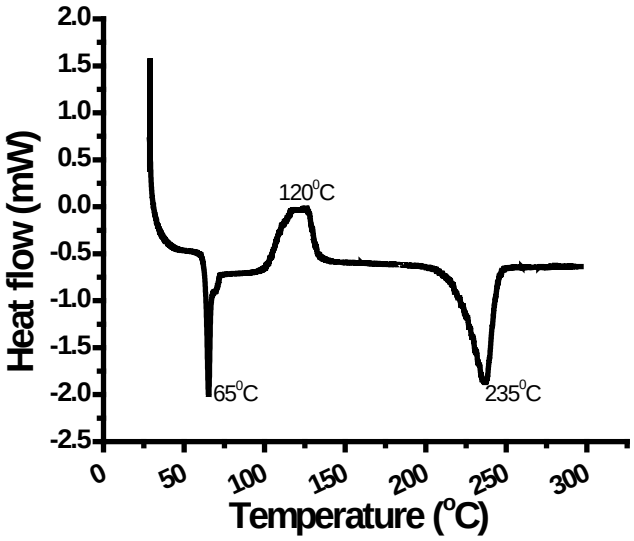

Figure 4.2. DCS thermal analysis of PET chips.

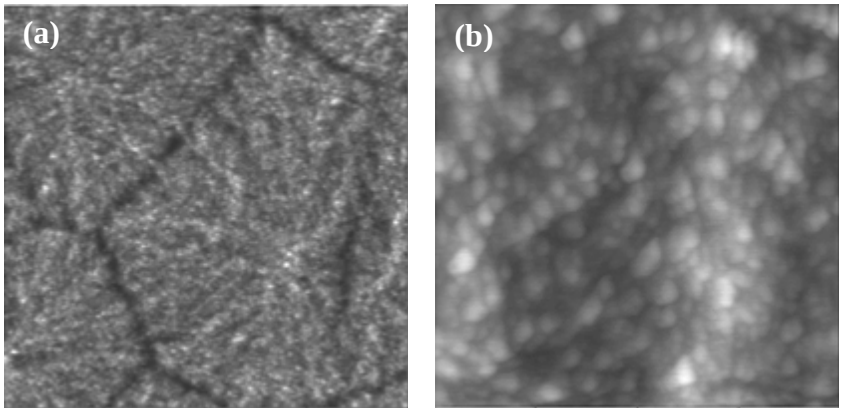

Figure 4.3. Topographical AFM images of the deposited PET film (69 nm) after annealing at 140°C for 3 hours. (a) and (b) 10x10 and 1x1 micron images, respectively. The vertical scale is 20 nm.

RMS surface roughness of the annealed PET film (69 nm) increased from 0.3 nm to ~2.6 nm and 2.3 nm for 10x10 and 1x1 micron scale images, respectively. The roughness change is attributed to crystal formation, and these results indicate that film

formed in this study can be used as a model surface for the systematic characterization of a polymer layer to be grafted to the PET fabric surface.

4.3.2. Surface modification of PET film with alkali treatment

Throughout this research, PGMA was used as an anchoring layer for the chemical modification of the surface using polymer grafting. The PGMA is capable of generating strong covalent interactions with a wide variety of substances (polymeric or inorganic surfaces) that have complementary functional groups, such as carboxy, hydroxy, amino, thiol, and anhydride.[55] However, the low level of surface functionality on virgin PET surfaces requires introducing functional groups to the PET surface to improve its binding activity.[56, 57]

Therefore, in order to enhance the PGMA binding efficiency to the PET (after formation of semi crystalline film), the surface was activated with plasma or alkali treatments. For a modification of the PET surface, plasma treatment, in general, is more popular for film or membrane surfaces,[22, 58-61] while alkali treatment is usually chosen for fibrous material surface modification.[14-18]

The hydrolysis of PET in aqueous NaOH occurs with the cleavage of ester linkages of the PET chains **(Figure 4.4).**[62] Hydrolysis assures increased surface functionality, but also, it degrades the PET surface and eventually leads to changes in surface morphology.[15, 17, 18] Alkali hydrolysis on the PET fabric surface has been reported to decrease weight and result in the formation of uneven cracks and voids on the fiber surface. Such morphology could lead to uneven polymer coating, and ultimately

influence wetting behavior of the surface. Thus, for this study, it is essential to select hydrolysis conditions to prevent extensive degradation of the surface.

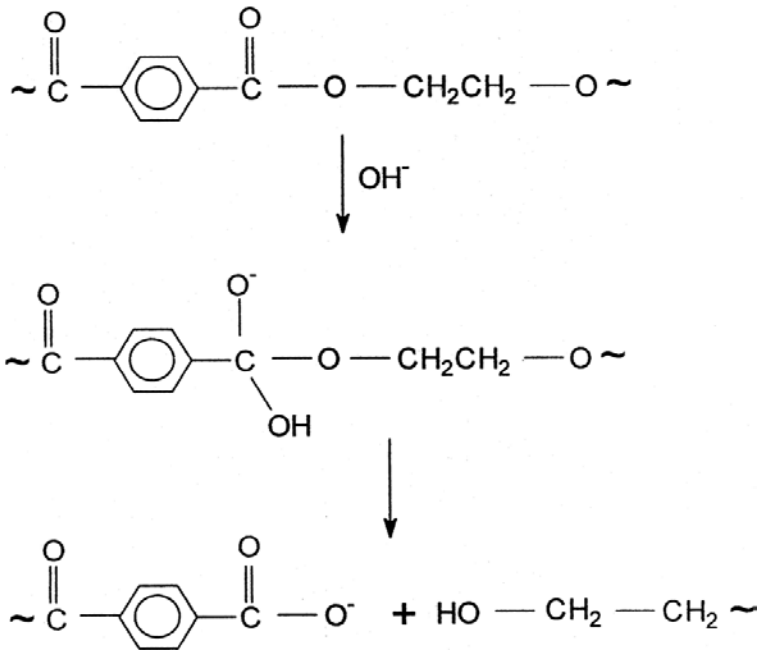

Figure 4.4. Cleavage of ester linkages of PET chains in an alkali environment.[62]

The effects of the NaOH treatment time on the PET film surface were systematically investigated. The thickness of the original dip-coated and annealed PET film was ~43 ± 1.0 nm. Ellipsometric thickness measurements indicate that the layer thickness was decreased by the alkali treatments, suggesting that hydrolytic etching had taken place. Changes in thickness versus alkali treatment time are plotted in **Figure 4.5a** for the originally ~43 nm thick films. The thickness change was 4 nm for 2 min of treatment, and surface degradation increased as alkali treatment time increased. In fact, the thickness changes after 2 min of treatment were significant. Namely, complete

degradation of the film was observed after 3 min of treatment. These results were in good agreement with previously reported studies in the literature for films[35] and fabrics.[15, 18]

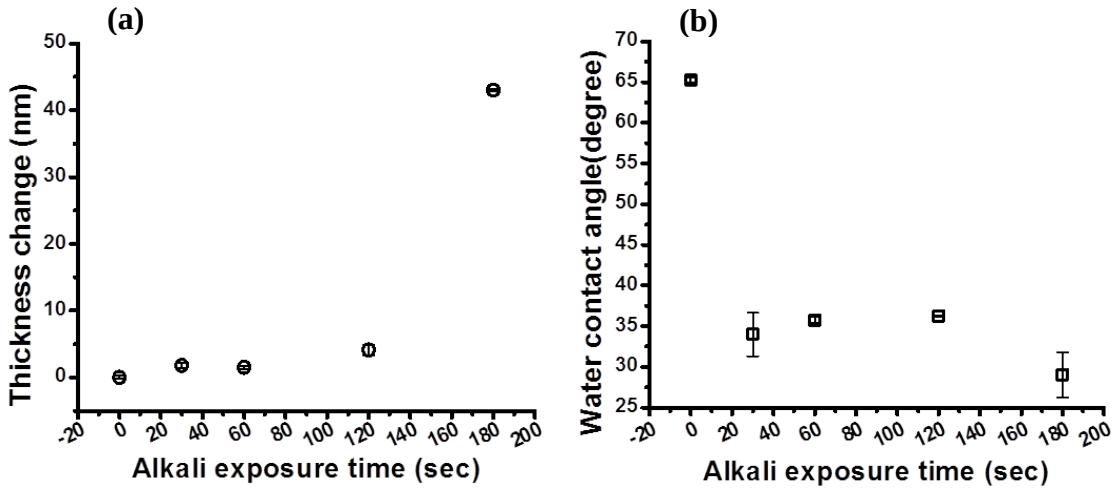

Figure 4.5. Effect of alkali treatment time on semi-crystalline PET film (43 nm thick). (a) Thickness change with change in alkali treatment time. (b) Water contact angle of the alkali treated surface at different times of alkali exposure.

The water contact angle of the PET film decreased to ~35^0 and lower after the treatment with the alkali solution **(Figure 4.5b)**. Reasons for the low contact angle can be explained by the occurrence of following events:[5] (a) increased number of polar groups due to chain scission, and (b) the increased roughness of the surface. A slight decrease in wettability for the 1 min and 2 min treatment times could be explained by two parallel events: the increasing number of polar groups by etching, and the removal of the etching residues from the surface. As the time of treatment increases, more oligomers with reactive ends are formed. Then, as a consequence of the rinsing process they are removed from the surface, thus, the surface ends up having a lower number of polar groups.

AFM images **(Figure 4.6)** of the hydrolyzed surface demonstrate that the semi crystalline structure remained intact and that the treatment was uniform. There were no significant changes in roughness.

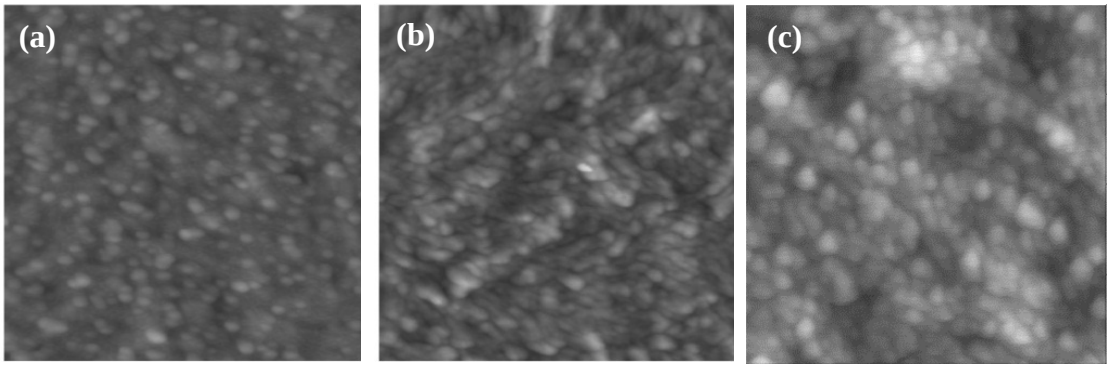

Figure 4.6. Topographical AFM images of the PET films (43 nm initial thickness) that were exposed to alkali treatments for (a) 30 sec, (b) 1 min, and (c) 2 min at room temperature. Images are 1x1 um, and the vertical scale is 20 nm.

4.3.3. Surface treatment of PET film by plasma modification

Another activation method that was employed in this study was plasma treatment. Etching with plasma occurs at the outermost part of the surface by producing surface oligomers. When the surface is rough, such as in fabric, the effects of plasma are more superficial when compared to alkali treatments since the plasma ions may not be able to diffuse and reach the inner fibers of the yarn. However, during hydroxide treatment, the solution can wick into the fabric and reach individual fibers.

Hwang et al. studied plasma interactions with polymeric substrates, and reported potential chemical interaction sites in the PET chain as demonstrated in **Figure 4.7**.[63] As reported in the literature, air plasma interacts with the CH_2 and phenyl rings **(Figure**

4.8).[37, 64] In fact, similar to hydrolysis, during plasma treatment two simultaneous events occur: oxidation and etching. It is important to control and optimize plasma treatment conditions to obtain reproducible surface of the PET film. Therefore, the model PET films after the plasma exposure were analyzed using ellipsometry and contact angle.

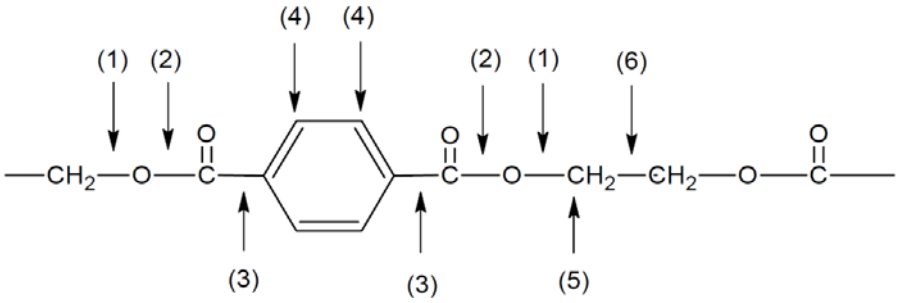

Figure 4. 7. Potential chemical interaction positions in PET chains.[56]

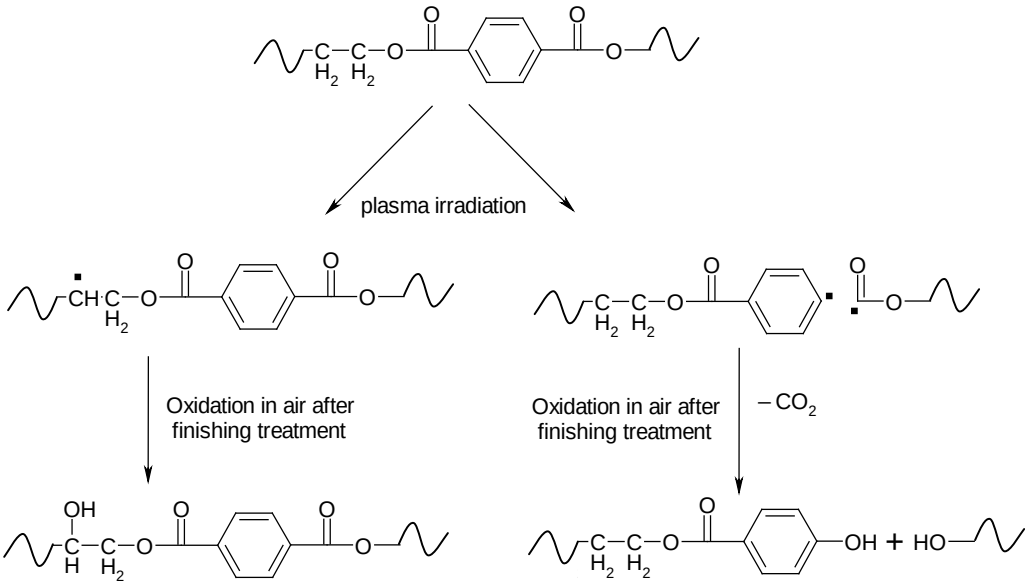

Figure 4.8. Plasma modification of PET chain. Air plasma interacts with the CH_2 and phenyl rings.[37, 64]

The thickness of the film was decreased after the plasma exposure, with the change in thickness being higher at longer treatments, reaching 8 nm decrease after 70 seconds **(Figure 4.9a)**. The decrease in the water contact angle suggests an increase in the hydrophilicity that is associated with the formation of hydrophilic polar groups **(Figure 4.9b)**. Wettability increases and reaches ~ 40^{o} after the 40 seconds of plasma exposure, and a slight decrease in the wettability was observed when treatment time is longer than 40 seconds. Similar relationships (increase then slight decrease in wettability with plasma application time) have also been observed previously by other scientists.[35, 37]

It has been deduced from the analysis of the thicknesses and WCA changes that when the plasma application is longer than 40 seconds, etching starts to dominate over surface activation. Therefore, 40 seconds of the plasma treatment time has been selected to employ for further study.

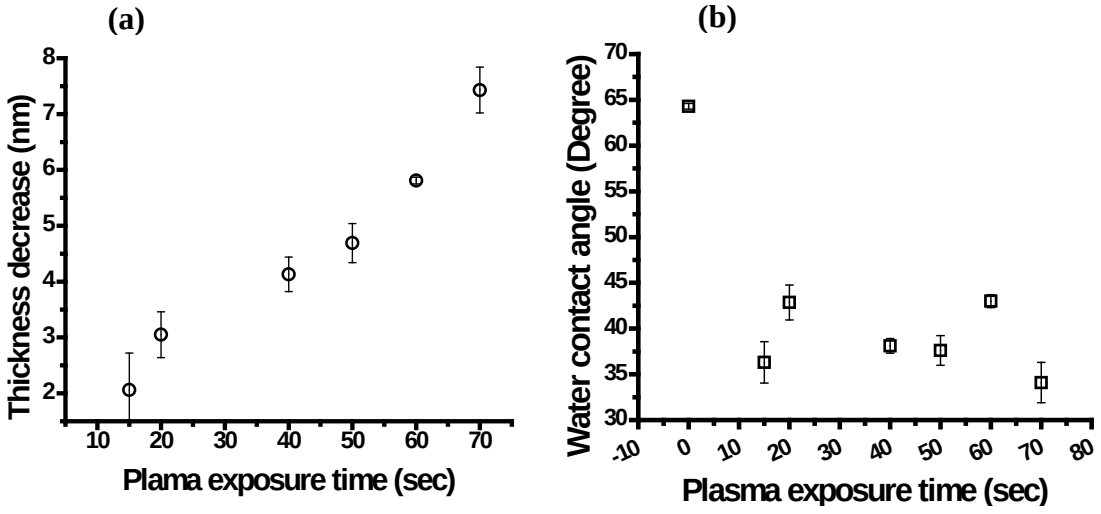

Figure 4.9. Effect of plasma exposure time on semi crystalline PET film (43 nm). (a) Thickness decrease. (b) Water contact angle.

The AFM images **(Figure 4.10)** show the morphology of film after the plasma treatment at different times. It was reported in the literature that the etching rate during plasma treatment is different in the amorphous part than the crystalline part;[35] therefore, it is reasonable to expect changes in the film roughness after the plasma treatment. However, no significant relationship between the roughness and the time of exposure was observed in this study. We suggest that the exposure time was not high enough to reveal the differences in the in RMS values. In fact, Burtovyy et al. also reported that roughnesses do not change significantly at low exposure time, and found only a 0.1 nm increase in the RMS roughness after the 40 seconds of plasma treatment.[37] It is also clear from the AFM images that the crystal structure after the plasma treatment was preserved, the treatment was uniform throughout the sample, and that the plasma did not destroy the film **(Figure 4.10)**.

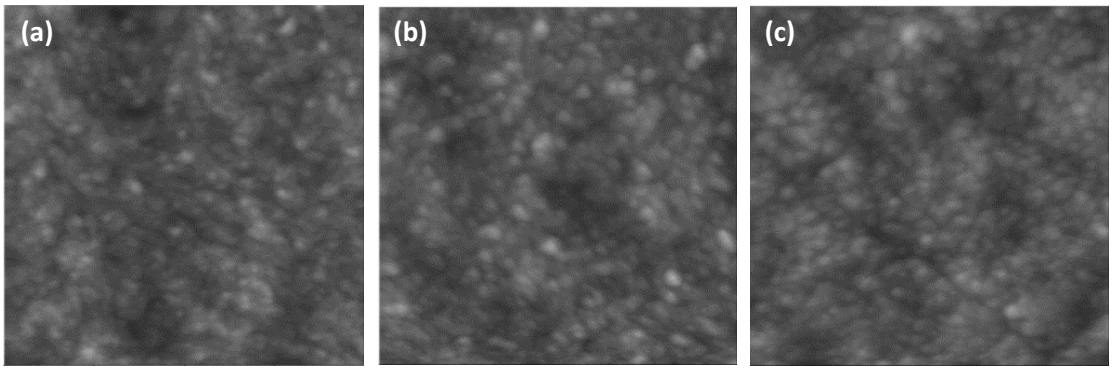

Figure 4.10. Topographical AFM images of the PET films (43 nm) exposed to plasma treatment for (a) 20 sec, (b) 40 sec, and (c) 60 sec at room temperature. The images are 1x1 um and the vertical scale is 20 nm.

The optimal treatment conditions were found to be 40 seconds of the plasma (6.8 W), and 2 min of the alkali treatments at room temperature. These conditions have very similar effects on the surface in terms of thickness change (~4 nm) and contact angle (~40^{o}). When these conditions are applied for the modification of a fiber surface, they will not change the bulk properties of the fibers.

4.3.4. PGMA anchoring layer deposition on the PET film surface

We studied the deposition of the PGMA layer by adsorption from the MEK solution on the model PET film treated with NaOH. For the anchoring of PGMA, the surface should have a sufficient amount of complementary groups that can be reached by the epoxy groups of the PGMA. For the PET film, the carboxyl and hydroxyl groups that were formed on the surface after the surface activation are capable of reacting with the epoxy groups of the PGMA. The reactive epoxy layer can, indeed, be deposited on the PET surface using this method.

It needs to be confirmed that during PGMA deposition from solution, the solvent does not age or remove the carboxyl groups from the surface. Thus, the influence of the solvent (for PGMA) on the surface of the film has been evaluated. After hydrolysis, the samples were washed with methanol to remove the oligomers that formed after chain scission. The water contact angle of this film was 36^{o}. Then, the hydrolyzed and methanol washed film was washed with chloroform or MEK. It was observed that the wettability of the surface decreased to $51^{0}\pm0.6^{0}$ after the chloroform wash, while it stayed the same after the MEK wash ($36.8^{0}\pm0.2^{0}$). Higher wettability indicates a greater number

of surface complementary groups available for PGMA grafting. Thus, for all PGMA deposition, MEK was used as a solvent.

4.3.4.1. Anchoring layer deposition on the alkali treated PET surface

The PGMA anchoring layer was deposited on the hydrolyzed PET film (65 nm), from a 0.5 wt/vol % PGMA-RhB solution in MEK, by adsorption at 50°C for 3 h. The unattached polymer was rinsed off with fresh MEK. A change in the water contact angle from 36° to 53° upon PGMA chemisorption confirmed deposition of the epoxy-containing polymer to the surface. In addition, deposition was also confirmed with ellipsometric measurements. The thickness of the PGMA layer deposited to the PET model film was determined to be 2.9±0.3 nm.

The surface coverage (Γ), the PGMA chain density (Σ), and the surface concentration of the epoxy groups present on the surface of the functionalized PET film (epoxy groups/nm^2 = ΣN, where N is the degree of PGMA polymerization, N ≈ 560) were estimated as described elsewhere.[65] Γ = 3.1 mg/m^2, Σ = 0.024 chain/nm^2, and the surface concentration of the epoxy groups ≈13 groups/nm^2 were obtained. The modification of the model substrate with a PGMA layer did not significantly alter the surface morphology of the PET film as represented by AFM images **(Figure 4.11)**. The PGMA layer was homogeneously anchored without dewetting, and the RMS roughness of the film after the PGMA deposition did not change.

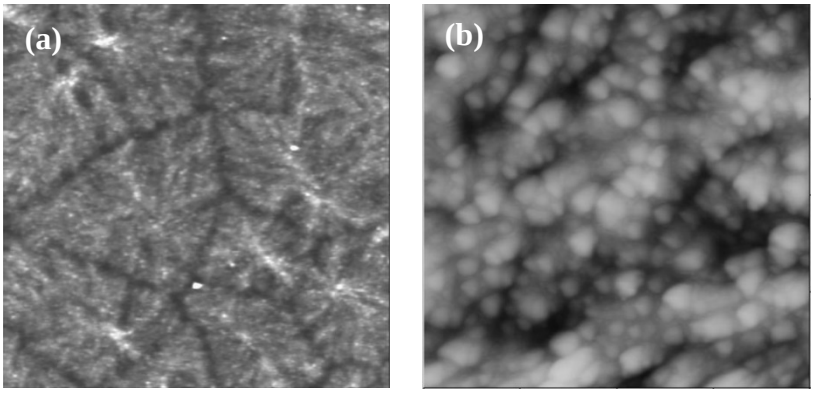

Figure 4.11. Topographical AFM images of the PGMA/PET film. PGMA was deposited on the alkali treated PET film (65 nm) by adsorption at 50^0C for 3 hrs. (a) 10x10 micron, (b) 1x1 micron images. Vertical scale: 20 nm.

4.3.4.2. Anchoring layer deposition on the plasma treated PET surface

The PGMA (Mw 176.000 g/mol) deposition by dip coating was also studied for the plasma activated PET film (~43 nm). Using the dip coating technique, a thicker PGMA layer (~80-90 nm) was deposited. This was done since one can speculate that the film deposited by the dip coating deposition technique will be relatively thick on a fibrous surface, when compared to the thickness of the film on a flat surface, due to the tightly packed dense weave structure of the fabric. The deposited layer was then annealed in a vacuum oven for 3 hours at 60^oC (slightly below the Tg of PGMA, 65-70 ^{o}C) for anchoring. With this technique, less than 10% of the deposited film (6-7 nm) was attached onto the surface. This thickness corresponds to the calculated parameters of Γ = 6.5 mg/m^2, Σ = 0.02 chain/nm^2, and the surface concentration of the epoxy groups ≈27 groups/nm^2. Therefore, it can be concluded that the thick layer deposition and low temperature annealing methodology for grafting can be used as a model for PGMA

anchoring layer formation on the fabric surface. The water contact angle of the PGMA layer was ~55^0, and a uniform coating was achieved as the AFM images represent **(Figure 4.12)**. RMS roughness of the film after the PGMA deposition did not change significantly. RMS roughness is 2 nm , and 1.3 nm for 10x10 and 1x1 images, respectively.

4.3.5. Surface modification of the PET film via "grafting to" approach

Different polymers that have functional groups complementary to epoxy have been grafted using the PGMA layer in order to confirm that the polymers can be grafted onto the PET fiber surface using the anchoring layer. The details of the polymer layer synthesis and analysis of the polymer layer will be reported in the next chapters. **Table 4.1** shows the parameters of the grafted layers. The properties of the polymers used for grafting are given in **Table 4.2**.

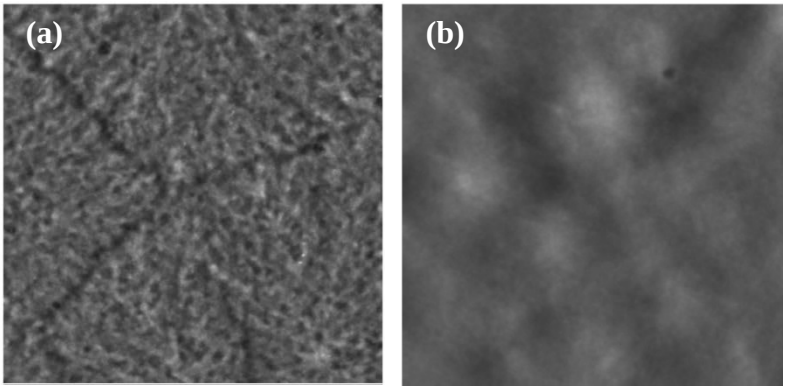

Figure 4.12. Topographical AFM images of the PGMA/PET film. PGMA was deposited on the plasma treated PET film (43 nm) by dip coating and annealed in 60^0C vacuum oven for 3 hrs. (a) 10x10 micron, (b) 1x1 micron images. Vertical scale: 20 nm.

Table 4.1. Grafting parameters of the polymer layers on the PET film. PS-COOH was grafted through a ~3 nm PGMA(M_n ≈176.000) layer, and PAA, P2VP-COOH, PSMA-h, and PEG-COOH were grafted through a ~3 nm PGMA(M_n ≈80.000) layer on a 65 nm NaOH treated PET film.

Grafted polymer layer	Thickness (nm)	Surface coverage (mg/m^3)	Chain density ($chains/nm^2$)
PEG	6.7±0.8	7.30	0.88
PAA	7.3±1.2	8.32	0.05
PVP	11±0.9	12.87	0.15
PSMA-h	7.6±0.6	9.65	0.02
PS	11	11.55	0.14

Table 4. 2. Parameters of the polymer used for grafting.

Grafted polymer layer	Number average molecular weight (g/mol)	Density (g/cm^3)
PGMA(80.000)	80000	1.08
PEG	5000	1.09
PAA	100000	1.14
PVP	53000	1.17
PSMA-h	350000	1.27
PS	48000	1.05
PGMA(176.000)	176000	1.08

The modification with polymer grafting changed the wettability of the surface by water that is attributed to the successful modification of PET with the mentioned polymers **(Figure 4.13)**. Among the grafted polymers, PS-COOH is the most hydrophobic and gave the highest water contact angle ($87±1^0$) when grafted to the film. These results are in good agreement with the previously reported data. Iyer et al.[35] studied

PS-COOH grafting via the PGMA anchoring layer to a PET surface with the "grafting from" technique, and reported a contact angle between 70^0 and 90^0 for the PS layer when thickness of the film is changing from 3 nm to 19 nm.

PSMA-h, PEG-COOH, PAA, and P2VP-OOH are the more hydrophilic polymers, and thus, a lower contact angle was observed. Among those, the PAA layer was the most hydrophilic one, and therefore, the water contact angle for the grafted layer on the PET was the lowest (~17^0). A strong relationship between the wettability and the thickness of the PAA layer was reported, which is ultimately related with the time and temperature of the grafting.[37] Another hydrophilic polymer that was grafted was PEG-COOH, and a 55^0 water contact angle was observed for the ~7 nm PEG layer. A lower contact angle (25-30^0) was reported in the literature.[66] We suggest that the high contact angle in our case could be explained with the formation of crystals. Iyer[35] reported water contact angle (WCA) of the PEG layer between ~35^0 and 45^0, with the WCA decreasing with the increasing amount of polymer grafting thickness. He did not conclude any relationship between the WCA and the crystallinity of PEG grafted layer; however, it was shown that the grafting thickness and the grafting density increased with the grafting time. A decrease in the density of the crystal domains with the increasing grafting time was also observed. Zdyrko et al.[32] reported a high water contact angle (58^0) for the thin PEG layer (3 nm), and a low contact angle for the thick PEG layer (9 nm-10 nm). It was suggested that the scattering of the WCA at intermediate thicknesses can be explained by the non-equilibrium wetting of the PEG crystals.

AFM images showed that the surface morphology of the PET film was altered by the grafting of the polymers **(Figure 4.14)**. The grafted polymer layers evenly covered the PET surface on micro- and nano-scale levels, and as reported previously in similar experiments, the PEG-grafted layers **(Figure 4.14 e, g)** formed crystalline structures on the surface.[32, 34, 36, 67]

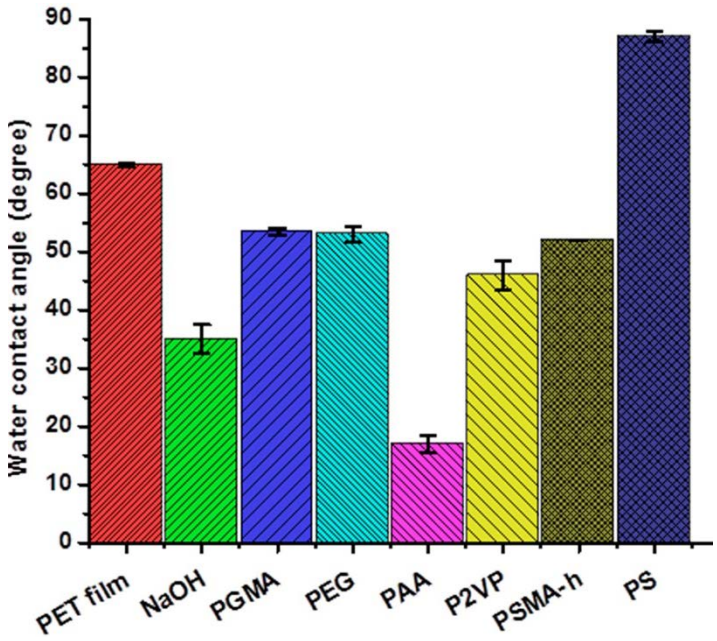

Figure 4.13. Water contact angle of polymer coated PET film surface. PS-COOH was grafted through a ~3 nm PGMA(M_n ≈176.000) layer, and PAA, P2VP-COOH, PSMA-h, and PEG-COOH were grafted through a ~3 nm PGMA(M_n ≈80.000) layer on a 65 nm NaOH treated PET film.

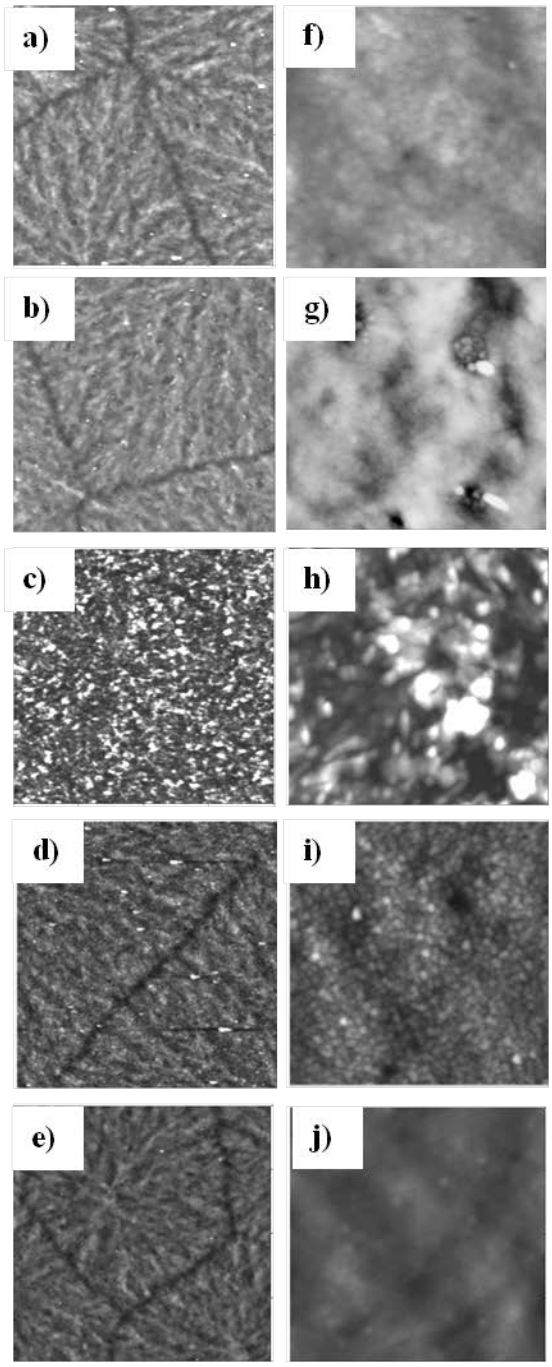

Figure 4. 14. Topographical AFM images of the PET film modified with a PGMA layer and grafted with P2VP (a, f) PAA, (b, g), PEG (c, h), PSMA-H (d, i), and PS (e, j). Vertical scale: 20 nm. Image size: (a, b, c, d, e) 10x10 and (f, g, h, i, j) 1x1 microns. PS-COOH was grafted through a ~3 nm PGMA(M_n ≈176.000) layer, and PAA, P2VP-COOH, PSMA-h, and PEG-COOH were grafted through a ~3 nm PGMA(M_n ≈80.000) layer on a 65 nm NaOH treated PET film

4.4. Conclusion

The model PET films on a silicon wafer were successfully fabricated. AFM studies indicated that initially deposited PET films were homogenous without presence of crystal formation. Crystals formed in the film after the annealing above its glass transition temperature. A reactive layer was formed on the PET film by plasma or alkali treatments. 40 sec plasma and 2 min alkali treatment have the similar effect on surface in terms of wettability, thickness change as well as PGMA layer formation.

Then, the anchoring polymer layer was deposited to obtain a highly reactive layer with a significant number of epoxy groups. The anchoring layer deposition was done by both dip coating and adsorption. Different polymers were then grafted to the surface via the “grafting to” technique through covalent bonding between the polymer and epoxy groups. The modification of the polymers is permanent due to the covalent bonding between the epoxy and the polymeric functional unit. With the grafting of different polymers, the wetting behavior of the film was changed.

4.5. References

1. Jiao, Y.-P.; Cui, F.-Z., Surface modification of polyester biomaterials for tissue engineering. *Biomedical Materials* **2007,** *2* (4), R24.

2. Vert, M.; Li, S. M.; Spenlehauer, G.; Guerin, P., Bioresorbability and biocompatibility of aliphatic polyesters. *J Mater Sci: Mater Med* **1992,** *3* (6), 432-446.

3. Öktem, T.; Ayhan, H.; Seventekin, N.; Piskin, E., Modification of polyester fabrics by in situ plasma or post-plasma polymerisation of acrylic acid. *Coloration Technology* **1999,** *115* (9), 274-279.

4. Gotoh, K.; Yasukawa, A., Atmospheric pressure plasma modification of polyester fabric for improvement of textile-specific properties. *Textile Research Journal* **2011,** *81* (4), 368-378.

5. Sanders, E. M.; Zeronian, S. H., An analysis of the moisture-related properties of hydrolyzed polyester. *Journal of Applied Polymer Science* **1982,** *27* (11), 4477-4491.

6. Kan, C. W.; Yuen, C. W. M., Static properties and moisture content properties of polyester fabrics modified by plasma treatment and chemical finishing. *Nuclear instruments and methods in physics research section B: beam interactions with materials and atoms* **2008,** *266* (1), 127-132.

7. Lau, K.; Chan, P.; Yeung, K.; Chan, K.; Gong, W., Surface properties of polyester fabrics induced by excimer laser processing. *Journal of materials processing technology* **1997,** *63* (1), 524-528.

8. Lehocký, M.; Mráček, A., Improvement of dye adsorption on synthetic polyester fibers by low temperature plasma pre-treatment. *Czechoslovak Journal of Physics* **2006,** *56* (2), B1277-B1282.

9. Leroux, F.; Campagne, C.; Perwuelz, A.; Gengembre, L., Atmospheric air plasma treatment of polyester textile materials. Textile structure influence on surface oxidation and silicon resin adhesion. *Surface and Coatings Technology* **2009,** *203* (20–21), 3178-3183.

10. Chappell, P. J. C.; Brown, J. R.; George, G. A.; Willis, H. A., Surface modification of extended chain polyethylene fibres to improve adhesion to epoxy and unsaturated polyester resins. *Surface and Interface Analysis* **1991,** *17* (3), 143-150.

11. Lin, T.; Wang, L.; Wang, X.; Kaynak, A., Polymerising pyrrole on polyester textiles and controlling the conductivity through coating thickness. *Thin Solid Films* **2005,** *479* (1–2), 77-82.

12. El-Gabry, L. K.; Allam, O. G.; Hakeim, O. A., Surface functionalization of viscose and polyester fabrics toward antibacterial and coloration properties. *Carbohydrate Polymers* **2013,** *92* (1), 353-359.

13. Chang, Y.-B.; Tu, P.-C.; Wu, M.-W.; Hsueh, T.-H.; Hsu, S.-h., A study on chitosan modification of polyester fabrics by atmospheric pressure plasma and its antibacterial effects. *Fibers and Polymers* **2008,** *9* (3), 307-311.

14. A. Bendak, S. M. E.-M., Effects of chemical modifications on polyester fibres. *Journal of Islamic Academy of Sciences* **1991,** *4* (4), 275-284.

15. Kish, M. H.; Nouri, M., Effects of sodium hydroxide and calcium hydroxide on polyester fabrics. *Journal of Applied Polymer Science* **1999,** *72* (5), 631-637.

16. Dave, J.; Kumar, R.; Srivastava, H. C., Studies on modification of polyester fabrics I: Alkaline hydrolysis. *Journal of Applied Polymer Science* **1987,** *33* (2), 455-477.

17. Rahman, M.; Alfaro, M., Degradation of polyester geotextiles in alkaline solutions under applied loading. In *Proceedings of the 57th Canadian Geotechnical Conference*, 2004; pp 33-39.

18. M.Dhinakaran, B. S. D., V.Subramaniam, A new method of investigating the structure by weigh loss of polyester fibers. *JTATM* **2010,** *6* (3).

19. Venkatachalam, S.; Nayak, S. G.; Labde, J. V.; Gharal, P. R.; Rao, K.; Kelkar, A. K., *Degradation and recyclability of poly (ethylene terephthalate)*. **2012**.

20. Kim, H.; Song, W., Lipase treatment of polyester fabrics. *Fibers and Polymers* **2006,** *7* (4), 339-343.

21. Zeronian, S. H.; Collins, M. J., Surface modification of polyester by alkaline treatments. *Textile Progress* **1989,** *20* (2), 1-26.

22. Egitto, F. D.; Matienzo, L. J., Plasma modification of polymer surfaces for adhesion improvement. *IBM Journal of Research and Development* **1994,** *38* (4), 423-439.

23. M. France, R.; D. Short, R., Plasma treatment of polymers: Effects of energy transfer from an argon plasma on the surface chemistry of poly(styrene), low density poly(ethylene), poly(propylene) and poly(ethylene terephthalate). *Journal of the Chemical Society, Faraday Transactions* **1997,** *93* (17), 3173-3178.

24. Hamerli, P.; Weigel, T.; Groth, T.; Paul, D., Surface properties of and cell adhesion onto allylamine-plasma-coated polyethylenterephtalat membranes. *Biomaterials* **2003,** *24* (22), 3989-3999.

25. Hochart, F.; De Jaeger, R.; Levalois-Grützmacher, J., Graft-polymerization of a hydrophobic monomer onto PAN textile by low-pressure plasma treatments. *Surface and Coatings Technology* **2003,** *165* (2), 201-210.

26. Ionov, L.; Sidorenko, A.; Stamm, M.; Minko, S.; Zdyrko, B.; Klep, V.; Luzinov, I., Gradient mixed brushes: ``grafting to" approach. *Macromolecules* **2004,** *37* (19), 7421-7423.

27. Russell, T. P., Surface-responsive materials. *Science* **2002,** *297* (5583), 964-967.

28. Ito, Y.; Ochiai, Y.; Park, Y. S.; Imanishi, Y., pH-Sensitive gating by conformational change of a polypeptide brush grafted onto a porous polymer membrane. *J. Am. Chem. Soc.* **1997,** *119* (7), 1619-1623.

29. Ionov, L.; Minko, S.; Stamm, M.; Gohy, J. F.; Jerome, R.; Scholl, A., Reversible chemical patterning on stimuli-responsive polymer film: Environment-responsive lithography. *J. Am. Chem. Soc.* **2003,** *125*, 8302-8306

30. Brittain, W. J.; Minko, S., A structural definition of polymer brushes. *Journal of Polymer Science Part A: Polymer Chemistry* **2007,** *45* (16), 3505-3512.

31. Zhao, B.; Brittain, W. J., Polymer brushes: Surface-immobilized macromolecules. *Progress in Polymer Science* **2000,** *25* (5), 677-710.

32. Zdyrko, B.; Varshney, S. K.; Luzinov, I., Effect of molecular weight on synthesis and surface morphology of high-density poly (ethylene glycol) grafted layers. *Langmuir* **2004,** *20* (16), 6727-6735.

33. Luzinov, I.; Julthongpiput, D.; Malz, H.; Pionteck, J.; Tsukruk, V. V., Polystyrene layers grafted to epoxy-modified silicon surfaces. *Macromolecules* **2000,** *33* (3), 1043-1048.

34. Ionov, L.; Zdyrko, B.; Sidorenko, A.; Minko, S.; Klep, V.; Luzinov, I.; Stamm, M., Gradient polymer layers by “grafting to” approach. *Macromolecular rapid communications* **2004,** *25* (1), 360-365.

35. Swaminatha Iyer, K. L. Multifunctional nanolayers via polymer brush approach: Synthesis and characterization. Dissertation, Clemson University, 2004.

36. Zdyrko, B. Thin polymer films for biomedical applications: Synthesis and characterization. Dissertation, Clemson University, 2005.

37. Burtovyy, O. Synthesis and characterization of macromolecular layers grafted to polymer surfaces. Dissertation, Clemson University 2008.

38. Burtovyy, O.; Klep, V.; Chen, H. C.; Hu, R. K.; Lin, C. C.; Luzinov, I., Hydrophobic modification of polymer surfaces via “grafting to” approach. *Journal of Macromolecular Science, Part B* **2007,** *46* (1), 137-154.

39. Hsieh, Y.-L.; Miller, A.; Thompson, J., Wetting, pore structure, and liquid retention of hydrolyzed polyester fabrics. *Textile Research Journal* **1996,** *66* (1), 1-10.

40. Fries, N.; Dreyer, M., An analytic solution of capillary rise restrained by gravity. *Journal of colloid and interface science* **2008,** *320* (1), 259-263.

41. Washburn, E. W., The dynamics of capillary flow. *Physical Review* **1921,** *17* (3), 273-283.

42. Wenzel, R. N., Resistance of solid surfaces to wetting by water. *Industrial & Engineering Chemistry* **1936,** *28* (8), 988-994.

43. Young, T., An essay on the cohesion of fluids. *Philosophical Transactions of the Royal Society of London* **1805,** *95*, 65-87.

44. Ramaratnam, K. Ultrahydrophobic surface modification of polymeric fibers and inorganic substrates. Dissertation, Clemson University, 2007.

45. Fox, J. D.; Capadona, J. R.; Marasco, P. D.; Rowan, S. J., Bioinspired water-enhanced mechanical gradient nanocomposite films that mimic the architecture and properties of the squid beak. *Journal of the American Chemical Society* **2013,** *135* (13), 5167-5174.

46. Kuttner, C.; Hanisch, A.; Schmalz, H.; Eder, M.; Schlaad, H.; Burgert, I.; Fery, A., Influence of the polymeric interphase design on the interfacial properties of (fiber-reinforced) composites. *ACS Applied Materials & Interfaces* **2013,** *5* (7), 2469-2478.

47. Burtovyy, O.; Klep, V.; Turel, T.; Gowayed, Y.; Luzinov, I., Polymeric membranes: Surface modification by "grafting to" method and fabrication of multilayered assemblies. In *Nanoscience and Nanotechnology for Chemical and Biological Defense*, American Chemical Society: 2009; Vol. 1016, pp 289-305.

48. Motornov, M.; Minko, S.; Nitschke, M.; Grundke, K.; Stamm, M., Mixed polymer brushes on polyamide substrates. *Polymeric Materials: Science & Engineering* **2003,** *88*, 264.

49. Salem, D. R., *Structure formation in polymeric fibers*. Hanser ; Hanser Gardner Publications: Munich; Cincinnati, 2001.

50. Knox, B. H.; Weigmann, H. D.; Scott, M. G., Interactions of non-aqueous solvents with textile fibers .5. Application of solubility parameter concept to polyester fiber-solvent interactions. *Textile Research Journal* **1975,** *45* (3), 203-217.

51. Riande, E. Polymer viscoelasticity stress and strain in practice. http://search.ebscohost.com/login.aspx?direct=true&scope=site&db=nlebk&db=nlabk&AN=28536.

52. Bikiaris, D. N.; Papageorgiou, G. Z.; Achilias, D. S., Synthesis and comparative biodegradability studies of three poly(alkylene succinate)s. *Polymer Degradation and Stability* **2006,** *91* (1), 31-43.

53. Tokiwa, Y.; Calabia, B., Biodegradability and biodegradation of polyesters. *Journal of Polymers and the Environment* **2007,** *15* (4), 259-267.

54. Lee, W.-K.; Gardella, J. A., Hydrolytic kinetics of biodegradable polyester monolayers. *Langmuir* **2000,** *16* (7), 3401-3406.

55. Tsyalkovsky, V.; Klep, V.; Ramaratnam, K.; Lupitskyy, R.; Minko, S.; Luzinov, I., Fluorescent reactive core–shell composite nanoparticles with a high surface concentration of epoxy functionalities. *Chemistry of Materials* **2007,** *20* (1), 317-325.

56. Kaihong, Q.; John, H. X.; Walid, A. D.; Chee Leung, M., Functionalizing polyester fiber with a self-cleaning property using anatase TiO2 and low-temperature plasma treatment. *International Journal of Applied Ceramic Technology* **2007,** *4* (6), 554-563.

57. Hashemizad, S.; Montazer, M.; Rashidi, A., Influence of the surface hydrolysis on the functionality of poly(ethylene terephthalate) fabric treated with nanotitanium dioxide. *Journal of Applied Polymer Science* **2012,** *125* (2), 1176-1184.

58. International Business Machines, C., IBM journal of research and development. *IBM journal of research and development.* **1957**.

59. Quoc Toan, L.; Pireaux, J. J.; Caudano, R.; Leclere, P.; Lazzaroni, R., XPS/AFM study of the PET surface modified by oxygen and carbon dioxide plasmas: Al/PET adhesion. *Journal of Adhesion Science and Technology* **1998,** *12* (9), 999-1023.

60. Le, Q. T.; Pireaux, J. J.; Verbist, J. J., Surface modification of PET films with RF plasma and adhesion of in situ evaporated Al on PET. *Surface and Interface Analysis* **1994,** *22* (1-12), 224-229.

61. Dmitriev, S. N.; Kravets, L. I.; Sleptsov, V. V.; Elinson, V. M.; Potryasai, V. V.; Orelovich, O. L., A high-frequency plasma-discharge effect on poly(ethylene) terephthalate films exposed to heavy ions. *Nuclear Instruments and Methods in Physics Research Section B: Beam Interactions with Materials and Atoms* **2000,** *171* (4), 448-454.

62. Bajaj, P.; Gupta, A.; Ojha, N., Antistatic and hydrophilic synthetic fibers: A critique. *Journal of Macromolecular Science, Part C: Polymer Reviews* **2000,** *40* (2-3), 105-138.

63. Hwang, Y. J. Characterization of atmospheric pressure plasma interactions with textile/polymer substrates. Nort Carolina State University, 2003.

64. Greenwood, O.; Hopkins, J.; Badyal, J., Non-isothermal O2 plasma treatment of phenyl-containing polymers. *Macromolecules* **1997,** *30* (4), 1091-1098.

65. Iyer, K. S.; Luzinov, I., Effect of macromolecular anchoring layer thickness and molecular weight on polymer grafting. *Macromolecules* **2004,** *37* (25), 9538-9545.

66. Piehler, J.; Brecht, A.; Valiokas, R.; Liedberg, B.; Gauglitz, G., A high-density poly(ethylene glycol) polymer brush for immobilization on glass-type surfaces. *Biosensors and Bioelectronics* **2000,** *15* (9–10), 473-481.

67. Zdyrko, B.; Klep, V.; Luzinov, I., Synthesis and surface morphology of high-density poly (ethylene glycol) grafted layers. *Langmuir* **2003,** *19* (24), 10179-10187.

CHAPTER FIVE

MODIFICATION OF TEXTILE SUBSTRATE: INFLUENCE OF POLYMER GRAFTING ON WETTABILITY OF PET FABRIC

5.1. Introduction

The level of wetting a fiber surface with liquids is an important characteristic of textile materials. Recently, introducing super-hydrophobicity or hydrophilicity to textile materials has gained interest from both the scientific and industrial communities, especially with regard to self-cleaning surfaces and fabric with moisture management features.[1-5]

The wetting behavior can be altered by two factors: surface energy and the geometry of the surface. Surface energy can be changed by surface modification via the grafting methodologies that have been reported for introducing new and stable functionality to textile substrates.[6-14] Recently, the "grafting to" method has been successfully employed to tailor textile surface hydrophilicity.[6, 11, 15-17] This method is based on the reaction between already synthesized polymers of known structure and the surface reactive groups.

Increased fiber hydrophobicity has been obtained by many groups via changing the chemical composition or/and introducing roughness to the surface. For example, lowering the surface energy by using hydrophobic macromolecules, such as fluoro-compounds, has been commonly employed to acquire hydrophobic textiles.[18] Ultra hydrophobicity and self-cleaning properties have been reached by decorating surfaces

with chemically functionalized particles.[6] For instance, Hoefnagels et al.[19] modified cotton surfaces that contained covalently attached silica particles with mono-epoxy-functionalized PDMS to obtain super hydrophobicity. The same surface was then modified with perfluoroalkyl silane to provide surface superoleophobicity. Super hydrophobicity for cotton was also achieved using diamond-like carbon (DLC) films.[20]

On the other hand, the wettability and wicking ability of textiles are two important and interrelated properties that play critical roles in many textile applications, such as hand towels, dishcloths, sports garments, liquid separation for scaled up oil-water separation, and liquid transport in micro scale sensors.[21, 22]

Wetting and wicking are related events. In fact, if liquid does not wet the fibers it cannot wick into the capillary formed by the fibers; therefore, fiber wettability is a prerequisite for wicking.[23] The difference between wetting and wicking can be stated by their definitions, "wettability is the initial response of fabric when brought in contact with water," whereas wick-ability is defined as the "ability to sustain capillary flow."[23-25] Ghali et al.[26] described wetting and wicking as a single process that is flow of a liquid in response to capillary pressure. Since capillary movement is the movement of liquid in capillary channels under the influence of its own surface and interfacial forces (causing capillary pressure), capillary flow is caused by wetting. In other words, in order for capillary flow to occur, liquid adhesion between the capillary and liquids should be greater than the cohesive forces of the liquid. This condition exists when the surface is wettable with the liquid (contact angle $< 90^0$). It is inevitable that a surface with capillarity will wick the wetting liquid.[23]

Numerous studies are dedicated to enhancing fiber surface wettability to increase dyeability,[27, 28] adhesion,[29-32] or the comfort of a garment.[33, 34] Plasma irradiation,[30] alkali oxidation,[35, 36] and grafting macromolecules[37] have been shown to increase wettability.

Wong et al.[38] studied the effects of plasma time on the wettability–wicking ability of linen, and showed that plasma treatments lead to an increase in the polar group content. Therefore, the surface energy of the fibers was increased, and consequently, a surface with improved wettability and wicking ability was obtained. It was shown that, when the treatment time was low, the fiber surface and pore structure did not change. Thus, a change in the wicking property was associated with a change in the chemical composition of the fibers.

The moisture related properties of hydrolyzed polyester fibers and fabric in both the weft and warp direction was studied.[39] It was reported that the wicking and moisture regain properties of PET fibers and fabrics increased with an increase in hydrolysis time. An improvement in wicking and wetting properties was correlated with a change in the pore size, as well as increased polar functionality on the surface.

The purpose of this part of dissertation is to describe the grafting of macromolecules onto a PET fabric, and evaluate the effect of that grafting on the wetting properties and wicking performance of the fabric. Wicking is a critical parameter to study since this dissertation specifically focuses on changing fluid transport properties of the fabric to use in microfluidics, and moisture management fabric.

5.2. Experimental

5.2.1. Fabric substrate modification

Fabric (Test Fabric Inc. #777H) was used in this section. Fabric preparation was explained in Section 3.5.2. The model study reported in **Chapter 4** for the PGMA deposition was followed at this point to form an anchoring layer on the fabric. The alkali treated PET fabrics were soaked in a 1 wt/vol % PGMA (Mn ≈ 176,000 g/mol) solution in MEK, and vacuum was applied several times to allow the polymer solution to penetrate into the yarns of the fabrics. The fabrics were kept in solution for 15 min at 50 °C for equilibration, then were taken out, dried at room temperature, and annealed in a vacuum oven at 60 °C for 3 hrs. After the PGMA layer annealing, the fabrics were washed several times with MEK and dried until constant mass was obtained. To obtain homogenous deposition, the vacuuming and equilibration were necessary and done for all polymer deposition on the fabrics.

The polymers that were used for the PET film modification in **Chapter 4**, PS-COOH, PEG-COOH, P2VP-COOH, and PAA, were then grafted to the epoxy functionalized PET fabric. Annealing conditions were kept the same as the annealing conditions for the PET film as reported in the **Chapter 4**. After grafting, the surface of the fabric was thoroughly washed with suitable solvent to remove unbound polymer, and dried until constant weight was achieved. Polymers have been chosen to achieve different wettability towards various liquids.

5.2.2. Microscopic characterization of polymer grafted textiles

Morphological changes in the PET fabrics were investigated by scanning electron microscopy (SEM), and the fluorescence microscopy was used to visualize polymer grafting.

5.2.3. Wettability analysis of polymer grafted textile[1]

For quantification of wettability, the static water contact angle and wicking kinetics on treated and non-treated fabrics were evaluated.

5.2.3.1. Water contact angle analysis

Static contact angle measurements were carried out using a contact angle goniometer (Kruss, Model DSA10). The contact angle measurements were conducted with the liquid of interest and a static time of 30 seconds before the angle recording. Calculations of the contact angles were made using the ImageJ (NIH) software.

5.2.3.2. Wicking analysis of modified fabric: Vertical wicking study

Flow under capillary pressure can be modeled using the Lucas-Washburn[40, 41] equation **(E.5.1)**, where L is the liquid front position or wicking length, and k and ε are the permeability and the porosity of the test sample, respectively. Pc is capillary pressure, η is the viscosity of the liquid, and t is time.

[1]The author would like to acknowledge Dr. Konstantin Kornev, Professor in the Department of Materials Science and Engineering Department, and Dr.Chen-Chih Tsai, graduate student in Dr. Kornev's, group for their help with this wicking set up, evaluation of the wicking results, and discussions.

$$L = \sqrt{\frac{2kP_c}{\varepsilon\eta}}t. \qquad \textbf{E.5.1}$$

The Lucas-Washburn relationship can also be used to approach wicking kinetics during the vertical wicking experiment. For the vertical wicking, one can rewrite Lucas-Washburn equation in terms of the weight gain of the fabric vs. time **(E.5.2)** by multiplying **E.5.1** with the porosity (ε),density of the liquid (ρ), and cross section of the sample (A). Capillary pressure (P_c) can be expressed as a function of the surface tension of the liquid (σ), liquid contact angle on the surface (Θ), and effective capillary radius (R) **(E.5.3)**.

$$\Delta W = \sqrt{\frac{2\varepsilon\rho^2 A^2 kP_c}{\eta}}t. \qquad \textbf{E.5.2}$$

$$P_c = 2\sigma\cos\theta / R \qquad \textbf{E.5.3}$$

$$C = \sqrt{\frac{2\varepsilon\rho^2 A^2 kP_c}{\eta}} \qquad \textbf{E.5.4}$$

The wicking properties of the surface modified fabric were tested using a vertical wicking experiment. A schematic of the vertical wicking set up is shown in **Figure 5.1**. A fabric strip (1x4 cm) is kept vertically with the lower end of the strip immersed into the liquid of interest. In this set up, spontaneous wicking occurs due to the capillary forces. The liquid reservoir was kept on the balance, and the balance was connected to a computer. As the wicking occurred into the fabric, weight loss (ΔW) from the reservoir was recorded as a function of time. When the results were plotted as weight loss (ΔW) vs.

the square root of the time, the wicking constant (C) (as given in **E.5.4**) can be extracted. Wicking constant is the slope of the ΔW vs. $t^{0.5}$ curve as defined by the Lucas-Washburn equation.[40, 41]

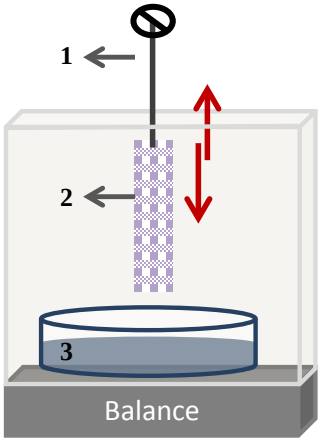

Figure 5.1. Illustration of vertical wicking setup. (1) Control apparatus (2) Fabric, (3) Liquid reservoir.

Hexadecane and DI water were used as wicking liquids. For the water wicking experiment, the balance was kept in a closed chamber saturated with water vapor. The samples were kept in a hanging position in the chamber for 30 minutes before immersing them into the DI water to prevent the effects of water evaporation. For the hexadecane wicking, the experiment started directly without waiting since the vapor pressure of hexadecane is low. The average of four measurements is reported.

The unknown parameters in **E.5.2**, permeability and porosity, were experimentally determined as described by Callegari et al.[42] The schematic configuration of the experimental setup for the permeability study is represented in **Figure 5.2**. During

measurement, a fabric strip with 1 cm in width (w) and 2 cm long (L) was placed in a gap between two highly permeable sponges that were immersed in a wetting liquid (hexadecane) reservoir. The height of the liquid in each reservoir was different and the distance between them was called the hydraulic head (H), which causes the liquid to flow thorough the fabric from one container (high pressure) to the other (low pressure). Using a scale (Sartorius, BP-221S), mass loss from the container, and thus mass flow through the sample, was monitored as a function of time. In this setup, after a certain time, the fabric was completely saturated. The liquid flow stabilized after complete saturation as shown in the sample plot for ΔW vs. time **(Figure 5.3).** The flow rate (Q) was calculated from the slope of **Figure 5.3**. To find the permeability, k, Darcy's law for porous material was applied **(E.5.5)**.[42] In the equation, d is the thickness, w is the width and L is the length of fabric, k is permeability, η is viscosity, ρ is fluid density, g is gravitational acceleration, and Q is the flow rate.

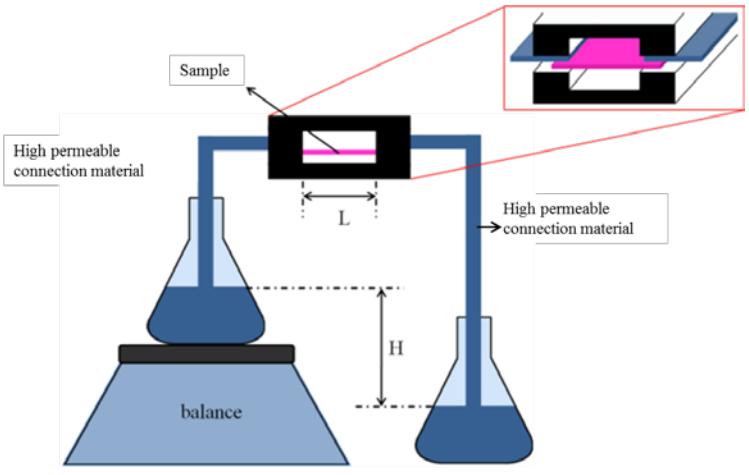

Figure 5.2. Experimental setup for the permeability test. Redrawn after the reference.[42]

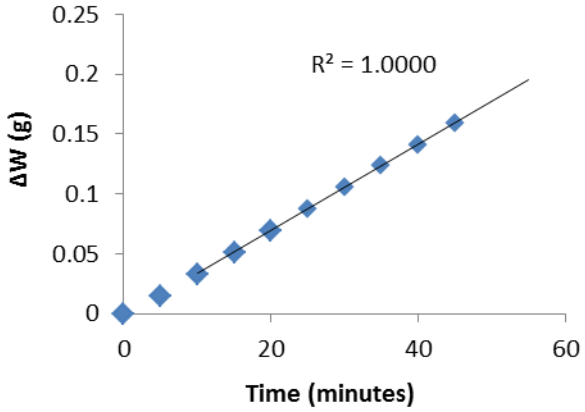

Figure 5.3. Plot of the liquid flow vs. time.

$$Q = dw(k/\eta)(\rho^2 gH)/L \qquad \textbf{E.5.5}$$

The porosity (ε) of the fabric (1x2 cm) was calculated by **E.5.6**, where m_w is the mass of the wet sample, m_d is the mass of dry sample, ρ is the density of the wetting liquid, and V_f is the sample volume. The masses of the dry and wet fabrics were measured before and after the fabric was completely saturated with the wetting liquid.

$$\varepsilon = (m_w - m_d)/(\rho V_f) \qquad \textbf{E.5.6}$$

The fabric volume was calculated as V_f = w*L*d, where w and L are the fabric width and the length, respectively, and d is the thickness of fabric. The sample thickness was determined by placing the fabrics in between two microscope slides and measuring the gap between the plates with a digital micrometer.

Hexadecane was chosen as a wetting liquid for the porosity and permeability experiments, since it is chemically inert, has low surface tension, and low vapor pressure,

which prevents evaporation of the liquid from the surface. The surface tension of the hexadecane was measured in our laboratory by using the pendant drop method, and found to be σ=27 mN/m, as reported in the literature. Hexadecane has a viscosity of η=3.34 cp, and a density of ρ=773kg/m^3.[42]

5.3. Results and discussion

5.3.1. Surface activation: Anchoring polymer deposition on the fabric surface

In the previous chapter, it was shown that the PET film was successfully formed, activated, and modified. The techniques used in the model study **(Chapter 4)** were then employed to activate and modify the surface of the PET fabrics.

The fabric preparation and activation were accomplished according to the procedure published elsewhere.[6] SEM images of the solvent cleaned fabric are presented in **Figure 5.4a,c**. The water contact angle measurements of the clean PET fabric surface revealed high hydrophobicity (133^0)**(Figure 5.5a).**

The surface was then subjected to the activation process by an aqueous hydroxide solution. Alkali hydrolysis is an accepted surface activation method that is commonly employed to increase the reactivity of a polyester fabric.[43] Additionally, the activation of polyester fabric with ethanolic sodium hydroxide is reported to lead to a significant improvement in the absorbency performance of the polyester fabric, such as the decrease in wicking time and the relative increase in the moisture regain percentages, when compared with the untreated PET fabric.[44]

Our model study clearly indicates that the number of polar groups on the surface after hydrolysis was increased. On the model film the water contact angle was decreased to 35^{o} from 65^{o} for the hydrolyzed PET surface **(Figure 5.5c, d)**. The decrease in wettability and decrease in thickness (3-4 nm) after hydrolysis supported the formation of polar groups through chain scission. However, the morphology of the PET film remained intact.

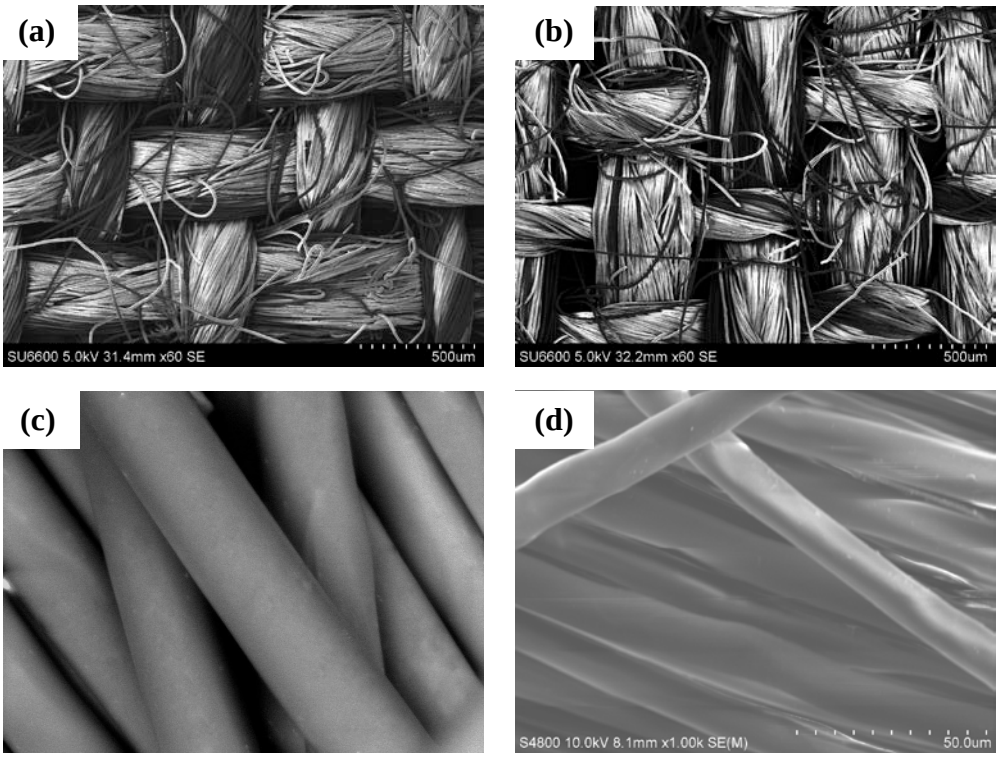

Figure 5.4. SEM images of PET fabric: (a,c) Non modified fabric, (b,d) hydroxide treated fabric surface.

We believe that the thickness change (3-4 nm), while a similar morphology was obtained after the hydrolysis, indicates that degradation of the film was not significant

during the treatment. In this study, the weight loss after hydrolysis was less than 0.2%, which is considered to be low, and indicated that the physical properties of the fabric and yarns were not affected. Smooth surface of PET remained intact. There was no presence of pits or voids. Thus, the effect of the alkali treatment on the fabric surface should be minimal, similar to the effect of treatment on the model film. This leads to the conclusion that the integrity of the fibers should remain intact as well.

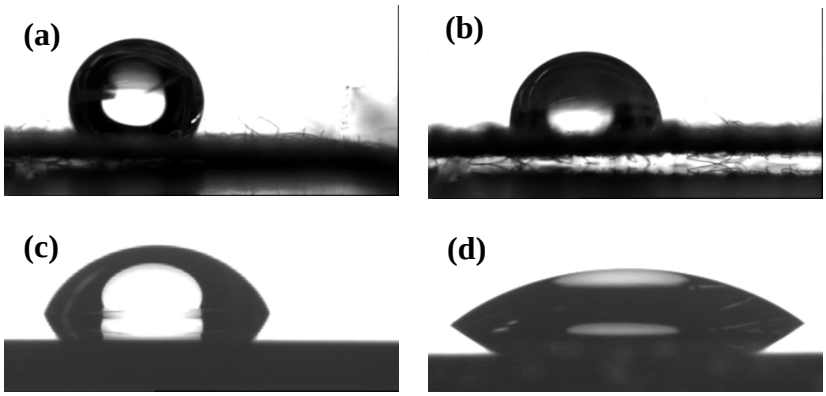

Figure 5.5. Water contact angle measurements on PET substrates: (a, b) fabric, (c, d) film, (a, c) non-treated PET substrates, and (b, d) alkali treated PET substrates.

The water contact angle of the clean fabric was measured to be ~133^{o}, which is higher than the PET film WCA (~65^{o}). After the alkali treatment, the water contact angle of the fabric decreased to ~95^{o} **(Figure 5.5a, b).** A similar decrease in the WCA of the film after hydrolysis was observed **(Figure 5.5c, d)**. Different wettabilities can be associated with the roughness of the fabric. These results are in good agreement with the literature data.[45, 46] It was reported that the fabric surface typically gave a higher contact angle than the film surface.[45] Hydrophobic nature of the fabric was expected due to the

nonpolar structure of the PET, organization of fibers in the structure, and the roughness factor. It should be noted that the water drop penetrated completely through for the hydrolyzed fabric after a certain time, but did not penetrate into the clean fabric. Thus, it is clear that the activity of the PET fibers was increased with the base treatment.

Next, the PGMA was deposited on the PET fabric from a solution (1 wt/vol % in MEK, Mn ≈176000 g/mol) by coating, drying and annealing. The SEM images of the fabric revealed that the PGMA did not form polymer aggregates on the fibers, or junctions between the fibers (that could be formed by the self-cross linking of the deposited polymer) **(Figure 5.6a)**. Formation of PGMA coating without the formation of bridges and aggregates is important for the wicking of the liquid in the fabric. Otherwise, the capillarity level would change between the fibers and complicate the wicking kinetics of the liquid in the PGMA coated fabric.

The PGMA can also be successfully anchored to the fiber surface when deposition is conducted by adsorption from a solution at a low temperature (50 ^{0}C, 3 hours). In order to visualize the PGMA attachment, rhodamine labeled PGMA was used in our experiments. The PGMA-RhB adsorption was done from a 0.5 wt/vol % PGMA-RhB solution in MEK. Fluorescence microscope images indicated that the surface was successfully covered with a PGMA layer **(Figure 5.6b)**.

The water contact angle of the PGMA modified PET fabric and film was measured as ~80^{o} and 54^{o} , respectively. The WCA on the fabric was higher than the respective WCA on the film, which could be related to the roughness of the fabric. The WCA on the hydrolyzed fabric was higher than the WCA on the PGMA modified PET

fabric, while on the film; the WCA on the hydrolyzed film was lower than on the PGMA modified film. This also may be related to the rough and hairy structure of the fabric.

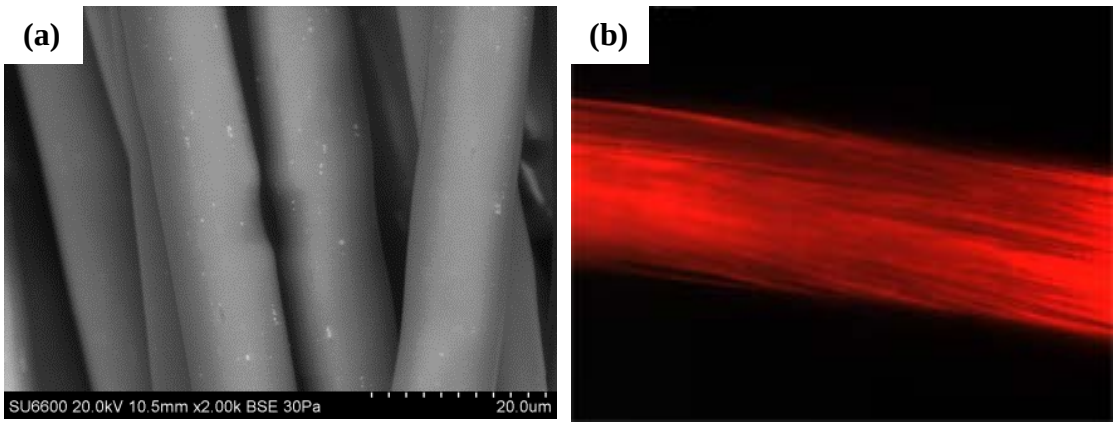

Figure 5.6. PGMA grafted PET fibers. (a) SEM images of the PGMA (~6 nm) coated PET fabric. (b) Fluorescence images of the PGMA (~3 nm) anchored to PET yarn.

5.3.2. Functional polymer grafting to the PET fabric surface

As discussed in **Chapter 4**, the PGMA layer provides a sufficient amount of epoxy groups on the surface, thus, different polymers can be anchored to the fibers with the "grafting to" approach. To this end, the hydrophilic polymers, PAA, P2VP-COOH, and PEG-CCOH, and the hydrophobic polymer, PS-COOH, were grafted to the PGMA/PET fabric surface. The influence of the polymer grafting on the fabric wetting parameters has been studied in this section.

Table 5.1 presents the water contact angle measurements of the modified PET fabrics. In general, among these polymers, the PS grafted surface had the highest water contact angle on both the PET fabric and the film. The PGMA attached fabric surface had

a WCA of ~80^{o}. After the PS coating was applied to the PGMA / PET fabric, a drastic change in WCA (increase to 150^{o}) was observed. The high contact angle confirms the PS-COOH grafting. The PAA grafted layer on the PET film has a very low contact angle (WCA 17^{o}). Similarly, a low contact angle (< 30^{0}) was observed on the PAA coated fabric as well, which indicates that the PAA was successfully grafted to the fabric.

Table 5.1. Contact angle of water drop on the PET film and fabric.

	Experimentally determined apparent contact angle(degree)	
	on film	on fabric
PET	65	143±14
Hydrolyzed PET	35	104±9.5
PGMA grafted PET	53.5	83±4.4
PEG grafted PET	53	68±9.5
PAA grafted PET	17	25±17
P2VP grafted PET	46	110±20
PS grafted PET	87	140±14

The water contact angle is a measurement of the very first interaction of a drop with the surface, which is controlled by the surface chemistry and the roughness. In our measurements, the water contact angle, after polymer grafting on the film, was found to be 46^{o} for the P2VP, 54^{o} for the PGMA, and 53^{o} for the PEG coated films. The water contact angles of these specific polymer layers on the fabric were found to be higher than the respective WCA on the PET film. This can be attributed to the roughness profile coming from the weave pattern and yarn structure of the textile fabric.[47, 48] Additionally,

those polymers were hydrophilic polymers, thus at the first sight, one might expect hydrophilic behavior for the treated fabrics as well. Contrary to the expectations, relatively high contact angles were recorded on the PGMA, PEG, and P2VP grafted fabrics. However, it should be mentioned that those measurements were taken in the first 30 seconds. In fact, the penetration of the water drop after a certain time was observed for all of the polymers except the hydrophobic polymer (PS) coated fabric. The penetration time for the drop on coated fabrics varied from 45 seconds to 2 minutes. Hairy structure of fabric also complicates the contact angle measurement, since baseline (that is used for measurement) is not easy to determine visually. Due to the mentioned factors, standard deviation for the fabric contact angle was high. Gallery of the contact angle pictures is given in **Figure 5.7.**

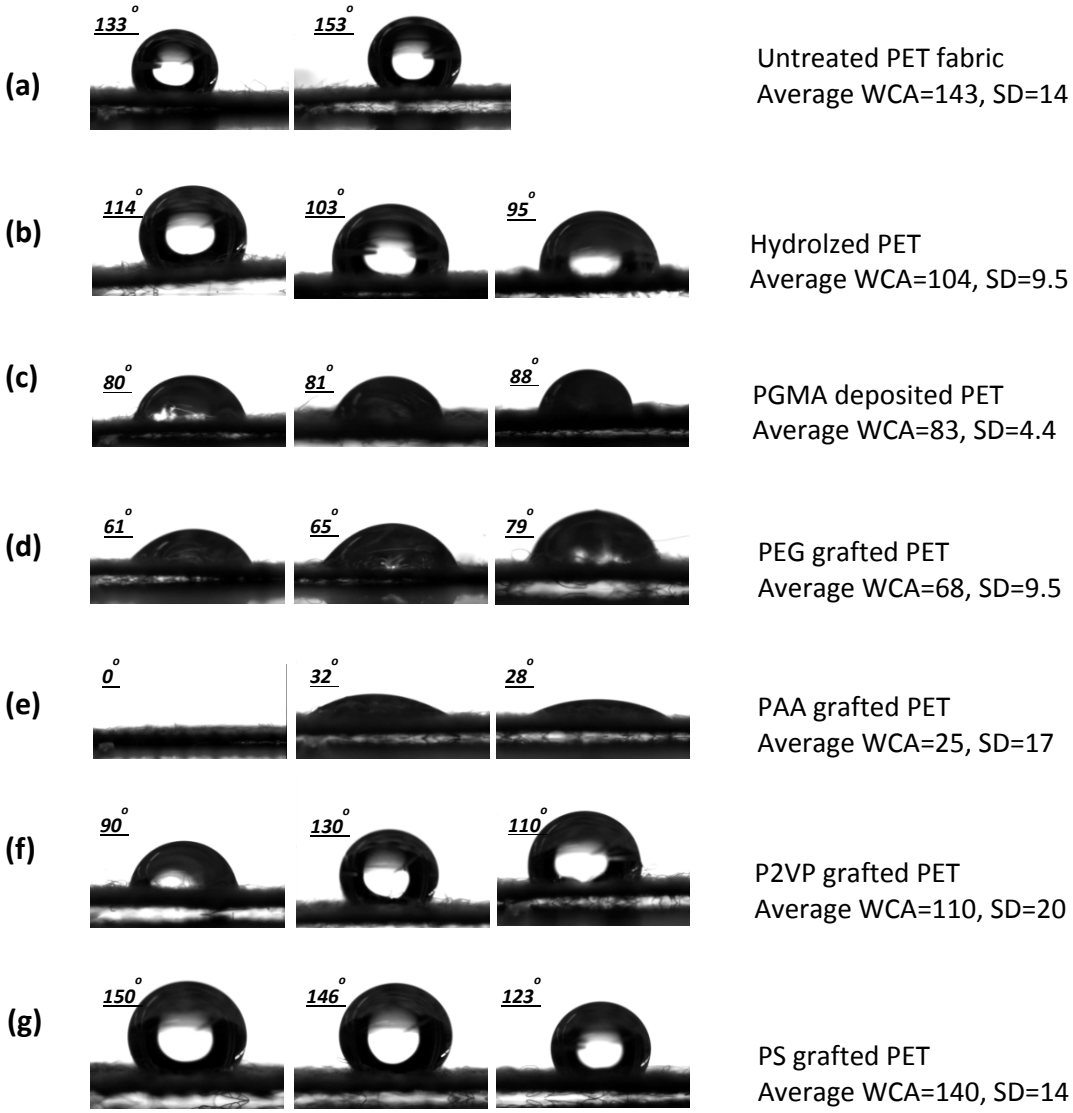

Figure 5.7. Gallery of contact angle on bare and surface modified PET fabrics.

5.3.3. Theoretical evaluation of fabric contact angle

Different wettability behaviors between the fabric and flat surface relate to the roughness factor.[23, 49-51] Roughness and surface energy are two parameters that influence the wetting behavior of any surface. Generally, initial contact angle can be used for the

qualitative evaluation of the surface energy. Also, contact angle of a surface can be predicted when the surface energies of the liquid and substrates are known. Young[52] modeled the relationship between surface energy and contact angle (Θ_e), where Θ_e is an equilibrium contact angle on a flat surface. However, Young's model is only valid for a flat surface. Theoretical models (Wenzel[53] and Cassie-Baxter[51]) have been developed to evaluate how the contact angle on a rough surface relates to the roughness factor and Young's equilibrium contact angle of the substrate. The Wenzel model **(E.5.7)** states that the surface with a contact angle of less than 90^o will have a lower contact angle with increased roughness. In our case, we obtained higher contact angle values, and thus, clearly, the Wenzel model was not suitable for explaining the roughness effect. In the equation below, Θ_e is the contact angle on a flat surface, Θ_r is the contact angle on a rough surface, r is level of roughness and defined as the ratio between the actual surface area and the apparent surface area of a rough surface. W stands for the predicted Wenzel contact angle.

$$\cos\theta_r^w = r\cos\theta_e \qquad \textbf{E.5.7}$$

The Cassie-Baxter[51] extended model includes the effects of porosity. When the liquid drop is placed on a porous surface, it is in contact with both a solid and air. Cassie and Baxter model suggested a relationship **(E.5.8)** between the Θ_e, Θ_r, f_1, and f_2, where f_1 is the surface area of the liquid in contact with the solid divided by the projected area **(E.5.9),** and f_2 is the surface area of the liquid in contact with air trapped in the pores of the rough surface divided by the projected area **(E.5.9).** CB stands for the predicted Cassie contact angle.

$$\cos\theta_r^{CB} = f_1 \cos\theta_e - f_2 \qquad \textbf{E.5.8}$$

$$f_1 = \frac{\text{area in contact with liquid}}{\text{projected area}} \qquad \textbf{E.5.9}$$

$$f_2 = \frac{\text{area in contact with air}}{\text{projected area}} \qquad \textbf{E.5.10}$$

The Cassie equation is rearranged for multifilament yarns and fabrics by Michielsen et al. **(E.5.11),**[49] where R is the radius (of fibers, or yarn) and d is half of the distance between the fibers or yarns. For the "basic weave" fabric pattern, d=R ($3^{0.5}$-1) ≈ 0.73R.

$$\cos\theta_r^{CB} = \frac{R}{R+d}(\pi - \theta_e)\cos\theta_e + \frac{R}{R+d}\sin\theta_e - 1 \qquad \textbf{E.5.11}$$

Similar to the previously published study,[49] we began by determining the apparent contact angle on the yarns using **E.5.11**. In this case, *R* is the radius of the fibers in the yarn, Θ_e is the contact angle measured on the flat surface, and *2d* is the fiber spacing and calculation made by assuming *d=R, d<R,* and *d>R*. Then, using the calculated values of Θ_r^{CB} for the yarns as the effective contact angle (Θ_e) for the fabric, the equation **(E.5.11)** can be solved to predict the Θ_r^{CB} of the fabric. The Θ_r^{CB} for the fabric was calculated for each apparent contact angle of the yarn (Θ_r^{CB} for yarn) that was calculated for the different fiber spacing as *d=R, d=R/2,* and *d=2R*. The fabric used in this study has a "basic weave" pattern, and thus the relation between the yarn radius and distance was taken as $d=R\,(3^{0.5}\text{-}1) \approx 0.73R$, with *R* being the yarn radius.

The predicted values were compared with the experimentally measured contact angles **(Table 5.2)** as well as the contact angles that were calculated using the wicking

kinetics of the fabric (This will be discussed later in the chapter). All measured WCA on fabric were higher than the measured values for the modified film; and therefore, the Cassie-Baxter model can be applied to understand high contact angle measured in our case. However, a better evaluation of the fiber spacing in the yarn is required. When the d<R(d=R/2), WCA prediction is lower than measured fabric WCAs. The model suggests that increasing the fiber spacing will lead to higher predicted contact angle values. Indeed, the predicted values are higher than the measured fabric WCAs when d=2R.

The predicted values were closer to the measured values when 2d=2R. These calculations suggest that d (fiber) is close to R (fiber). Slight difference could be due to high standard deviation for measured fabric WCAs. Such high deviation could be attributed to the uneven fiber spacing that is, in fact, unavoidable. It is obvious that (d) could be smaller at the inner side of the yarn due to twisting, or tension applied during the weaving process, while d becomes larger than R at the surface. Additionally, the model was developed for multifilament yarns and fabrics; but the fabric used in this study was spun bond PET fabric where a hairy nature is more distinct, inevitable, and uncontrollable. The model does not decisively define the initial wetting (WCA) behavior of modified fabric; however, it is suitable to use for the conclusion such that fabric roughness leads to a high contact angle on the PET fabric surface.

Table 5.2. Comparison of predicted and measured contact angles.

	Measured contact angle(degree)		Predicted contact angle for fabric(degree)*		
	on film	on fabric	CB angle (d=2R)	CB angle (2d=2R)	CB angle (d=R/2)
PET	65±0.4	143±14	149	122	98
NaOH	35±2.5	104±9.5	136	95.8	48
PGMA	53.5±0.6	83±4.4	*n*	*n*	*n*
PEG	53±1.4	68±9.5	*n*	*n*	*n*
PAA	17±1.4	25±17	*n*	*n*	*n*
P2VP	46±2.5	110±20	141	105	69
PS	87±1	140±14	157	138	125

* Prediction of contact angle on fabric was done by using the Michielsen approach for Cassie-Baxter model. Inter fiber distance was taken as (a) d=R/2, (b) d=2R, and (c) 2d=2R for calculation. Calculation was done only for fabric has WCA>90^{o}.

n Not calculated since WCA on fabric is below 90^{o}

Wicking is accepted to be more reliable approach for the wetting behavior evaluation of textile surfaces. The next part of this chapter will focus on the evaluation of wicking kinetics.

5.3.4. Wettability analysis by wicking

A change in wettability of the surface after various treatments has been demonstrated. However, the contact angle measurement of a droplet could be challenging and sometimes unreliable. For instance, the rapid penetration of the droplet by capillarity can occur, or the surface roughness, trapped air between the fibrils, and the hairy nature of the fabric can lead to high contact angle values. In fact, fabric roughness could have a significant influence on contact angle. The fabric used in this study is made of staple

yarns and has a hairy nature on the surface that it is almost impossible to control. Thus, the measurement of the droplet contact angle on the fabric would not be reliable for an accurate judgment of the wettability.[54]

One way to overcome the aforementioned problems would be an analysis of the wicking kinetics of the fabric.[23, 55] As mentioned in **Section 5.1**, wetting is a pre-requirement for wicking, therefore, wicking is affected by the parameters of wetting as well as the organization of the fibers or yarns in the fabric.[23]

Fabric is an assembly of yarns which in general, consist of fibers. Thus, the fabric structure contains micro size pores between the yarns, and smaller pores that are inside the yarns between the fibers. Clearly, fabric can be described as a network of capillary channels. When this system is in contact with a liquid, wicking will occur if the adhesion forces between the liquid and the surface are higher than the cohesive forces of the liquid. This is the case when the contact angles are lower than 90^0 as described by Young's equation. The relationship between capillarity, porosity, and permeability is generalized in Washburn's equation **(E.5.1 & E.5.2)**.[41]

To this end, a series of experiments were conducted to analyze the effects of fabric surface modification on the wicking of PET fabrics. Wicking is studied by using a vertical wicking setup, and weight loss from the liquid reservoir (or weight gain by the fabric) is monitored. In this way, **E.5.2** is more efficient for these calculations. Wicking constants are obtained from the wicking curves that are plotted as weight gain versus the square root of time. Several example of the wicking curves are given in **Figure 5.8**. Porosity and permeability are two unknown parameters of **E.5.2**, and moreover, they can

be straightforwardly determined using an experimental setup **(Figure 5.2)**. From the equation of wicking constant **(E.5.4)**, one can compute the contact angle for the probe liquid and make a better judgment regarding the effects of the surface modification. The wicking rate of at least two types of liquid is needed for these measurements.

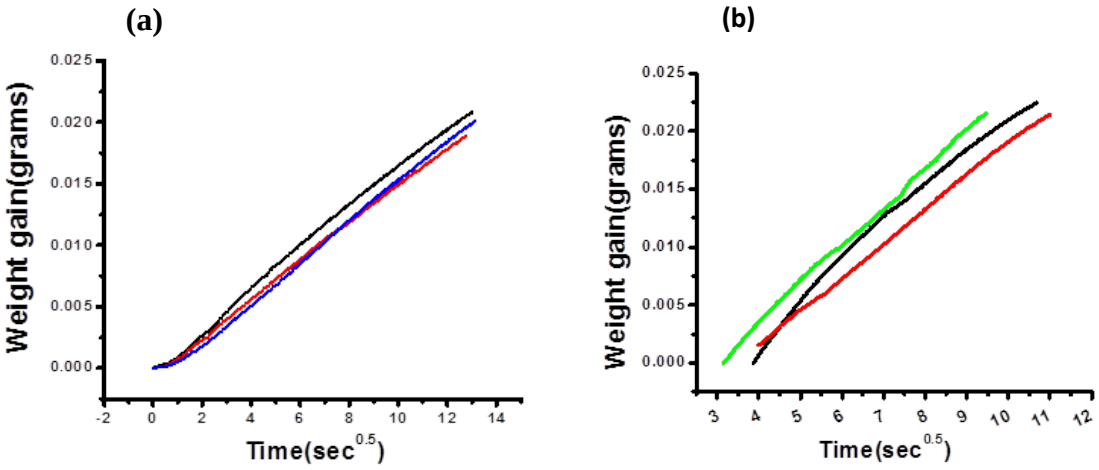

Figure 5.8. Sample wicking curves obtained from vertical wicking experiment. (a) Hexadecane wicking curve for PEG modified PET fabric. (b) Water wicking curve for PAA modified PET fabric.

5.3.4.1. Porosity and permeability analysis

Wicking depends on many factors including fabric structure, fiber alignment in the structure, and affinity of the material to the probe liquid. Structure can influence wicking in two ways. First, different structures will create different capillary channels, and if the structure is changed by surface modification, the size of the already existing capillaries will change. Also, accessibility of the active surface groups by the liquid and liquid surface affinity play crucial roles in the liquid-fabric interactions.

The literature suggests that the wicking performance of a porous surface, by the most general definition, is related to two fundamental phenomena: capillarity and permeability. Permeability defines the ability of a porous medium to allow fluid flow and it is a function of the porosity. Permeability can be calculated using Darcy's law[42] **(E.5.5)** after the determination of the mass flux experimentally, with the setup **(Figure 5.2)** as explained in **Section 5.2**.

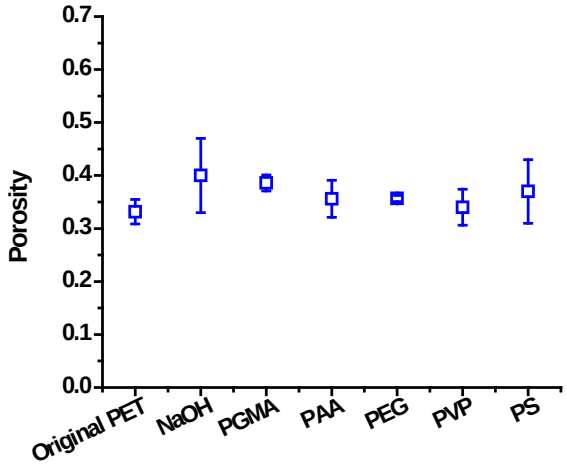

Figure 5.9. Porosity measurements of polymer grafted and non-modified PET fabric.

Flow depends on the shape, place, and size distribution of empty spaces (pores) in the structure;[56] therefore, wicking in fibrous structures will be influenced by porosity as clearly seen in Washburn's model **(E.5.1 & E.5.2).** During liquid flow in fibrous surface, not only the inter-yarn pore properties, but inter-fiber pore properties play a significant role.[56] It is therefore imperative to study the effects of polymer coating on porosity to understand whether a nano scale coating can change porosity.

We conducted experiments to analyze the effects of fabric etching and thin layer polymer grafting on porosity, and the results are reported in **Figure 5.9**. The measurements pointed out that fabric porosity was not altered significantly by the nano scale polymer coating.

The vertical wicking analysis was conducted and weight gain was monitored, instead of wicking high, for the following reason: the wicking liquid was selected to be colorless to avoid dye surface interactions, and therefore it was difficult to detect the wicking length. Secondly, the wicking height could be misleading since the wicking in larger pores could occur at a different rate then the wicking rate in smaller pores. The individual porosity components (inter and intra-yarn porosities) may be more important when analyses need to be done based on the wicking length (L), since the liquid will travel first in the small pores, then fill the larger pores, and thus complicate the observation of L.

Yang et al.[57] reported surface modifications of polypropylene non-woven fabric with acrylic acid, which was then grafted with N-isopropylacrylamide (NIPAAm), and followed by chitosan impregnation. Unlike our findings, they reported that the porosity was changed after modification. The change in the porosity was attributed to the change in density, and a significant difference between surface morphology of the pure PP and modified PP.

Figure 5.10 presents the permeability data for the modified and un-modified fabrics. The change in the permeability follows the same trend as the porosity of the fabric after various polymer grafting; however, the alteration of the average permeability

was not significant. High standard deviation is attributed to a shift in the fiber structure during handling. Indeed, after the alkali treatment the deviation was higher since the rinsing cycle with water was more aggressive compared to the gentle rinse with an organic solvent after the polymer grafting. The average results of four to six samples are reported here.

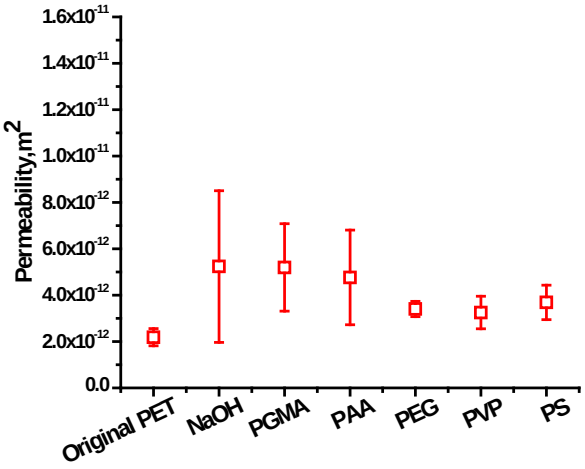

Figure 5.10. Permeability measurements of polymer grafted and non-modified PET fabric (wicking liquid is hexadecane).

Rahli et al.[58] studied the fluid flow thorough porous media made of randomly packed mono disperse fibers. The permeability was deduced experimentally and an increase in permeability with the increased porosity was found. In fact, an exponential relationship was observed. In our study, even though the variation in porosity and permeability was not significant, a higher standard deviation was observed for the permeability. However, sensitivity analysis suggested that deviations in permeability or porosity were not significant enough to cause difference in wicking rate of water.

Therefore, the variable that may influence wicking rate is surface-liquid affinity. Sensitivity analysis was done as follows: when WCA was assumed constant, measured ε, and k values were used to calculate wicking constant using **E.5.2**. In addition, measured k values and ε values individually were used for calculation by assuming constant WCA, ε, and constant WCA, k, respectively. For all sensitivity analysis, highest, lowest, and average values of ε and k for each polymer-coated fabric were used.

5.3.4.2. Wicking analysis

A vertical wicking experiment was done to evaluate the wicking rates of two different liquids in the surface modified PET fabrics (the vertical wicking setup used in this study is shown in **Figure 5.1**). We selected hexadecane and water to study the liquid wicking behavior in the modified woven fabric. Hexadecane was chosen since it was expected to wet the surface immediately with a nearly 0^0 contact angle due to its low surface tension. In fact, it was not possible to measure the contact angle of the hexadecane on the model PET film and fabric since the drop was virtually spreading on the surface. Thus, the contact angle of the hexadecane on the grafted PET substrates can be accepted as 0^0. Due to this, the liquid wicking will be independent of the fabric treatment, and the only factors that could influence the wicking rate of the hexadecane are the physical parameters of the fabric. Water was chosen since it has a different affinity to the grafted polymers. In this way we could determine the influence of the coating on the wicking rate of water. Then, the initial wetting contact angle could be extracted using **E.5.2**.

In order to compute the contact angle using Washburn's equation, the effective radius, R, is the only unknown factor that is needed. R can be calculated from the wicking rate of a highly wetting liquid, which was chosen as hexadecane. Therefore, the hexadecane wicking experiment has been conducted for all coated fabrics, and the R was computed from the wicking rate of hexadecane by using **E.5.4**. After the water wicking experiment, one can compute the water contact angle of the fabrics by inserting known values into Washburn's equation, where C is the wicking constant of water.

The experimental findings from the wicking studies are represented with **Figure 5.11** and **Figure 5.12**. The wicking constant of hexadecane (C_h) was not altered significantly with polymer grafting, since hexadecane was the wetting liquid for all polymers used in this study **(Figure 5.11)**. Thus, a slight deviation can be attributed to the slight variation in porosity and permeability, and in fact, the C_h trend is similar to the porosity and permeability trends.

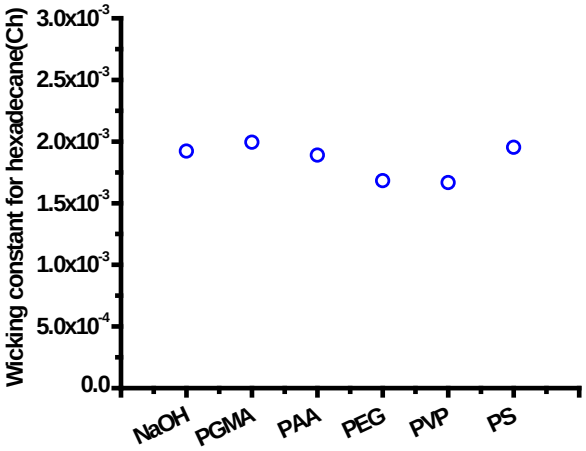

Figure 5.11. Hexadecane wicking constants for surface modified PET fabrics.

However, when we used water for the wicking experiments, which has some level of affinity to the surface, the wicking rate varied in a different way than the porosity and permeability variation among the polymers used for coatings. The wicking rates of water in the surface modified fabric and the plain fabric are represented in **Figure 5.12**. Clearly, the wicking rate of the probe liquid in the PET fabric can be altered by coating the polymers. PAA is the most hydrophilic polymer, has ~17 ^{0} water contact angle on the flat surface, and accordingly has the highest wicking rate. The wicking rate of water on the hydrophobic polymer (PS-COOH) coated surface was not detectable since water is a non-wetting liquid for PS coated substrates. The WCA on the PS layer was 85^0 and 150^0 on the film and fabric, respectively.

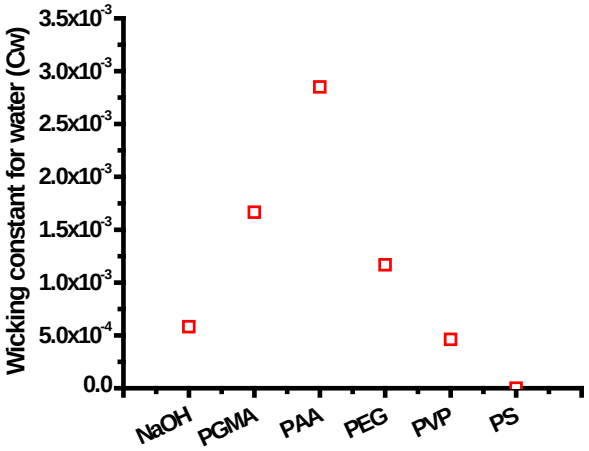

Figure 5.12. Water wicking constants for the surface modified PET fabrics.

The WCAs were computed from the wicking experiments, and using experimentally determined C_h, ε, and *k*, and taking the hexadecane contact angle as 0^0,

one can compute the R of the surface modified fabric. Then, using the computed R, and the experimentally determined C_w, *k*, and ε, the water contact angle can be calculated. These calculated results are provided in **Table 5.3**. All calculated contact angles were higher than 80 degree. However, as detected experimentally (**Figure 5.12)**, these contact angles allow water to wick at a different rate into the modified fabric.

Table 5.3. Calculated water contact angle and effective pore size. The wicking experimental results were used, and the calculation was done using Washburn's model.

	R-effective pore size (μm)	WCA calculated from wicking experiment* (degree)
NaOH	103	89.6
PGMA	91.5	87.2
PAA	85.8	80
PEG	77.7	88
PVP	71.7	89.7
PS	64.9	90

*Washburn equation is used for calculation after wicking experiment.

The water contact angles that were calculated from the wicking experiment using Washburn's relationship were compared with the Cassie-Baxter predicted WCAs that were calculated by assuming d=R, d<R, and d>R, where 2d and 2R are the inter fiber distance and fiber diameter, respectively. Since all the WCA (calculated from wicking experiment) were close to 90 degree, CB angle prediction was computed for the all polymer layers. It is clear that the Cassie model can be applied to explain the high initial wetting angle of the polymer grafted fabric. Comparison **(Table 5.4)** suggests that the

inter fiber distance (2d) is close to the fiber diameter (2R). Additionally, the contact angle calculated from the wicking experiment fits better with the model prediction **(Table 5.4 & 5.2).**

Table 5.4. Comparison of the contact angle for fabric calculated using Washburn's relationship with the predicted contact angle calculated using Michielsen approach of Cassie-Baxter model. Inter fiber distance is (a) d=R/2, (b) d=2R, (c) 2d=2R.

	Fabric WCA calculated from wicking experiment	Predicted contact angle for fabric		
		CB angle (d=2R)	CB angle (2d=2R)	CB angle (d=R/2)
NaOH	89.6	136	95.8	48
PGMA	87.2	144	117	82
PEG	88	144	111	80
PAA	80	132	84	0
P2VP	89.7	141	105	69
PS	90	157	138	125

5.4. Conclusion

The methodology used for polymer grafting to the PET film was successfully applied to graft various polymers to the PET fabric surface. Wettability was altered after polymer grafting. Liquid wetting behavior of the fabric was evaluated using the theoretical model. Michielsen's approach, which is indeed the modified Cassie model for fabric, was used here.

The experimental WCA measurements did not completely fit with the model predictions, which can be attributed to the fabric hairy surface or the probable variation in

fiber and yarn spacing of the fabric. However, comparisons suggested that when R/2<d<R, where d and R were fiber parameters.

The effect of the polymer grafting on the wicking property of the fabric has been evaluated using the vertical wicking set up. Porosity and permeability did not change significantly after polymer grafting, while the wicking rate of water did change. Therefore, it was concluded that the surface energy was a major parameter for wicking kinetic when the fabric was grafted with a thin polymeric film. Thus, the surface modification with polymer grafting is a suitable approach for designing fabric with controlled liquid transport properties, such as directional liquid transport.

We also computed the water contact angles from the well-known Washburn's equation by using experimentally determined wicking constants for water and hexadecane, then compared them with the predicted values calculated from the Cassie model. Good agreement indicates that the evaluation of the wicking kinetics was a better approach than the contact angle measurement for studying the effects of polymer grafting on the wetting behavior of the fabric.

5.5. References

1. Liang, J.; Zhou, Y.; Jiang, G.; Wang, R.; Wang, X.; Hu, R.; Xi, X., Transformation of hydrophilic cotton fabrics into superhydrophobic surfaces for oil/water separation. *Journal of The Textile Institute* **2012,** *104* (3), 305-311.

2. Xing, S.; Jiang, J.; Pan, T., Interfacial microfluidic transport on micropatterned superhydrophobic textile. *Lab on a Chip* **2013**.

3. Liu, Y.; Tang, J.; Wang, R.; Lu, H.; Li, L.; Kong, Y.; Qi, K.; Xin, J., Artificial lotus leaf structures from assembling carbon nanotubes and their applications in hydrophobic textiles. *J. Mater. Chem.* **2007,** *17* (11), 1071-1078.

4. Zimmermann, J.; Reifler, F. A.; Fortunato, G.; Gerhardt, L. C.; Seeger, S., A simple, one-step approach to durable and robust superhydrophobic textiles. *Advanced Functional Materials* **2008,** *18* (22), 3662-3669.

5. Hoefnagels, H.; Wu, D.; De With, G.; Ming, W., Biomimetic superhydrophobic and highly oleophobic cotton textiles. *Langmuir* **2007,** *23* (26), 13158-13163.

6. Ramaratnam, K.; Tsyalkovsky, V.; Klep, V.; Luzinov, I., Ultrahydrophobic textile surface via decorating fibers with monolayer of reactive nanoparticles and non-fluorinated polymer. *Chemical Communications* **2007,** *0* (43), 4510-4512.

7. Princi, E.; Vicini, S.; Proietti, N.; Capitani, D., Grafting polymerization on cellulose based textiles: A 13C solid state NMR characterization. *European Polymer Journal* **2005,** *41* (6), 1196-1203.

8. Hochart, F.; De Jaeger, R.; Levalois-Grützmacher, J., Graft-polymerization of a hydrophobic monomer onto PAN textile by low-pressure plasma treatments. *Surface and Coatings Technology* **2003,** *165* (2), 201-210.

9. Tsafack, M. J.; Levalois-Grützmacher, J., Towards multifunctional surfaces using the plasma-induced graft-polymerization (PIGP) process: Flame and waterproof cotton textiles. *Surface and Coatings Technology* **2007,** *201* (12), 5789-5795.

10. Gawish, S.; Ramadan, A.; Cornelius, C.; Bourham, M.; Matthews, S.; McCord, M.; Wafa, D.; Breidt, F., New functionalities of PA6, 6 fabric modified by atmospheric pressure plasma and grafted glycidyl methacrylate derivatives. *Textile Research Journal* **2007,** *77* (2), 92-104.

11. Burtovyy, O.; Klep, V.; Chen, H. C.; Hu, R. K.; Lin, C. C.; Luzinov, I., Hydrophobic modification of polymer surfaces via “grafting to” approach. *Journal of Macromolecular Science, Part B* **2007,** *46* (1), 137-154.

12. Chen, J.-P.; Chiang, Y.-P., Surface modification of non-woven fabric by DC pulsed plasma treatment and graft polymerization with acrylic acid. *Journal of Membrane Science* **2006,** *270* (1–2), 212-220.

13. Cristofor; Simionescu; Dénes, F.; Macoveanu, M. M.; Negulescu, I., Surface modification and grafting of natural and synthetic fibres and fabrics under cold plasma conditions. *Die Makromolekulare Chemie* **1984,** *8* (S19841), 17-36.

14. Mehta, I. K.; Kumar, S.; Chauhan, G. S.; Misra, B. N., Grafting onto isotactic polypropylene. III. Gamma rays induced graft copolymerization of water soluble vinyl monomers. *Journal of Applied Polymer Science* **1990,** *41* (5-6), 1171-1180.

15. Burtovyy, O.; Klep, V.; Turel, T.; Gowayed, Y.; Luzinov, I., Polymeric membranes: Surface modification by "grafting to" method and fabrication of multilayered assemblies. In *Nanoscience and Nanotechnology for Chemical and Biological Defense*, American Chemical Society: 2009; Vol. 1016, pp 289-305.

16. Pittman, J. J.; Klep, V.; Luzinov, I.; Marcus, R. K., Extraction of metals from aqueous systems employing capillary-channeled polymer (C-CP) fibers modified with poly(acrylic acid) (PAA). *Analytical Methods* **2010,** *2* (5), 461-469.

17. Zdyrko, B.; Luzinov, I., Polymer brushes by the “grafting to” method. *Macromolecular Rapid Communications* **2011,** *32* (12), 859-869.

18. Burtovyy, O.; Klep, V.; Chen, H. C.; Hu, R. K.; Lin, C. C.; Luzinov, I., Hydrophobic modification of polymer surfaces via ``grafting to`` approach. *Journal of Macromolecular Science, Part B* **2007,** *46* (1), 137-154.

19. Hoefnagels, H. F.; Wu, D.; de With, G.; Ming, W., Biomimetic superhydrophobic and highly oleophobic cotton textiles. *Langmuir* **2007,** *23* (26), 13158-13163.

20. Caschera, D.; Cortese, B.; Mezzi, A.; Brucale, M.; Ingo, G. M.; Gigli, G.; Padeletti, G., Ultra hydrophobic/superhydrophilic modified cotton textiles through functionalized diamond-like carbon coatings for self-cleaning applications. *Langmuir* **2013,** *29* (8), 2775-2783.

21. Wiener, J.; DejlovÃ¡, P., Wicking and wetting in textiles. *AUTEX Research Journal* **2003,** *3* (2), 64-71.

22. Kamath, Y. K.; Hornby, S. B.; Weigmann, H.-D.; Wilde, M. F., Wicking of spin finishes and related liquids into continuous filament yarns. *Textile Research Journal* **1994,** *64* (1), 33-40.

23. Kissa, E., Wetting and wicking. *Textile Research Journal* **1996,** *66* (10), 660-668.

24. Harnett, P.; Mehta, P., A survey and comparison of laboratory test methods for measuring wicking. *Textile Research Journal* **1984,** *54* (7), 471-478.

25. Wang, Y.; Moatamedi, M.; Grove, S. M., Continuum dual-scale modeling of liquid composite molding processes. *Journal of Reinforced Plastics and Composites* **2009,** *28* (12), 1469-1484.

26. Ghali, K.; Jones, B.; Tracy, J., Experimental techniques for measuring parameters describing wetting and wicking in fabrics. *Textile Research Journal* **1994,** *64* (2), 106-111.

27. Oktem, T.; Seventekin, N.; Ayhan, H.; Piskin, E., Modification of polyester and polyamide fabrics by different in situ plasma polymerization methods. *Turkish Journal of Chemistry* **2000,** *24* (3), 275-286.

28. Yao, Z. P.; Rånby, B., Surface modification by continuous graft copolymerization. III. Photoinitiated graft copolymerization onto poly(ethylene terephthalate) fiber surface. *Journal of Applied Polymer Science* **1990,** *41* (7-8), 1459-1467.

29. Krump, H.; Simor, M.; Hudec, I.; Jasso, M.; Luyt, A. S., Adhesion strength study between plasma treated polyester fibres and a rubber matrix. *Applied Surface Science* **2005,** *240* (1-4), 268-274.

30. Gotoh, K.; Yasukawa, A., Atmospheric pressure plasma modification of polyester fabric for improvement of textile-specific properties. *Textile Research Journal* **2011,** *81* (4), 368-378.

31. Leroux, F.; Campagne, C.; Perwuelz, A.; Gengembre, L., Fluorocarbon nano-coating of polyester fabrics by atmospheric air plasma with aerosol. *Applied Surface Science* **2008,** *254* (13), 3902-3908.

32. Krump, H.; Hudec, I.; Jasso, M.; Dayss, E.; Luyt, A. S., Physical-morphological and chemical changes leading to an increase in adhesion between plasma treated polyester fibres and a rubber matrix. *Applied Surface Science* **2006,** *252* (12), 4264-4278.

33. Choi, H.; Lee, J., The psycho-physiological response of polyethylene terephthalate irradiated by ultra-violet: Subjective fabric hand and wear comfort. *Fibers and Polymers* **2006,** *7* (4), 442-445.

34. Kan, C. W.; Yuen, C. W. M., Static properties and moisture content properties of polyester fabrics modified by plasma treatment and chemical finishing. *Nuclear instruments and methods in physics research section B: beam interactions with materials and atoms* **2008,** *266* (1), 127-132.

35. Liu, Y.; He, T.; Gao, C., Surface modification of poly(ethylene terephthalate) via hydrolysis and layer-by-layer assembly of chitosan and chondroitin sulfate to construct cytocompatible layer for human endothelial cells. *Colloids and Surfaces B: Biointerfaces* **2005,** *46* (2), 117-126.

36. Hsieh, Y.-L.; Miller, A.; Thompson, J., Wetting, pore structure, and liquid retention of hydrolyzed polyester fabrics. *Textile Research Journal* **1996,** *66* (1), 1-10.

37. Burtovyy, O. Synthesis and characterization of macromolecular layers grafted to polymer surfaces. Dissertation, Clemson University 2008.

38. Wong, K. K.; Tao, X. M.; Yuen, C. W. M.; Yeung, K. W., Wicking properties of linen treated with low temperature plasma. *Textile Research Journal* **2001,** *71* (1), 49-56.

39. Sanders, E. M.; Zeronian, S. H., An analysis of the moisture-related properties of hydrolyzed polyester. *Journal of Applied Polymer Science* **1982,** *27* (11), 4477-4491.

40. Lucas, R., Ueber das Zeitgesetz des kapillaren Aufstiegs von Flüssigkeiten. *Kolloid-Zeitschrift* **1918,** *23* (1), 15-22.

41. Washburn, E. W., The dynamics of capillary flow. *Physical Review* **1921,** *17* (3), 273-283.

42. Callegari, G.; Tyomkin, I.; Kornev, K. G.; Neimark, A. V.; Hsieh, Y.-L., Absorption and transport properties of ultra-fine cellulose webs. *Journal of colloid and interface science* **2011,** *353* (1), 290-293.

43. Hashemizad, S.; Montazer, M.; Rashidi, A., Influence of the surface hydrolysis on the functionality of poly(ethylene terephthalate) fabric treated with nanotitanium dioxide. *Journal of Applied Polymer Science* **2012,** *125* (2), 1176-1184.

44. Bendak, A.; Raslan, W. M., Dyeability improvement of polyester pretreated with some alkoxides. *Journal of Applied Polymer Science* **2008,** *108* (1), 7-13.

45. Sanders, E. M.; Zeronian, S. H., An analysis of the moisture-related properties of hydrolyzed polyester. *Journal of Applied Polymer Science* **1982,** *27* (11), 4477-4491.

46. Donelli, I.; Freddi, G.; Nierstrasz, V. A.; Taddei, P., Surface structure and properties of poly-(ethylene terephthalate) hydrolyzed by alkali and cutinase. *Polymer Degradation and Stability* **2010,** *95* (9), 1542-1550.

47. Patankar, N. A., Mimicking the lotus effect: Influence of double roughness structures and slender pillars. *Langmuir* **2004,** *20* (19), 8209-8213.

48. Ramaratnam, K. Ultrahydrophobic surface modification of polymeric fibers and inorganic substrates. Dissertation, Clemson University, 2007.

49. Michielsen, S.; Lee, H. J., Design of a superhydrophobic surface using woven structures. *Langmuir* **2007,** *23* (11), 6004-6010.

50. Mhetre, S.; Parachuru, R., The effect of fabric structure and yarn-to-yarn liquid migration on liquid transport in fabrics. *Journal of The Textile Institute* **2010,** *101* (7), 621-626.

51. Cassie, A. B. D.; Baxter, S., Wettability of porous surfaces. *Transactions of the Faraday Society* **1944,** *40* (0), 546-551.

52. Young, T., An essay on the cohesion of fluids. *Philosophical Transactions of the Royal Society of London* **1805,** *95*, 65-87.

53. Wenzel, R. N., Resistance of solid surfaces to wetting by water. *Industrial & Engineering Chemistry* **1936,** *28* (8), 988-994.

54. Yildirim, I. Surface free energy characterization of powders. http://scholar.lib.vt.edu/theses/available/etd-05042001-163337.

55. Quantifying wetting and wicking phenomena in cotton terry as affected by fabric conditioner treatment. http://hdl.handle.net/1854/LU-152307.

56. Turan, R. B.; Okur, A.; Deveci, R.; Açıkel, M., Predicting the intra-yarn porosity by image analysis method. *Textile Research Journal* **2012**.

57. Yang, J. M.; Lin, H. T., Properties of chitosan containing PP-g-AA-g-NIPAAm bigraft nonwoven fabric for wound dressing. *Journal of Membrane Science* **2004,** *243* (1–2), 1-7.

58. Rahli, O.; Tadrist, L.; Miscevic, M.; Santini, R., Fluid flow through randomly packed monodisperse fibers: the Kozeny-Carman parameter analysis. *Journal of fluids engineering* **1997,** *119* (1), 188-192.

CHAPTER SIX

FABRIC WITH WETTABILITY GRADIENT

6.1. Introduction

Gradient surfaces have attracted scientists for both theoretical and practical purposes. For example, the wettability gradient has been used to investigate the behavior of small droplets on surfaces and modeling and understanding the effect of surface tension on droplet motion.[1-5] In addition, the variation of properties on one single surface is a great advantage for many combinatorial studies, such as the interaction of biological compounds with modified surfaces and the movements of molecules and bacteria.

A variation in number of functional groups, molecular weight, chemical composition, grafting density of polymer layers or particle concentration, or combination of those parameters on a surfaces can be achieved in gradual manner. Previous chapters of this study have covered that wettability is a function of surface tension. Therefore, a wettability gradient on a surface can be achieved with creation of a surface tension gradient.

Many chemical reactions between two compounds are temperature- and time-dependent. Therefore, the temperature gradient stage and the gradual immersion of a substrate to the reaction media have been two tactics widely employed for developing the wettability gradient. The first wettability gradient was developed by Elwing et al. in 1987.[6] The diffusion technique has been applied to form a gradient of methyl groups on a surface. In fact, it was the first study that employed a gradient approach to analyze the

surface energy dependence of the adsorption of proteins (such as human fibrinogen, γ-globulin, and lysozyme) on solid surfaces.[6] Later, the diffusion technique was applied to develop a wettability gradient surface; however, studies were limited to hydrophilic inorganic substrates. Pitt et al.[7, 8] and Lee et al. [9, 10] reported wettability gradient on polymer surfaces obtained using plasma and corona discharge techniques. The gradients, on a polyethylene (PE) surface, was achieved by a knife-type corona electrode whose power was manipulated gradually during the treatment; thus, concentrations of oxygen-containing constituents progressively altered, which led to gradual change in wettability.[9, 10]

As discussed herein before, grafting of end-functionalized polymers to the surface allows alteration of surface properties[11-16] and evidently can be applied to form a wettability gradient on the surface. Indeed, the grafting-to and the grafting-from techniques have been used to obtain a gradient coating on surfaces.

Ionov et al.[17-19] prepared a polymer layer with a gradient in grafting density. Grafting of end functionalized hydrophobic polymer (PS-COOH) to the PGMA anchoring layer in gradient manner has been achieved on a surface by using a temperature stage that generates a temperature gradient on the surface; thus, a gradual increase in gradient density can be achieved from the cold to hot ends of the sample. Mixed gradient polymer brushes have also been synthesized using the temperature gradient stage.[18]

Yu et al.[20] prepared a wettability gradient from super-hydrophilic to super-hydrophobic on a gold surface. They utilized time dependency of reaction kinetics.

Mainly, the reaction time on the sample was regulated by adding more solution to the reaction container that changed the upper solution level. Therefore, reaction time was longer on the bottom part of the sample as compared to the reaction time on the upper part of sample.

The wettability gradient prepared by the above-cited methods appears to be a useful and time-saving approach for many studies. However, most of them involve inorganic substrates and/or polymer films with limited flexibility. From the functional materials perspective, it is desirable to bring gradient properties to flexible fibrous substrates such as textile fabrics. Fabric possessing a gradient polymeric coating that introduces a wettability gradient property can be used to control and move liquid away from human skin to increase comfort. To the best of our knowledge, wettability gradient on a fabric in the long length scale has not been reported.

When the skin releases moisture, either it will evaporate, or the garment will absorb it. The garment should allow moisture evaporation to maintain user comfort. Thus far, moisture management with textile done by using micro fibers to introduce high capillary, or apply different finishes on both sides of fabric. The inner side is designed to be hydrophobic, and the outer side is hydrophilic. Therefore, moisture easily transfers through the fabric and evaporates. This design is successfully utilized in sport and summer clothing. However, in many cases, especially with the cold weather garments with several layers, water is trapped in the inner fabric, and evaporation is limited by several outer structures. Particularly for soldiers on the battlefield, sweat most likely is

absorbed and trapped by the inner fabric. In that case, wetness reduces comfort, and the sensation of cold ensues because of reduced thermal insulation.

This study focuses on synthesizing gradient polymer layers and fabricating fabric with a wettability gradient. The experimental development reported in this chapter represents the formation of wettability gradient through the long length scale of the PET fabric and the feasibility of using such a fabric in a laminated structure for moisture management in a body armor garment.

6.2. Experimental

6.2.1. Model film preparation, activation and PGMA anchoring layer formation

Model film preparation (~43nm), activation, and anchoring layer formation were done as explained in Chapter 4. Plasma activation time was 40 seconds for all samples, and PGMA ($M_n \approx$ 176,000 g/mol) layer (~6-7nm) formation was done at 60°C in a vacuum oven for 3 hours.

6.2.2. Single component polymer coating and formation of non-gradient mixed polymer brushes on PET film under static conditions

To obtain a wettability gradient, we followed two-step procedures. In the first step, a hydrophobic gradient polymer layer was synthesized on the film or fabric substrate. In the second step, a hydrophilic polymer was grafted to the surface containing hydrophobic gradient polymer layer.

In order to study grafting kinetics and obtain a reference polymer brush with uniform thickness, polymers were coated separately on the PGMA/PET film and annealed in a vacuum oven under static conditions for varying times at set temperatures.

To analyze the PS-COOH grafting capacity of the PGMA anchoring film (~6 nm), polymer solution (2% vol/wt PS-COOH in toluene) was deposited on the surface of PGMA/PET film by drop casting. After films were dried at room temperature for 30 minutes, samples were placed in a vacuum oven and annealed at 150°C for different times under static conditions. Then samples were washed thoroughly in toluene to remove unbonded PS-COOH chains. Film thicknesses were measured by ellipsometry.

Single–component polyacrylic acid (PAA) layer was also grafted to the PGMA/PET film. Deposition was done by dip coating form a1 wt/vol % PAA solution in methanol. PAA-deposited samples were annealed in a 120°C vacuum oven for different annealing times.

To obtain a reference brush for gradient layer preparation, non-gradient mixed polymer brush were formed. Samples with variable PS layer grafting density were prepared and rinsed with MEK, a good solvent for the PGMA anchoring layer. Then, a hydrophilic polymer PAA was deposited by dip coating on the PS/PGMA/PET layer. Annealing was done under static conditions in a 120°C vacuum oven for 6 minutes.

6.2.3. Preparation of gradient polymer coating on the PET film

To achieve grafting density gradient in the polymer layer grafted to the model PGMA/PET /silicon wafer, a gradual immersion technique was used. Setup consisted of

an oven and a motor-controlled dip-coating mechanism **(Figure 6.1).** The speed of immersion could be varied. The achievable minimum running speed was 0.5 mm/sec. The oven has an upper opening that allowed sample immersion. Dip coating apparatuses made it possible to gradually immerse and pull out a sample with a controlled speed. Thus, the annealing time could be varied.

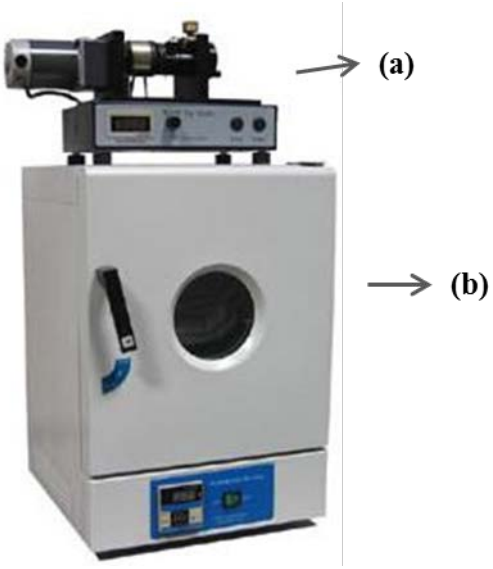

Figure 6.1. Desktop dip coater with digital controlled temperature chamber. (a) dip coater unit,(b) oven unit.

The initial PS-COOH film was deposited on the PGMA/PET layer by drop casting. The grafting of the deposited PS-COOH layer was done in dynamic mode by immersing the substrate in the oven and varying the annealing time simply by gradually removing it from the oven to form a polymer coating with grafting density gradient by controlling the annealing time. PS-COOH ungrafted macromolecules were removed with

multiple washing in toluene. The oven temperature was kept at 150°C, and the time of the sample pull was arranged to be 100 minutes total for 12 cm long samples.

Due to the high thermal conductivity of silicon wafers compared to fabric, in a dynamic model experiment, four SiO_2 (1x4 cm) samples were placed in an individual holder made of aluminum foil; each folder was attached with cotton yarn. Yarn joined the foil holders to prevent sample connection and heat transfer. In addition, the assembly allowed us to immerse them in the oven by dip coater. PGMA/PET films were initially formed on wafer surface. Then PS-COOH was deposited and dried at room temperature before placing wafers into the holder.

After dynamic annealing, PS-COOH was removed with toluene rinse. Samples were then washed with MEK to bring the PGMA chains to the surface. Then, PAA was deposited from 1 wt/vol % PAA in methanol by dip coating followed by grafting at static mode in a vacuum oven at 120^{o}C for 6 minutes. The surface was then rinsed with methanol many times to remove free polymers.

6.2.4. Surface modification of PET fabric

The preparation and activation of PET fabric (Test-FabricInc.#777H) and PGMA anchoring layer formation were explained in **Section 3.5.2** and **5.2.1**, respectively.

6.2.4.1. Single-component polymer grafting on fabric

The polymers under investigation, PS-COOH, and PAA, were grafted to the epoxy-functionalized PET fabric. PS-COOH-deposited fabric was annealed in a 150°C

vacuum oven for 100 minutes. PAA-deposited fabric was annealed in a 120°C vacuum oven for 1 hour.

6.2.4.2. Formation of wettability gradient on fabric.

A wettability gradient was formed on the fabric surface in the following manner. PS-COOH was deposited on a 12 cm long PGMA/PET fabric and dried at room temperature. Then annealing was done in dynamic mode using the dip-coater oven assembly. After rinsing the surface with toluene to remove unattached PS-COOH chains, the fabric was dried and rinsed with MEK. Finally, PAA was deposited and annealed in a 120°C vacuum oven for 6 min. Polymer concentrations and annealing conditions were kept the same as annealing conditions for the model study. After the grafting, surfaces were thoroughly washed with a suitable solvent to remove unbounded polymer and dried until a constant weight was achieved. Polymers were chosen to achieve different water wettability.

6.3. Results and discussion

The main goal of this part of the dissertation is to form mixed polymer grafting layers using a homogeneous anchoring layer. **Figure 6.2** demonstrates the formation of mixed polymer brushes with a concentration gradient of two polymers in an opposite direction. As the schematic shows, three types of macromolecules are attached to the surface. Polymer 1 is the PGMA anchoring layer. Polymer 2 is the terminally

functionalized hydrophobic polymer PS-COOH layer, and Polymer 3 is the hydrophilic polymer PAA layer.

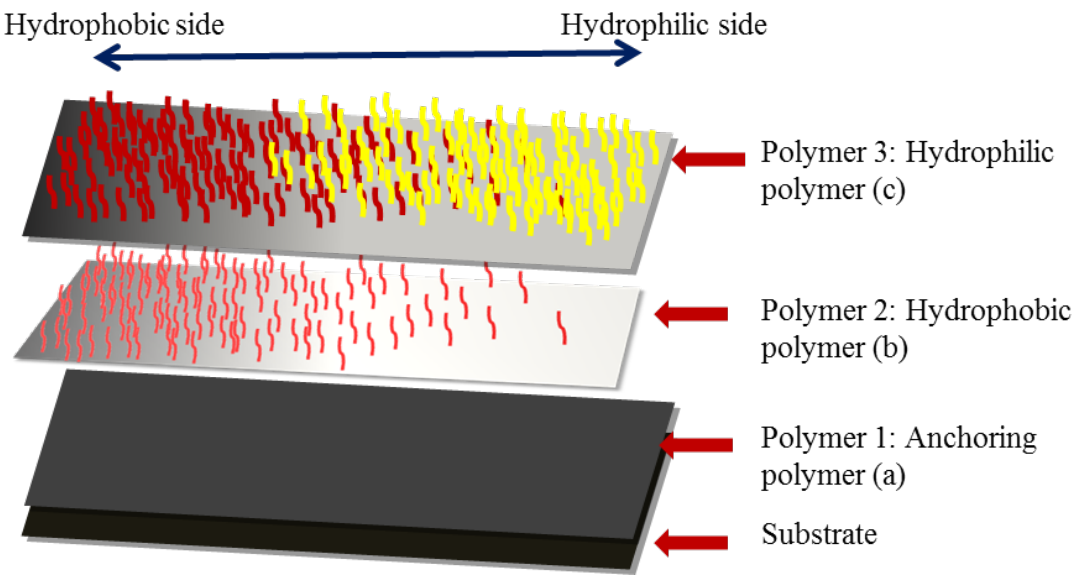

Figure 6.2. Schematic illustration of synthesis of the mixed polymer brushes with a concentration gradient of two polymers in reverse directions.

PGMA anchoring layer was previously used to obtain mixed polymer brushes[21] and mixed polymer layers with thickness gradients.[22, 23] Simply by varying the grafting density of a secondary polymer, mixed polymer brush surfaces at various concentrations of polymers can be obtained. The concentration of mixed brush constituents can also gradually varied by gradual change in reaction condition. Therefore, the mixed brush system, where concentrations of each component change in reverse directions across the sample length, can be formed.

Initially, uniform PGMA film was formed on the surface of activated PET film. A discussion on anchoring layer preparation was provided in **Chapter 4**. After the anchoring layer formation, hydrophobic polymer film (PS) synthesized on the PGMA/PET layer with grafting density gradient. When proper experimental conditions are used, PS brushes will be dominant on one side of the surface, and the other side will have minimal or no PS brushes **(Figure 6.2b).** The composition of the surface in **Figure 6.2b** can be altered to extend PGMA chains; hence, epoxy functionality will be exposed to the surface. This can be achieved by treating the surface with a good solvent for PGMA. When epoxy group concentration is increased on the surface, PAA can be grafted. The surface in **Figure 6.2c** will have a mixed brush where concentration of the polymers gradually changes not only along the surface, but also in reverse directions to each other.

Here, work was done to determine optimal grafting conditions to obtain a gradient polymer layer consisting of mixed brush on the PET surface that is suitable to acquire a wettability gradient on PET fabric. To optimize experimental conditions for synthesis of the gradient polymer brushes on the fabric and on the model PET film surface, we first evaluated kinetics of single component polymer grafting.

6.3.1. Single-component PS brushes

Grafting of the single component PS-COOH has been studied to evaluate the effect of annealing time on thickness and determine the conditions needed to obtain a PS film with concentration gradient. Thicknesses measured by ellipsometry indicated that PS grafting density increased with annealing time **(Figure 6.3).** When annealing time was

below 40 minutes, no significant amount of PS-COOH was grafted to the surface. The highest grafting was achieved when reaction time was 100 minutes. Different grafting amounts of PS-COOH on ~6 nm PGMA indicated that not all epoxy groups reacted with PS-COOH functionality at low annealing times.

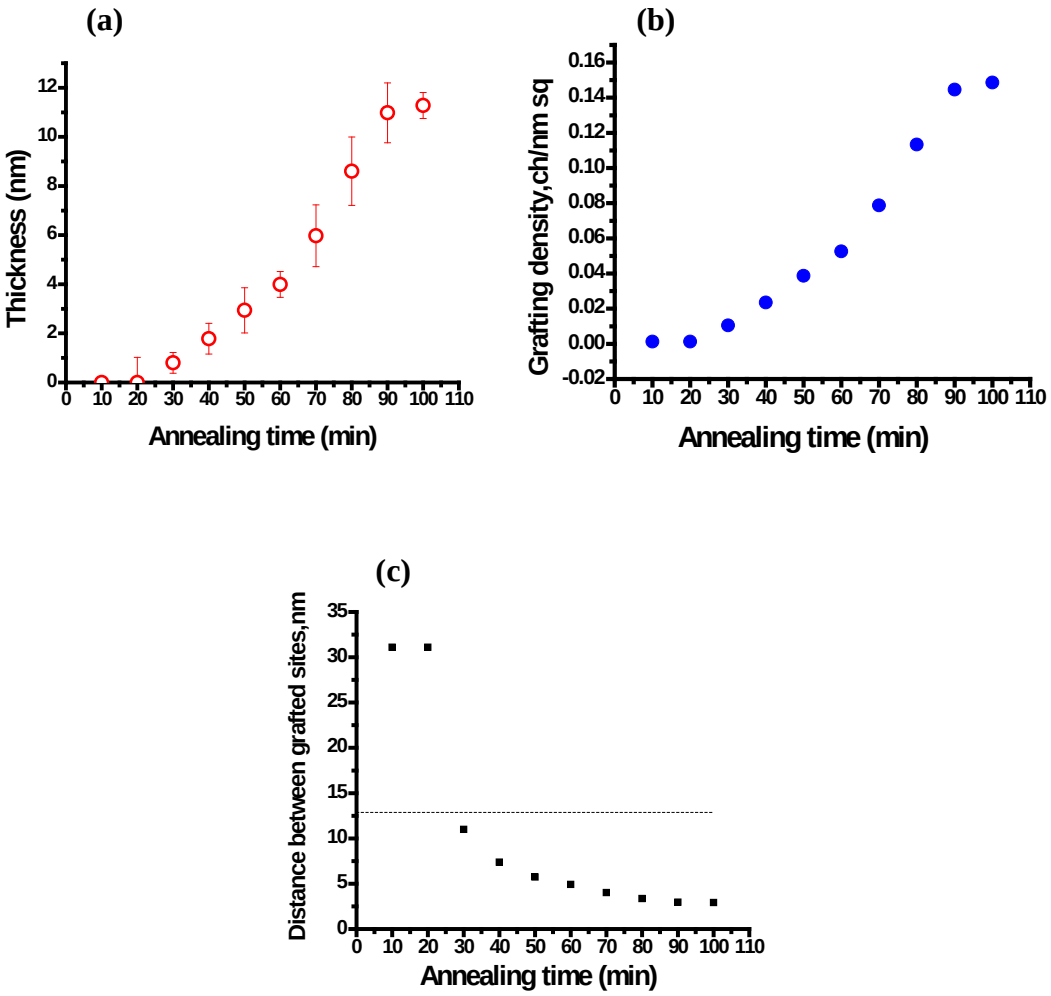

Figure 6.3. PS (a) layer thickness, (b) grafting density, and (c) distance between grafting sites variation with annealing time at 150°C. The substrate is a PGMA/PET/silicon wafer. Dash line shows the end-to end distance of PS macromolecules.

Distance between grafting sites (*D*) for the layers synthesized at the long annealing time is lower than the bulk end-to-end distance for the PS macromolecule (12.9 nm), indicating that the PS macromolecules are densely grafted and are in the ``brush regime``**(Figure 6.3c).**

Iyer et al.[21]reported the formation of mixed polymer system containing a PS and anchoring PGMA layer and showed that surface wettability of the PS/PGMA layer can be tailored by a selective solvent treatment. To this end, PS/PGMA/PET surfaces have been rinsed with MEK and toluene that is a good solvent for PGMA and PS, respectively. After rinsing with each solvent, the water contact angle was measured. Results are reported in **Figure 6.4c,d.** The Cassie equation[24] **(E.6.1)** and the surface's experimentally determined contact angle were applied to evaluate the PS composition of the PS/PGMA/PET surface.

$$\cos\theta = \varphi\cos\theta_A + (1-\varphi)\cos\theta_B \qquad \textbf{E.6.1}$$

In the equation, Θ is the water contact angle on the PS/PGMA layer. Θ_A and Θ_B are the water contact angles of the homo-polymer PS and PGMA layers, respectively, and the φ is the fraction of the surface that was covered by PS. The water contact angle on the PS and PGMA homopolymer brushes were 87° and 55°, respectively. It should be mentioned that the water contact angle on the PS/PGMA layer depends on the fraction of PS in the PS/PGMA layer.

PS/PGMA thickness ratio was increasing with annealing time **(Figure 6.4a)**. Cassie calculation indicated that and PS fraction on PS/PGMA layer depends on PS layer annealing time, and solvent that surface is exposed **(Figure 6.4b).**

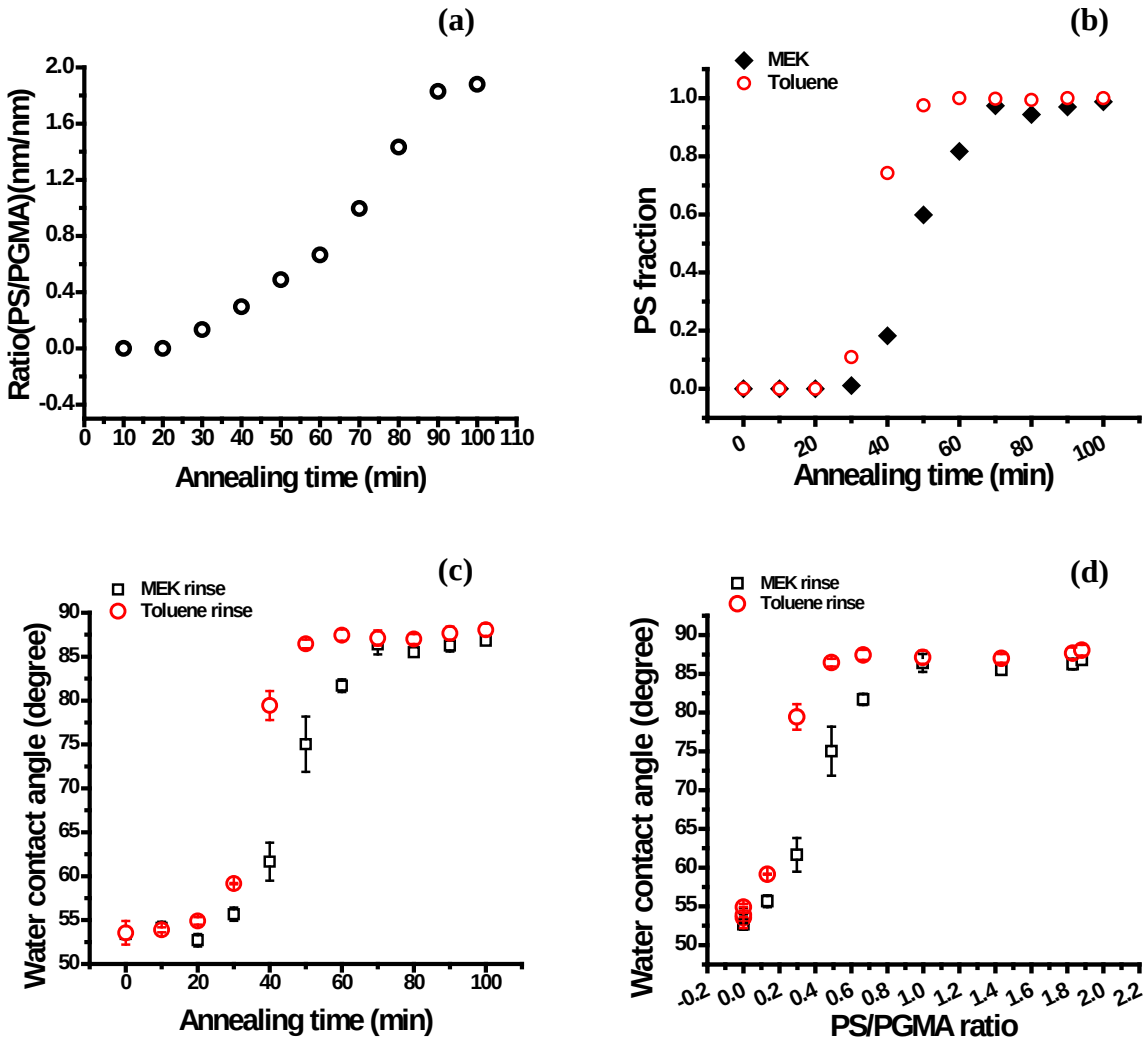

Figure 6.4. (a) PS/PGMA thickness ratio versus PS annealing time. (b) Fraction of grafted polystyrene on the surface after toluene and MEK rinse calculated using the Cassie equation. Water contact angle on the PS grafted layer versus (c) annealing time and (d) PS/PGMA ratio. The annealing temperature was 150°C. The surface was PGMA/PET film.

Generally, higher WCA on the surface after toluene treatment was observed. Changes in contact angle were plotted versus PS/PGMA thickness ratios **(Figure 6.5).** No switching in WCA was observed when annealing time was below 20 minutes, which corresponds to the 0 PS/PGMA ratio. The lowest degree of switching was observed when the PS/PGMA ratio was above 1 (70 minutes annealing). Switching was unrelated to PS layer thickness when the PS/PGMA ratio was above 1. The highest degree of switching was observed at ~0.3 PS/PGMA ratio that corresponds to the 2 nanometer PS layer thickness and 40 minutes annealing. Decreased WCA (after MEK) indicated that polymers adapted a new conformation and more epoxy groups were exposed to the surface. It can be also concluded that the switching in WCA on the surface was related to grafted polymer ratios. When ratios were between 0.2 to 1, surfaces with a clear switching ability were obtained. Obviously, more epoxy would be available on the mixed brush surface for another polymer grafting after MEK rinse. **Figure 6.6** illustrates the conformational changes on the mixed polymer brush grafted surface after the rinsing surface with a selective solvent.

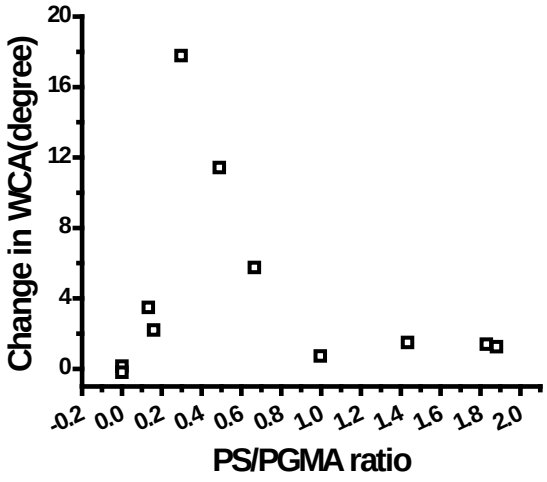

Figure 6.5. Change in WCA versus PS/PGMA thickness ratio after a selective solvent rinse. Surfaces were rinsed with first toluene, then MEK. WCAs were measured after each solvent rinse.

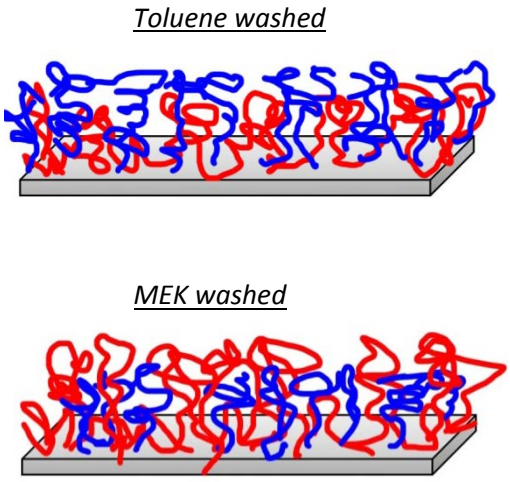

Figure 6.6. Illustration of PS/PGMA mixed brush after selective solvent rinse.

On the other side regardless of solvent, that surface is exposed; stepwise increase in water contact angle is observed with increase in annealing time, while change in thickness and ratio is linear **(compare Figure 6.3a and 6.4c).** This can be explained with the non-linear dependence for the fraction of surface screened with PS chains. Therefore, for better understanding of the wettability, coverage of surface with the PS macromolecules have been estimated.

6.3.1.1. Modeling of PS gradient brushes

Wettability of the surface modified with the grafted polymer chains depends on the grafted layer parameters. When distance between the grafted sites (D) is low, chains overlap and forced to stretch away from the interface (``brush regime``). When D is high, polymer chains may adapt ``mushroom `` like or ``pancake`` like conformation, and do not screen the surface.[25]

Sofia and coworkers[26] studied how protein adsorption on PEO surface related to the PEO grafting density, PEO molecular type, molecular weight, and protein size. They proposed a physical model to explain the effect that polymer chain arrangement has on protein adsorption. The model is illustrated in **Figure 6.7. It is** based on the same approach that WCA is depend on the area occupied by the polymer that is directly related with the grafting density of the polymer molecules. The correlation assumes that *Rg* does not change until the brush regime (Regime III) is reached.

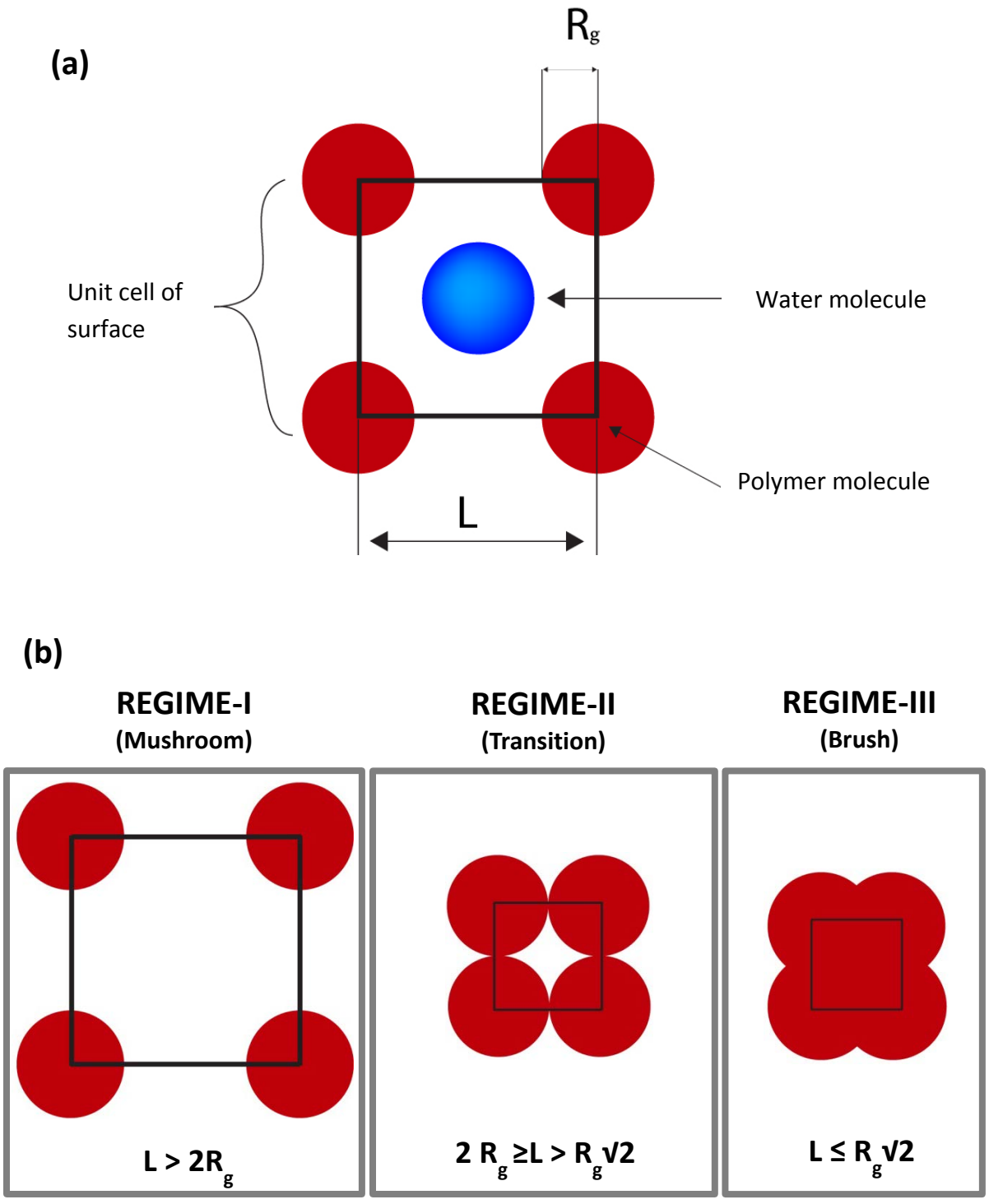

Figure 6.7. 2D geometric model of surface coverage. (a) The radius of the disc is equal to the Rg of polymer molecule. (b) A mathematical representation of different regimes for surface coverage. *Redrawn after Ref* [26].

Mei et. al [27] used the model and derived equations to correlate surface coverage with the grafted polymer thickness, radius of gyration (R_g), and molecular weight. S_{block} is a fraction of the surface occupied by the PS chains, and S_{open} is the fraction that is not occupied by PS chains. Model states that summation of S_{block} and S_{open} equals to one, where A_R, and $A_{covered}$ is the area of unit cell, and surface area covered by PS chains, respectively (E.6.2&3).

$$S_{block} + S_{open} = 1 \qquad \textbf{E.6.2}$$

$$S_{open} = 1 - S_{block} = \frac{A_R - A_{covered}}{A_R} \qquad \textbf{E.6.3}$$

In Regime-I, attached polymer chains are too far from each other to interact, thus are in the ``mushroom ``regime and satisfy the $L>2R_g$ correlation. S_{block} for Regime-I can be calculated with E.6.4.

$$S_{block} = 1 - \frac{L^2 - \pi R_g^2}{L^2} \qquad \textbf{E.6.4}$$

Regime –II defines the case where polymer chains start to overlap (with the increasing grafting density) but not completely cover the entire surface. This regime is a transition from ``mushroom`` to ``brush`` regime and satisfies the $2R_g \geq L > 2^{1/2} R_g$ relation. S_{block} for Regime-II can be calculated using the following equation(E.6.5), where a is the one dimensional length of a polymer segment and is ~0.6nm for PS.[28]

$$S_{block} = 1 - \frac{L^2 - \pi R_g^2 + 2R_g^2(2R_g^2 a \cos(L/2R_g) - L\sin(a\cos(L/2R_g)}{L^2} \qquad \textbf{E.6.5}$$

In Regime–III, $L \leq 2^{1/2} R_g$ correlation is satisfied. Grafting density is high enough to completely cover the surface. There is no open surface, thus S_{open} is equal to zero.

$$S_{open} = 0, \qquad S_{block} = 1$$

For our calculation radius of gyration (R_g) and average distance between chains (L) was estimated using the following equations, where N is degree of polymerization, h is dry thickness of polymer layer, p is dry polymer density, and M_n is the number average molecular weight.

$$R_g = a(N/6)^{1/2} \qquad \textbf{E.6.6}$$

$$L = (M_n / \rho h N_A)^{1/2} \qquad \textbf{E.6.7}$$

Fraction of the surface (S_{block}) that is covered with PS chains versus the grafting density of PS macromolecules is plotted in **Figure 6.8**. Results clearly revealed that fast transition in WCA is related with the surface screening with the PS chains. When PS grafted chains are in Regime-I, low WCA is obsereved(~ 60 degree). For the PS polymer used in this study (Mn 48000g/mol), Regime-I is observed when annealing time is lower than 40 minutes. Above 40 minutes annealing time, Regime –II and Regime-III are observed.

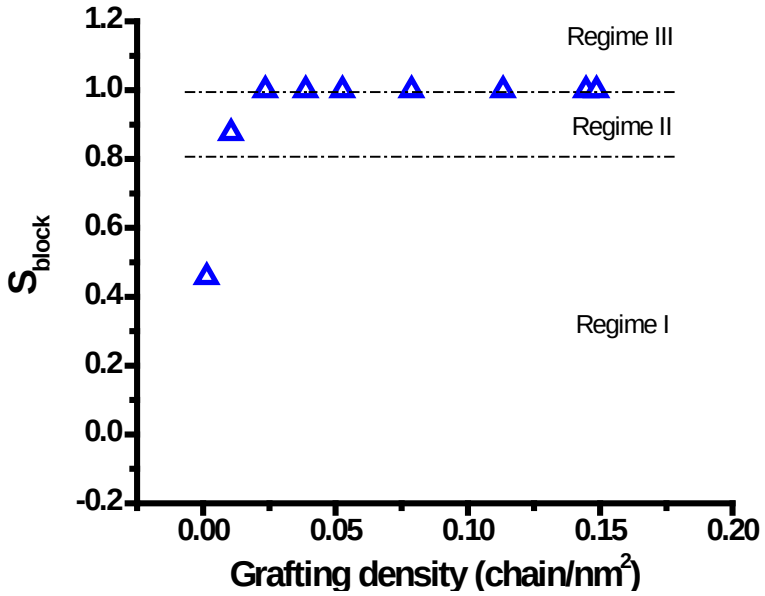

Figure 6.8. Fraction of surface that is covered with the PS as a function of grafting density.

Surface morphologies after the solvent treatments were analyzed with AFM, and the images are presented in **Figure 6.9**. The surface with the highest PS/PGMA ratio (1.88) has a smooth surface morphology after exposing it to a good solvent (toluene) for PS. At the 1.88 PS/PGMA ratio (~12 nm PS), PS grafting is close to saturation. A smooth surface with very low roughness (RMS 0.9 nm for PS/PGMA 1.88) indicates a homogenously covered surface. When the same surface is treated with a good solvent (MEK) for PGMA but a bad solvent for PS, epoxy groups, if there are any at the high PS/PGMA ratio, will be exposed to the surface. Indeed, surface roughness after MEK treatment slightly increases to ~1.1 nm for the sample with the highest PS/PGMA ratio.

This observation indicates that a small amount of PGMA exists on the surface even at the ratio of 1.88.

When the PS film annealing time was less than 40 minutes, the surface coating exhibits a rougher morphology, with 1.6±0.2 nm RMS roughness, after the toluene treatment; at low PS grafting times, the surface contains both PS and PGMA segments. After rinsing the surface with toluene, rougher and bumpier morphologies (for ratios <1) were observed. This is probably due to the collapsing of surface dominant polymer chains, PGMA, with toluene rinse. When the sample was washed with MEK, a good solvent for PGMA, the surface became smoother with 1.2 nm RMS roughness. After rinsing the surface with MEK, PS chains collapse, and PGMA chains extend **(Figure 6.6).** Thus, when the PS/PGMA ratio is low, PGMA chains are dominant on the surface. Hence, the surface adapts a smoother morphology after rinsing with MEK, compared to the morphology of the same surface after rinsing in toluene **(Figure 6.9)**.

A globular surface morphology was observed when the PS/PGMA ratio was below 0.3. The roughness of the globular surface decreased slightly with increased grafting thickness and virtually disappeared at the highest grafting thickness corresponding to a 1.88 PS/PGMA ratio after toluene rinse.

Thickness and water contact angle measurements revealed that, by controlling the PS concentration on a surface, one can graft another polymer by utilizing free epoxy groups. When the polymer ratio is between 0.2 and 1, a surface with clear wettability switching can be obtained, and a mixed polymer layer can be formed.

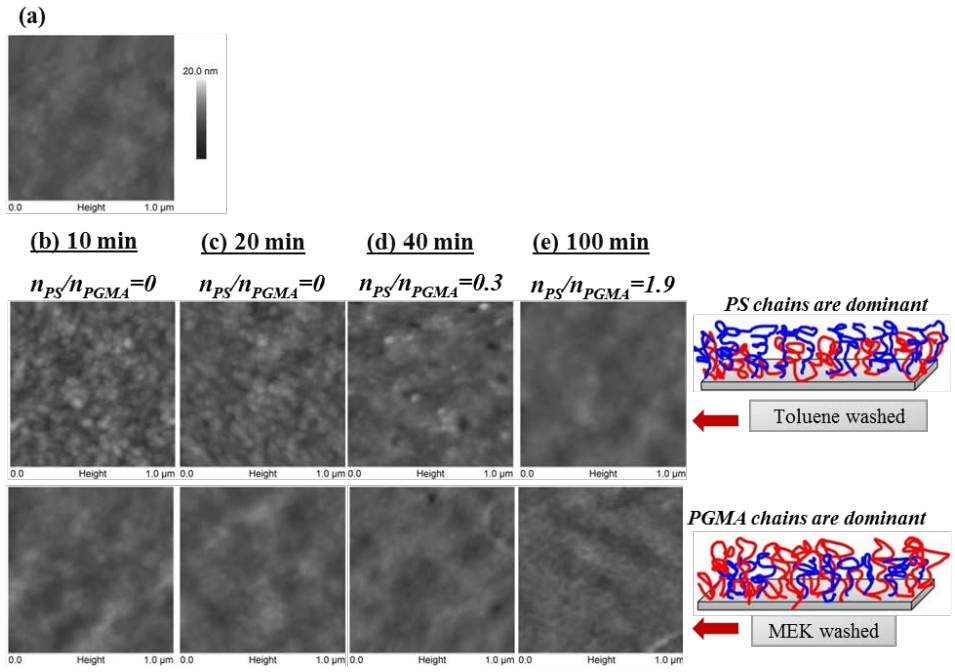

Figure 6.9. (a) Morphology of ~6 nm PGMA film. Morphology of PS layers on PGMA/PET film: (b) 10 minutes, (c) 20 minutes, (d) 40 minutes, and (e) 100 minutes annealing time. In images (b-e), top raw is after toluene rinse, and bottom raw is after MEK rinse.

6.3.2. Single-component PAA brushes

The wettability of a mixed-brush coated surface depends on the ratio between components and the solvent to which the surface has been exposed. Hence, the PAA/PS ratio in the mixed-brush layer is an important parameter to evaluate. In general, the grafting is controlled by two mechanisms: the reaction between complementary groups that are time- and temperature-dependent and the diffusion. In the current study PAA chains should diffuse through the PS grafted layer in order to reach free epoxy functionality.

We first studied single component PAA grafting to a PGMA-modified surface. The temperature was kept constant at 120^{o}C, and the annealing time was varied. A single-component grafting study shows that the grafting thickness of the PAA (on the ~6 to 7 nm PGMA film) layer increases with annealing time and reaches a maximum level after 30 minutes of annealing **(Figure 6.10a)**. PAA grafted to the PGMA surface even at room temperature.

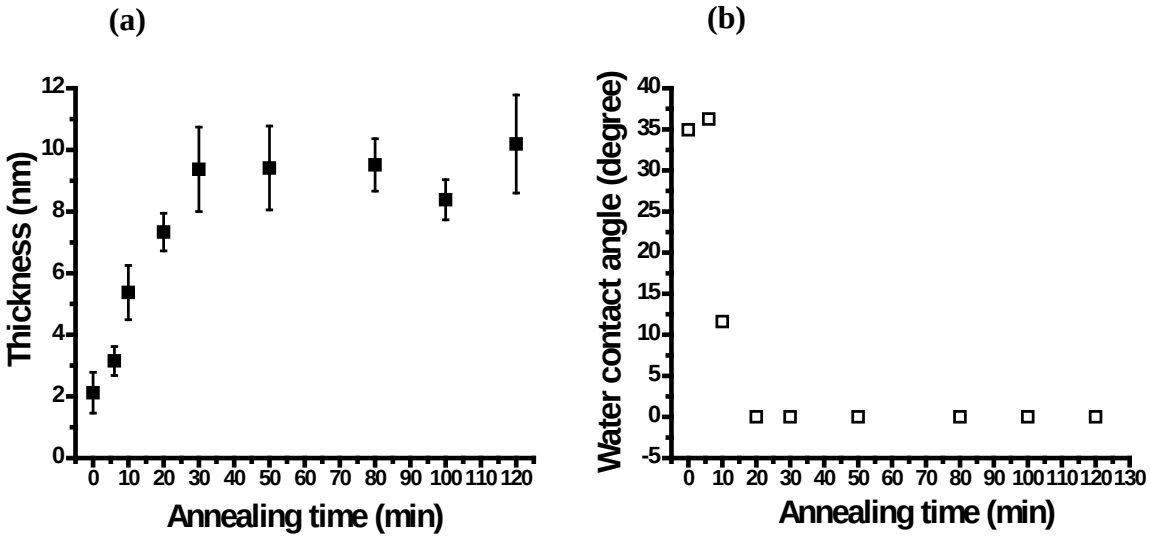

Figure 6.10. Properties of the PAA/PGMA/PET film after rinsing in methanol. (a) Thickness (b) Static water contact angle.

The static water contact angle for the PAA-grafted surface is presented in **Figure 6.10b.** The water contact angle indicates that, the surface becomes hydrophilic (WCA~37°) even when the annealing time was low as 6 minutes. A drop of water spread on the surface in less than 30 seconds when the annealing time was 20 minutes and higher **(Figure 6.10b)**.

The morphology of the PAA coated surface **(Figure 6.11)** shows the typical morphology of PAA film. PAA grafted to the surface homogeneously without dewetting even at the low annealing time. The surface demonstrated a cluster structure regardless of the annealing times. The cluster morphology of PAA can be attributed to the multiple connections between PAA chains and the surface, since PAA has –COOH in each monomeric unit. Similar morphologies have been reported by Gupta et al.[29] and Li.[30] Li reported an increased surface roughness with an increase in PAA grafting. In the current work, surface roughness did not change with the grafting amount. These differences can be related to anchoring layer thickness or the substrate, which in our case was PET film.

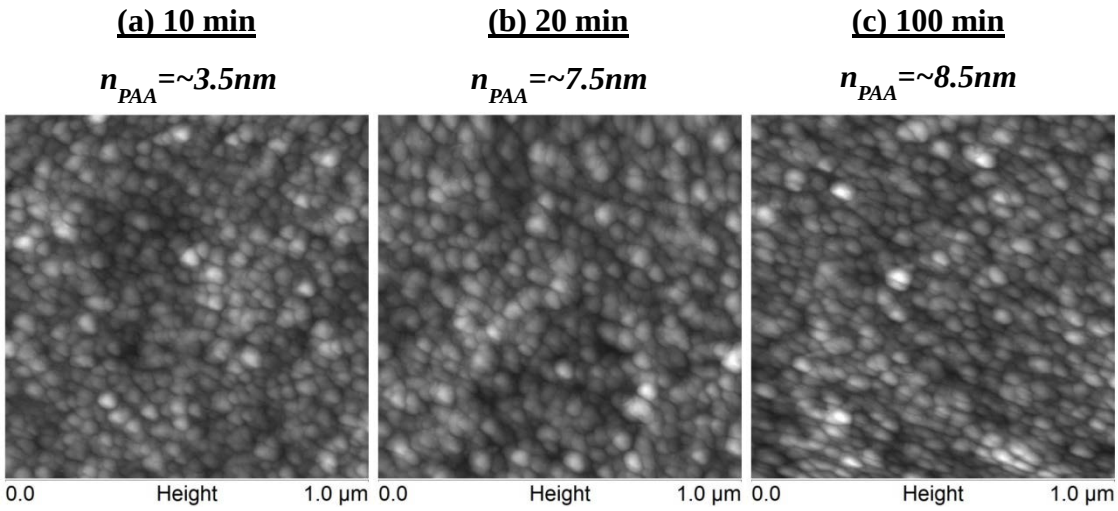

Figure 6.11. Morphology of PAA layer on the PAA/PGMA/PET film. (a) 10 minutes, (b) 20 minutes, and (c) 100 minutes annealing time.

6.3.3. Gradient mixed and non-gradient mixed polymer grafted layer

Previous sections analyzed grafting of the single-component PAA and PS-COOH macromolecules. This section is devoted to PAA grafting to the PS/PGMA surface. The PS grafted surfaces reported in **Section 6.3.1** were used here as substrates for the PAA grafting. The surfaces were initially treated with MEK to allow PGMA chains to extend to the surface.

The thickness of the PAA-grafted layer anchored to the PS/PGMA/PET substrate is given in **Figure 6.12a**. PAA is grafted to the PS/PGMA/PET surface even when the PS/PGMA ratio is as high as 1.88 (~11 nm PS layer). **Figure 6.12** can be divided into two regions, above and below the PS/PGMA thickness ratio of 0.5. The relationship between the PS/PGMA ratio and PAA grafting thickness is plotted in **Figure 6.12b**. The PAA grafting thickness was higher for the ratio below 0.5. Below the 0.5 ratio, there was no significant relationship between the ratio and PAA grafting.

PAA grafting on the PS/PGMA layer is controlled by the availability of epoxy groups and the diffusion of the PAA chains. The number of available epoxy groups decreases with increased PS thickness. As discussed before, PS-COOH virtually did not graft to the surface when the time of annealing was lower than 20 minutes, which means abundant epoxy groups were available for PAA grafting on the PS/PGMA surfaces that were annealed less than 20 minutes. This explains higher grafting thicknesses of the PAA layer on the samples that have the PS/PGMA ratio below 0.5. The diffusion of the chains is a function of temperature and time, and also restricted by PS chains that are already grafted to the surface. As evident from the graph, PAA can graft to the surface even at the

high PS grafting ratio. The results suggest that PAA can diffuse through the PS layer and reach the PGMA chains. This led us to conclude that the diffusion of the PAA chains at 120°C can overcome the PS layer steric hindrance effect.

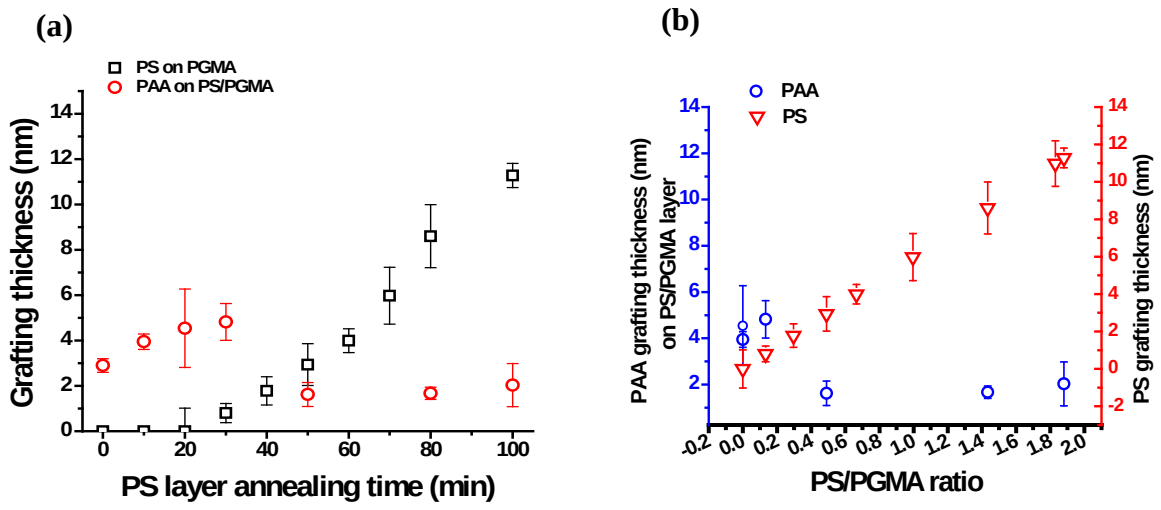

Figure 6.12. (a) Thickness of PAA layer in the PAA/PS/PGMA/PET film for different PS annealing times. (b) PS/PGMA ratio versus PAA and PS grafting thickness on PS/PGMA/PET film and PGMA/PET film, respectively.

The water contact angle measurements for the PAA-grafted layers after solvent treatment are given in **Figure 6.13a**. **Figure 6.13b** represents the change in the wettability of the PAA grafted surface with the change of PS/PAA thickness ratio. Clearly, the wettability of the PAA layer of the PAA/PS/PGMA grafted substrate can be altered by changing the thickness of the PS grafted layer. WCA can be varied from 0° to 80°.

AFM topography of the PAA layer (on PS/PGMA/PET) after selective solvent treatment is presented in **Figure 6.14**. After rinsing with methanol, the PAA-grafted surfaces for the low PS/PGMA ratios revealed a cluster morphology, which is similar to the single-component, PAA-grafted surface. This behavior can be explained with the collapsed PS chains and extended PAA brushes. A sample with a high PS/PGMA ratio has a smoother surface after the methanol rinse, similar to the single-component, PS-grafted surface. This is probably due to the low PAA concentration on the sample surface, which has a high PS/PGMA ratio(1.9). Consequently, the effects of the methanol rinse that collapses PS brushes and extends PAA brushes is not apparent on AFM images.

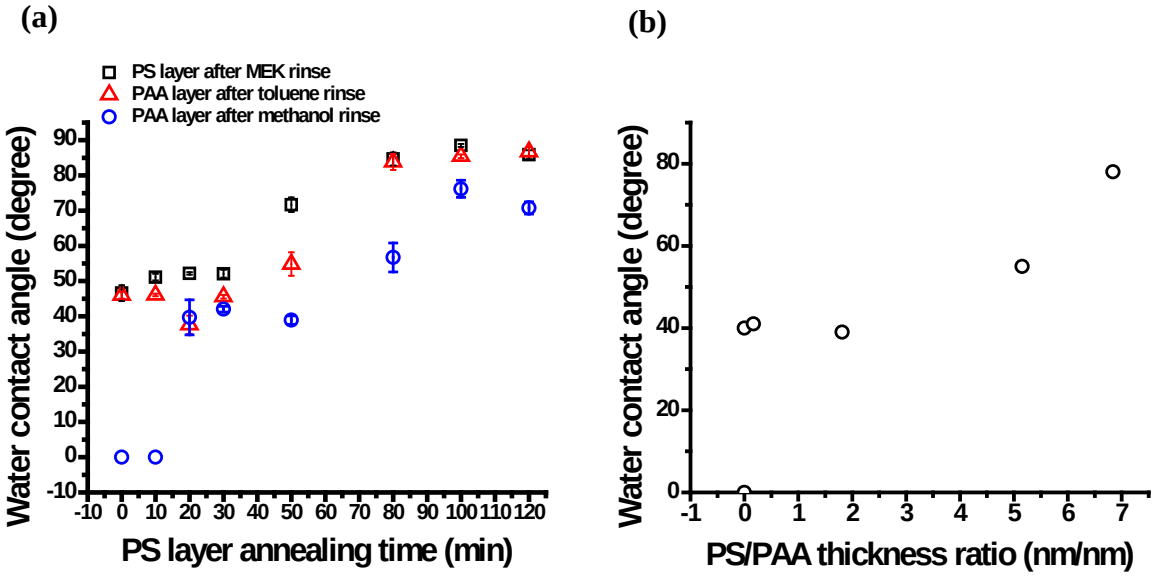

Figure 6.13. Water contact angle for the PAA/PS/PGMA/PET film versus (a) PS annealing time. (b) PS/PAA ratio of PAA/PS/PGMA/PET film.

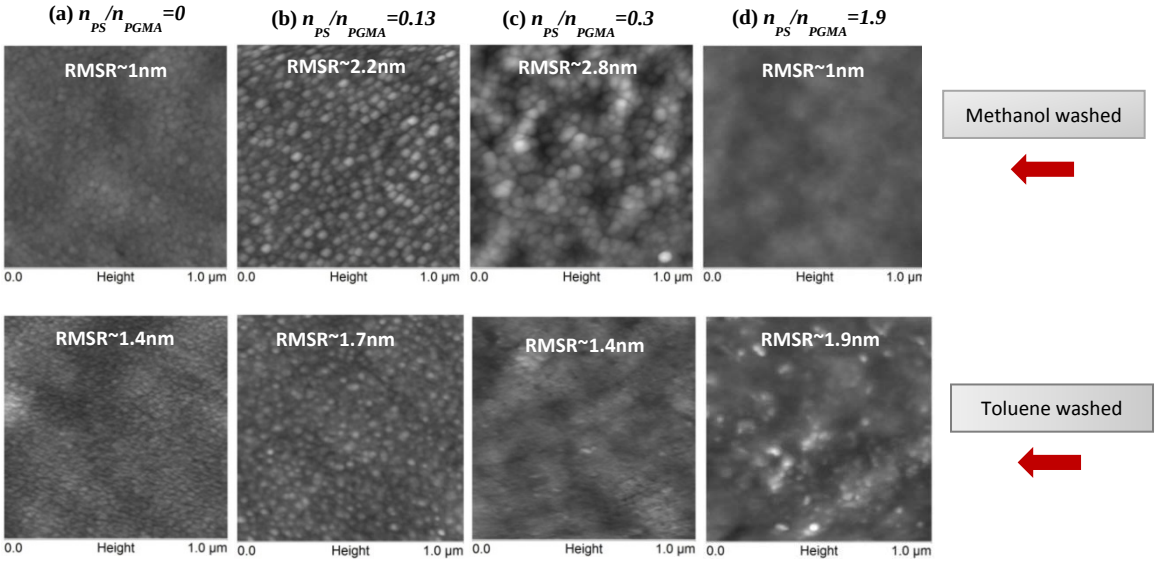

Figure 6.14. AFM topologies of PAA layer after selective solvent treatment. PAA layer is on the film (PS/PGMA/PET) with PS/PGMA ratio 0, 0.13, 0.3, 1.9 for image a, b, c, d, respectively.

After the successful formation of a mixed polymer brush with different polymer concentrations, a gradient mixed polymer surface was formed on the model PET film. PS was dropped on samples and samples were allowed to dry at room temperature for 30 minutes. Four PS deposited films were placed in an individual aluminum holder and holders connected with a cotton yarn. Then, the assembly was directed into the annealing oven by dip coating mechanism. Mixed brush with gradual change in concentration of constituents formed by gradual change of annealing time. Estimated time of annealing for each samples with corresponding measured grafting thickness and water contact angle are presented in **Figure 6.15**. In fact, gradient PS grafting was obtained. After treating surface with MEK to reveal epoxy functionalities, PAA was grafted on gradient PS coated surfaces. A variation of PAA grafting amount **(Figure 6.15)** with PS grafting

thickness was similar to the homogeneous mixed polymer-grafted surface. However, the obtained values shifted, which can be explained with the slow cooling of the silicon wafers and therefore, a longer annealing time. The water contact angle shows the gradient wettability property of the surface.

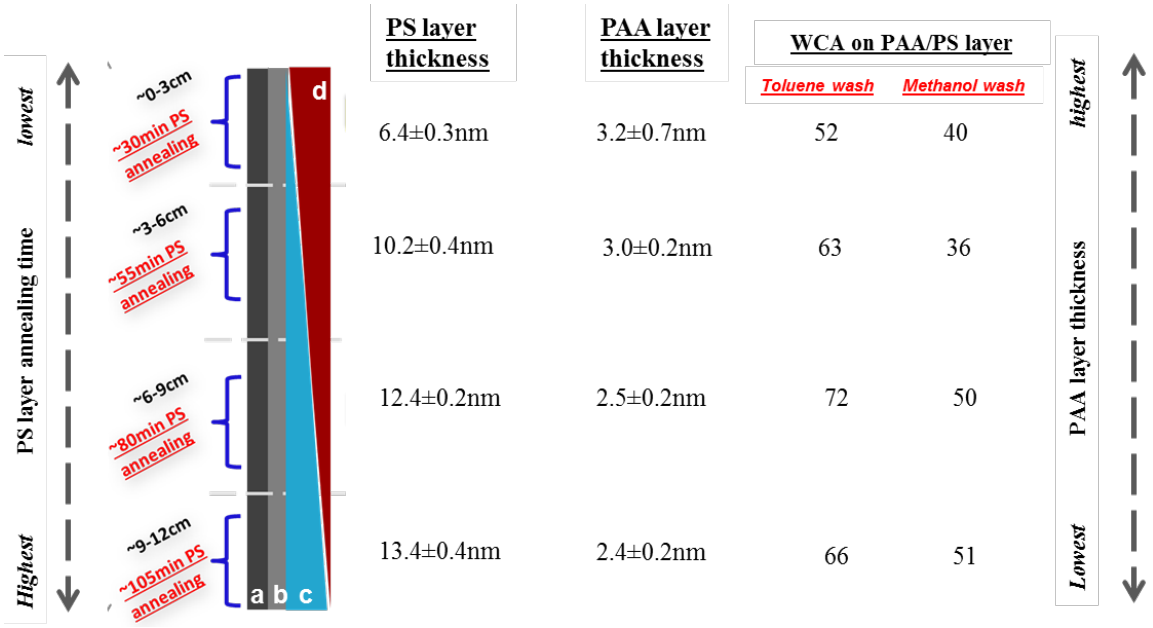

PS layer thickness	PAA layer thickness	WCA on PAA/PS layer	
		Toluene wash	Methanol wash
6.4±0.3nm	3.2±0.7nm	52	40
10.2±0.4nm	3.0±0.2nm	63	36
12.4±0.2nm	2.5±0.2nm	72	50
13.4±0.4nm	2.4±0.2nm	66	51

Figure 6.15. Properties of surface at different steps of wettability gradient synthesis. PS gradient formed under dynamic conditions. Time of annealing for the sections of PS gradient also represented. Substrate is PGMA/PET/silicon wafer.

Figure 6.16 shows dependence of water contact angle on PS/PAA ratio after rinsing the surface with the selective solvents. Measurements for samples formed at dynamic **(Figure 6.16a)** and static **(Figure 6.16b)** grafting conditions were compared. The result indicates that the same degree of switching can be achieved by both dynamic and static annealing when certain PS/PAA ratios are obtained. Thus, it is clear that the wettability gradient was successfully obtained with the proposed methodology.

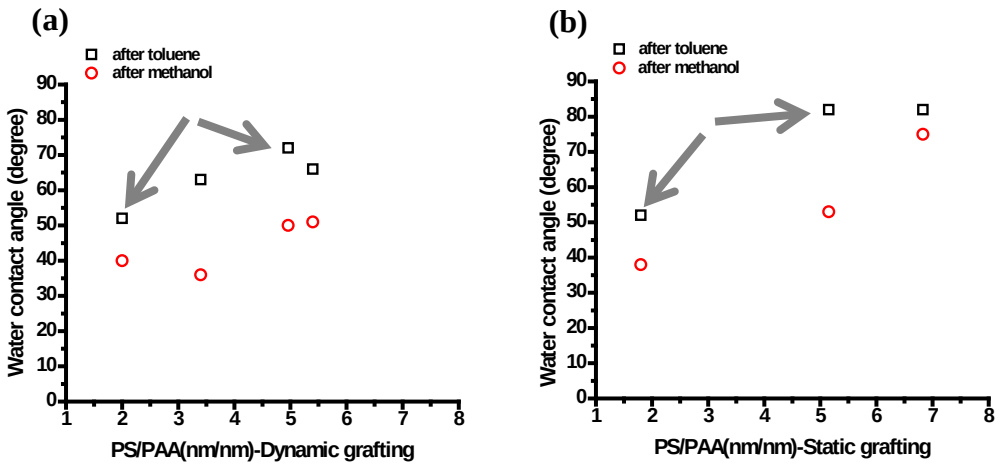

Figure 6.16. Dependence of water contact angle on PS/PAA (nm/nm) ratio. Circles-Methanol treated sample. Square-Toluene treated sample. Substrate: PAA/PS/PGMA-PET film. (a) Dynamic annealing, (b) Static annealing.

6.3.4. Wettability gradient on the PET fabric

The demonstrated gradient polymer layer formation strategy was employed to modify the fabric surface to obtain a wettability gradient along the fabric. The PET fabric was grafted with PS in gradient manner using dip coater-oven assembly, and then PAA was grafted on the PS/PGMA/PET surface at 120°C for 6 minutes. Wettability measurements of PAA/PS/PGMA grafted PET fabric are given in **Figure 6.17**. A wettability gradient has been successfully formed on a 12-centimeter-long PET fabric. The obtained fabric with wettability gradient can be used to transfer liquid.

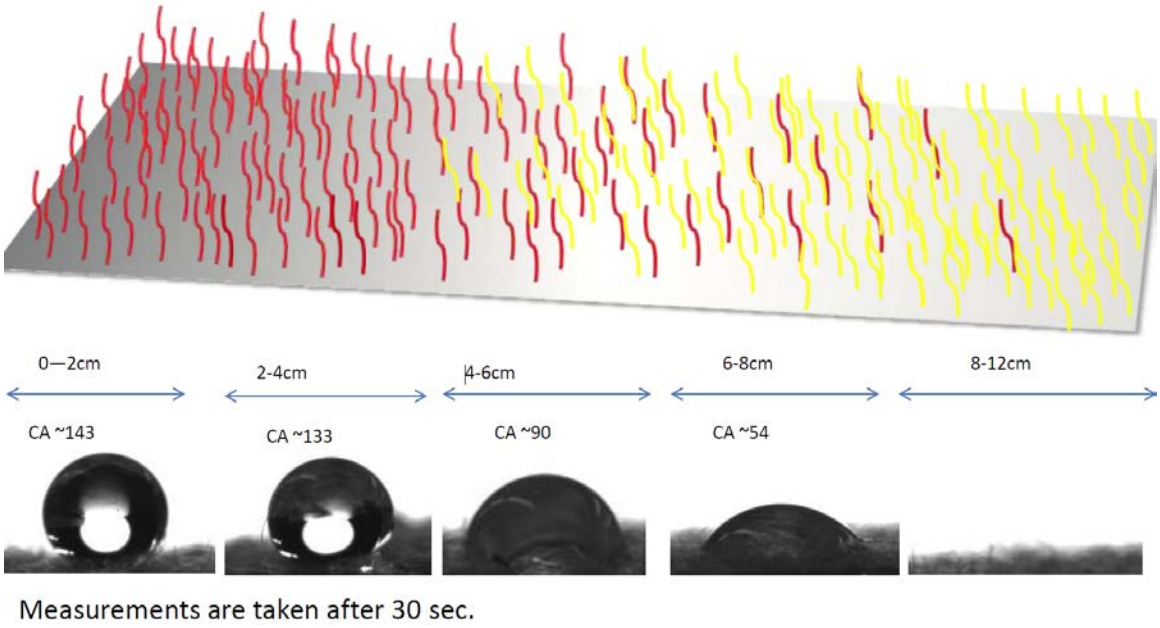

Figure 6.17. Water contact angle on fabric surface. Substrate: PAA/PS/PGMA/PET fabric. Coating is done to obtain gradually changing wetting property on the fabric.

We foresee that this fabric can be employed to stimulate cooling for body when it is used in laminated garment design. In the garment assembly, the hydrophobic part should be in contact with the body so perspiration can wick to the fabric by direct contact, then the penetrated liquid will wick toward the more hydrophilic side, which is exposed to air (outer part of garment). Then drying can occur by evaporation as illustrated in **Figure 6.18.**

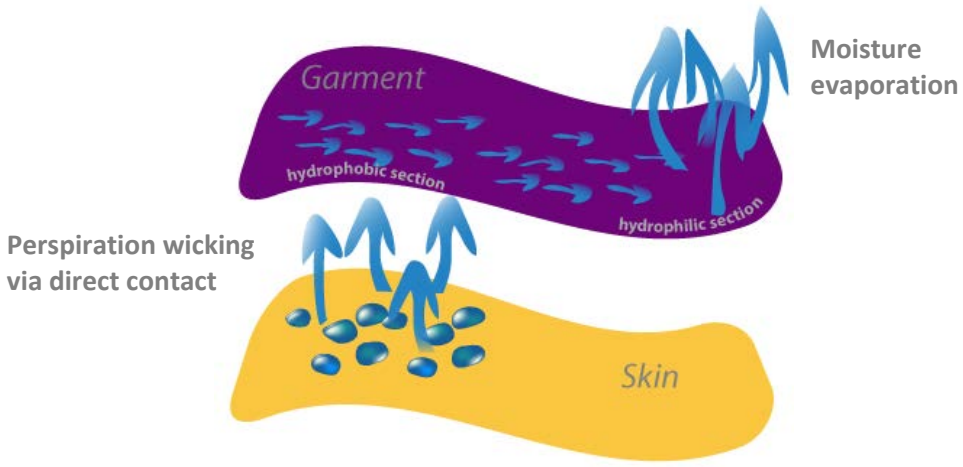

Figure 6.18. Illustration of liquid transport by gradient fabric.

6.3.5. Analysis of fabric cooling performance using surface differential scanning calorimeter[1]

The efficiency of evaporative cooling depends on ultimate garment design and clothing material. The effect of clothing material on cooling efficiency was tested using surface differential scanning calorimetry (SDSC) developed by Burtovyy et al.[31] Principles of the equipment are based on differential scanning calorimetry (DSC) methodology. Using the SDCS, one can assess cooling efficiency of the materials under development.

6.3.5.1. Surface differential scanning calorimetry (SDSC)

The basic components of SDSC are illustrated in **Figure 6.19.** The SDSC consists of a computer, a data acquisition system (Keithley 2700), two power suppliers (TDK-Lambda

[1] Fabric cooling efficiency tests were performed by Mahmut Oguz Kesimci and Dr. Ruslan Burtovvy

ZUP) to heat thin, flexible Kapton heaters with low lateral heat loss (Omega Engineering, Inc.), and RTD (Resistance Temperature Detector) sensors (Omega Engineering, Inc.) placed at the center and the corner of the heaters. The computer runs a LabView program implementing a proportional integral (PI) control algorithm and data logging.

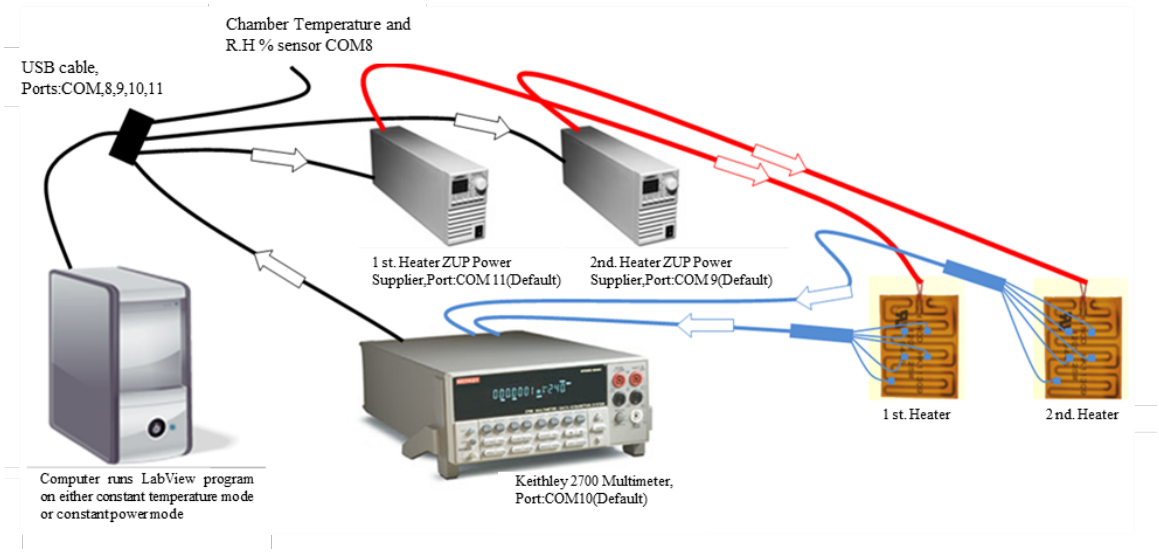

Figure 6.19. Illustration of the SDSC experimental set-up.

The two heating systems of the SDSC, the reference and sample systems, are presented in **Figure 6.20.** The reference system simulates non-evaporating conditions; therefore, it is isolated from the ambient environment by covering the fabric's surface with a plastic film and Styrofoam insulation to prevent evaporation and obtain the temperature and power values for the non-evaporating condition. The sample system is used to test the evaporative heat transfer of the cooling arrangement, and it incorporates the material to be tested (modified fabric) and the top Styrofoam insulation ("the

clothing"). In the sample system **(Figure 6.21),** a thin, flexible 10x10 cm^2 Kapton heater films **(Figure 6.21a)** are placed onto the Styrofoam insulation **(Figure 6.21b).** Thus, the direction of the heat flow is upward. The heaters in both systems are covered entirely by cotton fabrics **(Figure 6.21c).** Cotton fabrics are dipped into water **(Figure 6.21d)** to keep them wet, thus simulating a body surface. Materials under testing **(Figure 6.21e)** (modified fabric) are positioned between the cotton fabric and the top insulation.

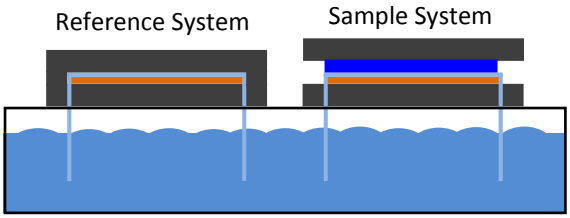

Figure 6.20. illustration of the two heating system arrangement of the SDSC set-up: The reference system and the sample system.

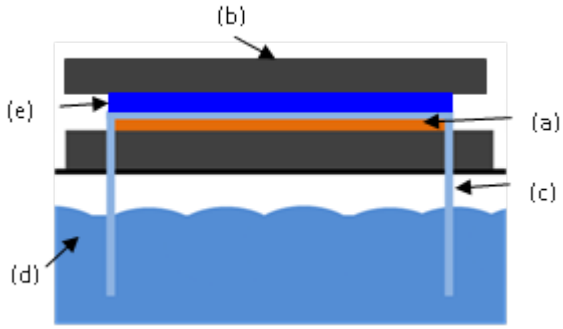

Figure 6.21. Detailed illustration of the sample system.

SDSC can detect the temperature difference between the two systems when supplied power is constant or power can be regulated to keep reference and sample system at the same temperature. In that case, the difference between the power levels

required to maintain the two systems at the same temperature is used as another characteristic of the efficiency of the evaporative cooling.

6.3.5.2. Measurement of cooling efficiency using the SDSC

To carry out actual experiments, the SDSC was placed in a controlled temperature-humidity chamber (Thermal Product Solutions). The PET fabrics (10x10cm) that were modified with pure PAA and PS layer were tested with SDSC. In initial experiments on the gradient fabric preparation, a mono-directional gradient was created (from completely hydrophobic on one end to completely hydrophilic on another end) **(Figure 6.17)**. For actual testing of the cooling arrangements, a bi-directional gradient fabric was obtained (from completely hydrophobic at the center to completely hydrophilic on the sides).

Gradient and pure polymer modified fabric were attached to the top insulation. Samples are tested both using constant temperature and constant power modes. Thus, the supplied power difference to keep temperature constant and the temperature difference of the two systems when same power is supplied were measured. The obtained results are presented in **Figure 6.22** (conditions: T=35.5 ^{o}C, RH=55%, air gap - 3 mm).

It is evident that the gradient fabric stimulates cooling comparatively higher than the hydrophobic and hydrophilic fabrics. A wettability gradient on the fabric surface speeds up the process of water evaporation from the body's surface. PAA-modified fabric is the most hydrophilic surface; therefore, drying is slow, thus, the pure PAA-coated fabric shows the lowest cooling effect.

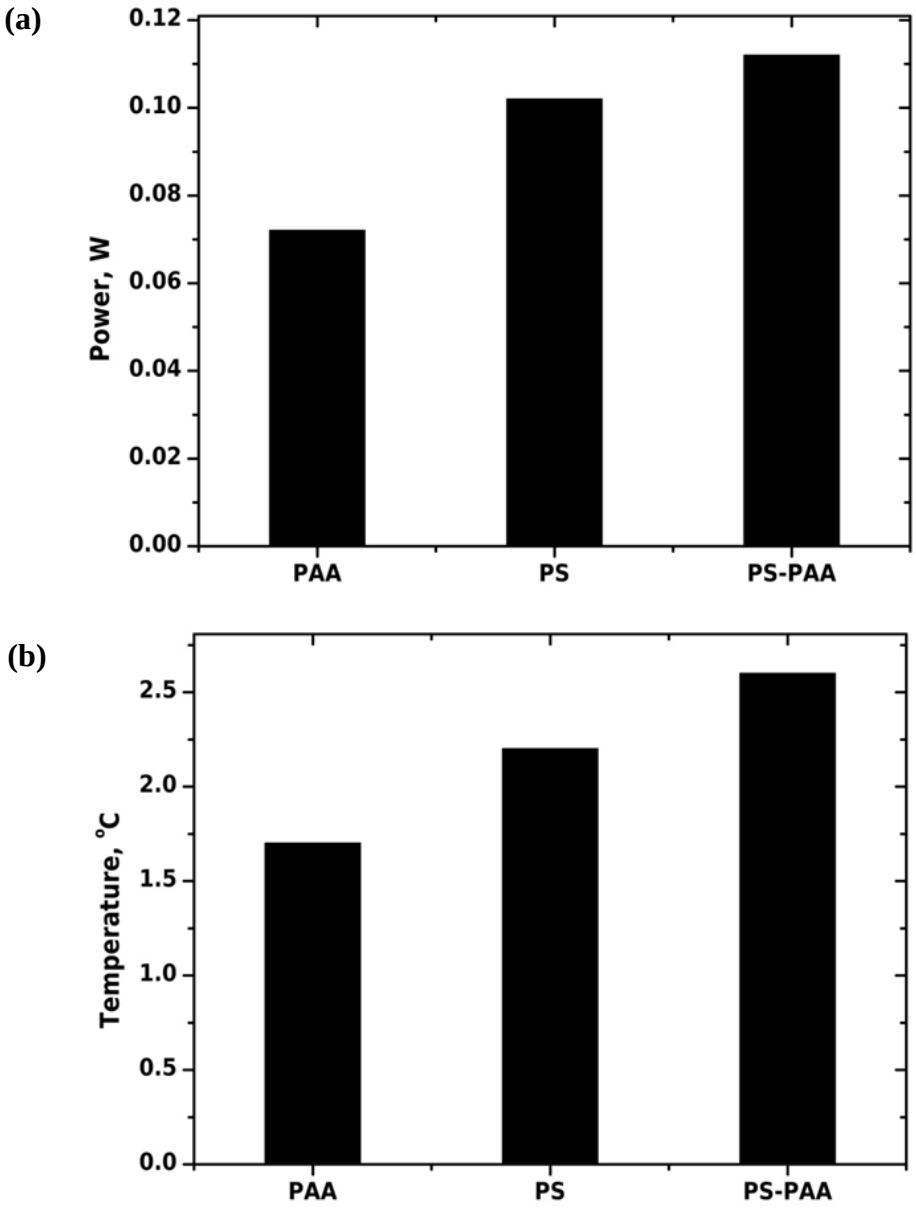

Figure 6.22. (a) Cooling power and (b) temperature effect measured with polymer modified fabrics.

6.4. Conclusion

PGMA layer anchored to a PET surface provides adequate functionality to form a gradient mixed polymer brush on PET film and fabric substrate.

Extend of single component polymer grafting vs annealing time was investigated. Water contact angle analysis, AFM morphology study, and ellipsometry measurements indicated single component hydrophilic (PAA), and hydrophobic polymer (PS) layers were successfully obtained. Thickness measurements suggest that PS grafting thickness increases with annealing time. PAA grafting thickness increases during the first 30 minutes and then reaches maximum grafting at 120^{o}C. Non-gradient mixed polymer brushes with different ratio of the components were formed. Contact angle analysis shows switching properties of the surface upon selective solvent treatment. The morphology of gradient mixed polymer brush after solvent treatment suggested variation in composition of components influenced switchability of the surface. Thus, if grafting of a hydrophilic polymer on a hydrophobic polymer is needed, the surface that was grafted with hydrophobic polymer through the anchoring layer should be treated with a proper solvent before deposition of the hydrophilic polymer.

A dual gradient mixed polymer film was also synthesized successfully using dip-coater-oven assembly. Assembly allows controlling the annealing time of polymer grafting and consequently the formation of a gradient in grafting density and wettability.

A dual gradient mixed polymer coating was applied to a fabric surface. Wettability gradient in one direction on the fabric was successfully obtained. Cooling

efficiency improvement was also demonstrated. Namely, the gradient fabric demonstrated enhanced cooling performance compared to the fabrics with uniform wettability.

6.5. References

1. Sun, C.; Zhao, X.-W.; Han, Y.-H.; Gu, Z.-Z., Control of water droplet motion by alteration of roughness gradient on silicon wafer by laser surface treatment. *Thin Solid Films* **2008,** *516* (12), 4059-4063.

2. Xu, L.; Li, Z.; Yao, S., Directional motion of evaporating droplets on gradient surfaces. *Applied Physics Letters* **2012,** *101* (6), 064101-064101-4.

3. Malouin, B. A.; Koratkar, N. A.; Hirsa, A. H.; Wang, Z., Directed rebounding of droplets by microscale surface roughness gradients. *Applied Physics Letters* **2010,** *96* (23), 234103-234103-3.

4. Longley, J. E.; Dooley, E.; Givler, D. M.; Napier, W. J.; Chaudhury, M. K.; Daniel, S., Drop motion induced by repeated stretching and relaxation on a gradient surface with hysteresis. *Langmuir* **2012,** *28* (39), 13912-13918.

5. Subramanian, R. S.; Moumen, N.; McLaughlin, J. B., Motion of a drop on a solid surface due to a wettability gradient. *Langmuir* **2005,** *21* (25), 11844-11849.

6. Elwing, H.; Goelander, C. G., ChemInform Abstract: Protein and detergent interaction phenomena on solid surfaces with gradients in chemical composition. *ChemInform* **1991,** *22* (7), no-no.

7. Pitt, W. G., Fabrication of a continuous wettability gradient by radio frequency plasma discharge. *Journal of Colloid and Interface Science* **1989,** *133* (1), 223-227.

8. Gölander, C. G.; Pitt, W. G., Characterization of hydrophobicity gradients prepared by means of radio frequency plasma discharge. *Biomaterials* **1990,** *11* (1), 32-35.

9. Lee, J. H.; Khang, G.; Lee, J. W.; Lee, H. B., Interaction of different types of cells on polymer surfaces with wettability gradient. *Journal of Colloid and Interface Science* **1998,** *205* (2), 323-330.

10. Lee, J. H.; Kim, H. G.; Khang, G. S.; Lee, H. B.; Jhon, M. S., Characterization of wettability gradient surfaces prepared by corona discharge treatment. *Journal of Colloid and Interface Science* **1992,** *151* (2), 563-570.

11. Inoue, H.; Uyama, Y.; Uchida, E.; Ikada, Y., Scanning electron-microscope observation of lubricious polymer surface for medical use. *Cells Mat.* **1992,** *2* (1), 21-28.

12. Luzinov, I.; Minko, S.; Senkovsky, V.; Voronov, A.; Hild, S.; Marti, O.; Wilke, W., Synthesis and behavior of the polymer covering on a solid surface. 3. Morphology and mechanism of formation of grafted polystyrene layers on the glass surface. *Macromolecules* **1998,** *31* (12), 3945-3952.

13. Norton, L. J.; Smigolova, V.; Pralle, M. U.; Hubenko, A.; Dai, K. H.; Kramer, E. J.; Hahn, S.; Berglund, C.; DeKoven, B., Effect of end-anchored chains on the adhesion at a thermoset-thermoplastic interface. *Macromolecules* **1995,** *28* (6), 1999-2008.

14. Ruckenstein, E.; Byungip Chung, D., Surface modification by a two-liquid process deposition of A–B block copolymers. *Journal of Colloid and Interface Science* **1988,** *123* (1), 170-185.

15. Ruckert, D.; Geuskens, G., Surface modification of polymers—IV. Grafting of acrylamide via an unexpected mechanism using a water soluble photo-initiator. *European Polymer Journal* **1996,** *32* (2), 201-208.

16. Tomita, N.; Tamai, S.; Okajima, E.; Hirao, Y.; Ikeuchi, K.; Ikada, Y., Biomaterials lubricated for minimum frictional resistance. *Journal of Applied Biomaterials* **1994,** *5* (2), 175-181.

17. Ionov, L.; Zdyrko, B.; Sidorenko, A.; Minko, S.; Klep, V.; Luzinov, I.; Stamm, M., Gradient polymer layers by “grafting to” approach. *Macromolecular rapid communications* **2004,** *25* (1), 360-365.

18. Ionov, L.; Sidorenko, A.; Stamm, M.; Minko, S.; Zdyrko, B.; Klep, V.; Luzinov, I., Gradient mixed brushes: ``Grafting to`` approach. *Macromolecules* **2004,** *37* (19), 7421-7423.

19. Uhlmann, P.; Ionov, L.; Houbenov, N.; Nitschke, M.; Grundke, K.; Motornov, M.; Minko, S.; Stamm, M., Surface functionalization by smart coatings: Stimuli-responsive binary polymer brushes. *Progress in Organic Coatings* **2006,** *55* (2), 168-174.

20. Yu, X.; Wang, Z.; Jiang, Y.; Zhang, X., Surface gradient material: From superhydrophobicity to superhydrophilicity. *Langmuir* **2006,** *22* (10), 4483-4486.

21. Swaminatha Iyer, K. L. Multifunctional nanolayers via polymer brush approach: Synthesis and characterization. Dissertation, Clemson University, 2004.

22. Burtovyy, O. Synthesis and characterization of macromolecular layers grafted to polymer surfaces. Dissertation, Clemson University 2008.

23. Zdyrko, B. Thin polymer films for biomedical applications: Synthesis and characterization. Dissertation, Clemson University, 2005.

24. Cassie, A., *Discuss. Faraday Soc.* **1948,** *3*, 11.

25. Advincula, R. C.; Brittain, W. J.; Caster, K. C.; Rühe, J., *Polymer brushes*. Wiley Online Library: 2004.

26. Sofia, S. J.; Premnath, V.; Merrill, E. W., Poly(ethylene oxide) Grafted to Silicon Surfaces: Grafting Density and Protein Adsorption. *Macromolecules* **1998,** *31* (15), 5059-5070.

27. Mei, Y.; Elliott, J. T.; Smith, J. R.; Langenbach, K. J.; Wu, T.; Xu, C.; Beers, K. L.; Amis, E. J.; Henderson, L., Gradient substrate assembly for quantifying cellular response to biomaterials. *Journal of Biomedical Materials Research Part A* **2006,** *79A* (4), 974-988.

28. Sperling, L. H., *Polymeric multicomponent materials: an introduction*. Wiley New York, NY: 1997.

29. Gupta, B.; Plummer, C.; Bisson, I.; Frey, P.; Hilborn, J., Plasma-induced graft polymerization of acrylic acid onto poly(ethylene terephthalate) films: characterization and human smooth muscle cell growth on grafted films. *Biomaterials* **2002,** *23* (3), 863-871.

30. Li, Z. Protein interactions with mixed poly(ethylene glycol)/polyacrylic acid brushes. Master Thesis, Clemson University, 2008.

31. Burtovyy, R.; Rubin, B.; Kesimci, M. O.; Luzinov, I.; Owens, J.; Kornev, K. G., Surface differential scanning calorimeter for evaluation of evaporative cooling efficiency. *Journal Of Engineered Fibers And Fabrics* **2012,** *7*, 58-62.

CHAPTER SEVEN

TOWARD FABRIC-BASED FLEXIBLE MICROFLUIDIC DEVICES: POINTED SURFACE MODIFICATION FOR PH SENSITIVE AQUEOUS LIQUID TRANSPORT

7.1. Introduction

The development of economical, accurate, and user friendly microfluidic devices has attracted great attention in the field of bioengineering, drug development, and medical diagnosis.[1, 2] Indeed, microfluidic chips that are engineered to transport small volumes of fluids to a precise location, are extensively reported in literature.[1-7] Currently, lithographic techniques are regularly and successfully used to create microchannels in silicon, glass, and polymer substrates for the transport of liquids.[8-10] However, the complexity and the relatively high cost of lithographic manufacturing are continuous stimuli for the development of more economical and scalable approaches to the fabrication of microfluidic devices.[11-16] Specifically, fibrous materials, such as paper and threads (yarns), are under consideration for the capillarity-driven distribution of fluids without the utilization of external pumping devices.[17]

High wicking ability is the most prominent characteristic of paper-based microfluidic devices (μPADs).[18-25] Further advantages of paper-based devices are that paper is inexpensive, lightweight, biodegradable, broadly available, compatible with biological samples, and easy to functionalize.[26] On the other hand, paper wicks liquid

isotropically, and to fabricate a microfluidic device, it is necessary to create flow channels using lines of hydrophobic polymers[13, 14] The micropatterns on paper have been fabricated with simplified lithography, plasma activation, and deposition of a hydrophobic polymer with an inject printer or pen.[18, 21, 24, 27, 28] To date, an analysis of blood type, pH value, and glucose and protein content in urine with μPADs has been successfully performed.[20, 22, 29]

Recently, threads/yarns have become alternative material for low-cost point-of-care (POC) diagnosis.[11, 13-16, 30] Many types of yarn, such as cotton,[16] nylon,[14] polyester,[31] and silk,[11] PVDF[17] have been used to develop thread-based microfluidic devices (μTADs). Protein, nitrite, and ketone colorimetric assays, enzymatic colorimetric assay for glucose and alkaline phosphate detection, uric acid analysis, and antibody-antigen reaction have been performed with μTADs.[11, 14, 16] Numerous advantages of the yarn can be mentioned: flexibility, lightweight, one-dimension capillary flow, straightforwardness of chemical modification, possibility of large volumetric flow, and vast potential for mass production.[13, 14, 32] The potential for thread to control fluid direction and to be incorporated into complex microfluidic structures has been recently demonstrated. For example, Li et al.[16] tailored the wettability of cotton yarn with plasma oxidation and sewed the yarn into the polymer surface to fabricate μTAD. Reches et al.[14] demonstrated three different designs for the μTAD: woven array, branching design, and sewn array design. In addition, the wicking properties of nine different threads before and after plasma treatment were examined. It was also shown that thread knots can be employed as effective mixers, splitters, and locations for the detection zone.[14, 15] The flow resistance of

knots with different topologies has also been studied.[30] Bahandari et al.[11] utilized a conventional weaving technique to fabricate a fabric-based sensor. Specifically, silk yarns (with different wicking properties) were used to form strip-control units in fabric. Owens et al.[13] utilized hydrophobic polypropylene (PP) and hydrophilic poly(ethylene terephthalate) (PET) yarns to systematically engineer woven textile fabric to create amphiphilic microchannels with defined orientations and locations. As a result, the microfluidic co-flow of immiscible liquids (water and dodecane) within the textile structures was demonstrated.

In general, either unmodified or premodified threads/yarns are used to obtain the thread-/yarn-based microfluidic prototype devices. To scale up the production of the devices, traditional textile machinery has to be used and various sizing agents should be applied to the yarns before the manufacturing. Therefore, an extensive cleaning procedure to remove sizing agents (after the fabric is made) is needed to expose the fiber surface. During the cleaning procedures, the surface properties of the unmodified and premodified fibers constituting the yarns will be changed and may not possess the necessary characteristics. One of the ways to overcome this limitation is to produce textile materials of necessary structure from unmodified yarns only that can be later locally modified using high-throughput (e.g., ink-jet printing) techniques to target a specific application. To this end, we report here a methodology for pointed surface modification of model textile microfluidic devices to produce functional (pH sensitive, acidic and basic reported here) yarn-based channels in the textile device.

Specifically, fabrication of model microfluidic textile chips woven from PP and PET fibers was studied in this work. PP fibers were used to form hydrophobic boundaries for the yarn microchannels made of PET. Next, the PET yarns were modified with a nanoscale layer of epoxy-containing polymer to introduce the epoxy reactive groups to the fiber surface. The modification did not affect the PP parts of the fabric, leaving them hydrophobic and nonreactive. As a result, generic reactive channels were obtained. Finally, the reactive channels were locally modified with polymers of dissimilar nature via the "grafting to" technique,[33] and fabric was obtained, possessing PET yarn-based channels having carboxylic (acidic) and pyridine (basic) surface functionalities within each channel. The dimensions of the modified area can be controlled via the volume of a droplet of a reactive polymer solution placed on a predetermined location on the fabric. We foresee that, using ink-jet printing techniques, the method reported in this publication can be easily scaled-up and employed to mass produce yarn-based microfluidic devices.

7.2. Experimental

7.2.1. Model substrates

Model PET film preparation was reported in **Section 3.5.1**. alkali surface activation, PGMA anchoring layer formation ,and polymer grafting for model film were done using same methods explained in **Section 4.2.** PET layer was ~70nm, PGMA-RhB (Mn ≈ 80,000 g/mol) layer was ~3nm. PAA, P2VP-COOH, and PEG-COOH were selected polymer to be grafted.

7.2.2. Fabric substrates

PET multifilament yarn (500/70 Denier-3Ztwist) was provided by Middleburg Yarn Processing Co Inc. PP multifilament yarn (100/40 Denier) was provided by Fiber Visions, Inc. and was twisted (4Z) with Saurer Allma Assembly Twisting Machines to achieve required mechanical properties for weaving.

Woven fabrics were manufactured in Clemson laboratory using computer-controlled AVL 40 in., 24-harness Industrial Dobby Loom **Figure 7.1**). To start with, one-component PET, PP and two-component PET/PP blended fabrics were manufactured. Then, model textile microfluidic chips (**Figure 7.2**) comprising both PET and PP yarns were fabricated. Fabric cleaning and activation were accomplished as explained in Section 3.5.2.

Figure 7.1. AVL 40 inches, 24-harness Industrial Dobby Loom. (1)Shuttle box, (2)Control unit, (3)Warp beam, (4)Harnesses, (5)Reed, (6)Fabric beam.

The alkali-treated fabrics were soaked in a 0.5 wt/vol % PGMA-RhB solution in MEK and vacuum was applied several times to allow polymer solution to penetrate into the yarns of the fabrics. The fabrics were left immersed in the PGMA solution for 3 h at 50°C. After treating with PGMA, the fabrics were washed several times with MEK and dried until constant mass was obtained. PEG, P2VP-COOH, and PAA were then sequentially grafted to the PET yarns in the PET/PP assembly. This was accomplished by sequentially depositing ~ 30µl of each solution drop-wise via a micropipette in a specified location(A, and B on **Figure 7.2**) for each polymer to create demanded patterns made of different grafted polymers. Annealing each polymer layer was conducted for 1 h at 120°C prior to depositing the next polymer.

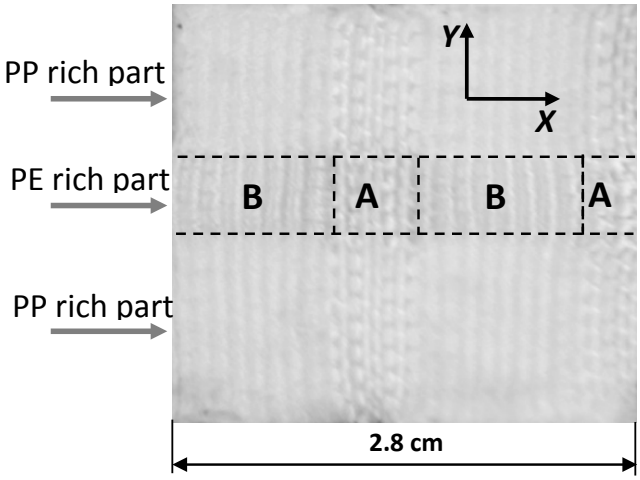

Figure 7.2. Model textile microfluidic chip where PET-rich woven stripes are generated in PP hydrophobic fabric matrix. PET rich part A: fabric with two-directional (weft and warp) positioning of the PET yarns. Section A does not contain any PP threads. PET rich part B: fabric where PET yarns are positioned in the *X* direction only. Perpendicular (*Y*) fibers in the section B are made of PP.

The samples were not rinsed to remove unattached polymers until the grafting of all polymers was completed since unattached polymer can reach with PGMA. At the end of the grafting, the samples were rinsed several times with methanol to remove any ungrafted polymers.

7.3. Results and Discussion

7.3.1. Model textile microfluidic chip

Model textile microfluidic chips comprised of a fabric possessing a weave pattern where PET-rich stripes were embedded in the PP hydrophobic fabric **(Figure 7.2)**. The fabric based chips were cut of the larger piece of fabric produced using a dobby loom. In this fabric structure, the PP fibers were used to form hydrophobic boundaries for the yarn microchannels made of PET. PET rich part of the chip contained two structural sections (marked A and B on **Figure 7.2**). The section A is the fabric with two-directional positioning of the PET yarns. This section does not contain any PP threads. An aqueous liquid placed on A should readily propagate without preferential path in both perpendicular (*Y*) and parallel (*X*) directions until it reaches PP rich part of the textile chip. The section B is the fabric where PET yarns are positioned in the *X* direction only. Perpendicular (*Y*) fibers in the structure are made of PP. Therefore, an aqueous liquid will move preferentially into *X* direction. In fact, when water was placed on the different sections of the chip we observed isotropic *(X-Y)* and anisotropic (*X*-direction) propagation of the liquid placed on A and B, respectively. It is important to highlight that movement of water into the PP rich or pure PP part of the chip was not observed.

In the textile chip, element B is envisioned as a logical element where a liquid possessing a certain characteristics is propagating, while movement of another liquid can be arrested. In this work we targeted to control the movement of an aqueous system based on its pH. To create pH sensitive elements nanoscale layers of pH sensitive polymers were grafted to the yarns in the sections B. Section A is envisioned as a distribution center in the textile microfluidic chip. Liquid placed there is propagating isotropically and, therefore, all yarns in the sections B are supplied with a liquid of interest. To modify fibers in the section A a pH insensitive polymer was employed.

7.3.2. Surface modification of PET fibers with an epoxy-containing polymer

Developing a procedure for the surface modification of PET fibers within the PET/PP fabric with a reactive epoxy-containing polymer was the first key step in our study. We selected a PGMA that contained an epoxy group in every repeating unit for the modification of the fiber surface. The polymer was demonstrated to be an effective macromolecular anchoring layer for grafting polymers to inorganic and polymeric surfaces using the "grafting to" and "grafting from" approaches.[33-37] This method of surface modification was previously used in our laboratory to successfully modify fibrous polymer materials.[38-42]

In our initial experiments, fabric consisting of only PET yarn was used. Specifically, to modify the PET threads in the fabric, PGMA macromolecules were adsorbed on the fiber surface from a solution in MEK. In previous two chapters, it was shown that PGMA can be grafted on hydrolyzed PET film and fabric. It was proven with the model study **(Chapter 4)** that the reactive layer can be deposited on the PET surface

using this method. The chemisorption of the polymer chains was achieved via the reaction between the epoxy groups in the macromolecules and the carboxyl/hydroxyl groups on the fiber surface.[43]

Prior to the adsorption, surface of the PET fabric is activated with the procedure reported in **Chapter 5**. We treated the PET fabric with NaOH solution to increase the concentration of the reactive carboxyl groups on the surface. This procedure is an accepted surface hydrolysis method that is commonly employed to increase the reactivity of a polyester fabric.[44] NaOH treatment is selected specifically, since PP does not hydrolyzed in the alkali environment. Thus, alkali hydrolysis allows creation of reactive PET channel in PET/PP blended fabric, as PP remains intact (non-reactive) after treatment. In the model experiment **(Chapter 4)** conducted for the thin PET film deposited on a silicon wafer, we estimated by ellipsometric measurements that only about 3–4 nm of the film (and therefore the fiber) is removed during the treatment. As a result of chain scission, the water contact angle for the film changed from 65° to 35°, indicating the formation of a significant number of polar (carboxyl and hydroxyl) groups on the PET surface. AFM imaging of the model sample demonstrated that there was, in fact, no significant change in the morphology of the PET film after treatment with NaOH **(Chapter 4 Figure 4.2b, Figure 4.5c).** Likewise, the SEM study confirmed that the PET fibers were intact after the 2 min exposure to the alkali solution **(Chapter 5 Figure 5.3b)**.

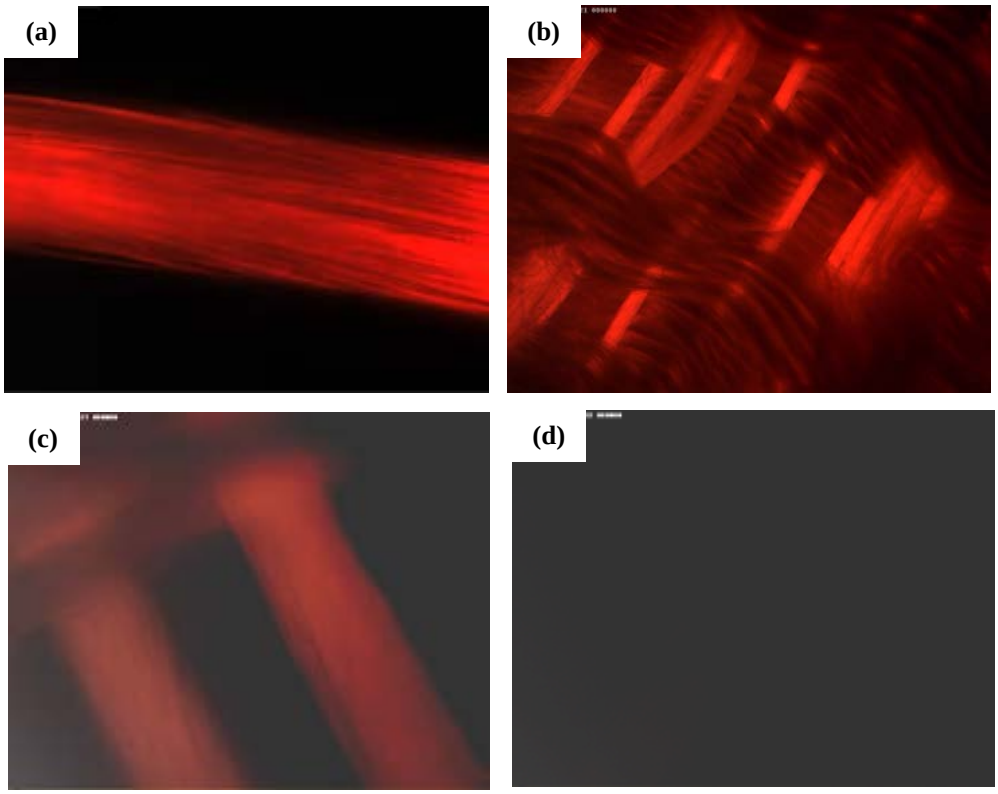

Figure 7.3. Fluorescent microscope images of (a) PET yarn,(b) PET/PP blended fabric, (c) PET yarn in blended fabric, (d) PP yarn in blended fabric (no fluorescence signal detected).

The surface modification approach used to treat the model PET film was applied to the one-component PET, PP, and PET/PP blended fabrics. Macromolecules labeled with Rhodamine B were used to confirm homogeneous deposition of the PGMA chains on the fiber surface. Fluorescent microscopy of the textile material treated with fluorescent tagged PGMA showed that the fibers in the PET yarn were evenly covered with the reactive polymer**(Figure 7.3a)**, and when the surface modification method was applied to the PP yarns, no fluorescent signal was observed. This latter result indicated that PP fibers were not covered with the PGMA adsorbed layer, and demonstrates that

this treatment method can be used to selectively modify fibers in the PET/PP blended fabric. In fact, when the PET/PP fabric was subjected to the PGMA solution, only PET fibers were modified with the reactive polymer, as evidenced by fluorescent microscopy **(Figure 3b-d).**

Surface modification with NaOH followed by PGMA grafting on PET/PP fabric surface can create hydrophilic and reactive PET yarn channels within hydrophobic and inert PP threads. Water contact angle measurements conducted for the PET/PP blended fabric confirmed the point modification of the textile structure. **Figure 7.4a,b** show the high contact angle of a water droplet deposited onto the PP yarns and the absorption of a water droplet when deposited onto the PET yarns.

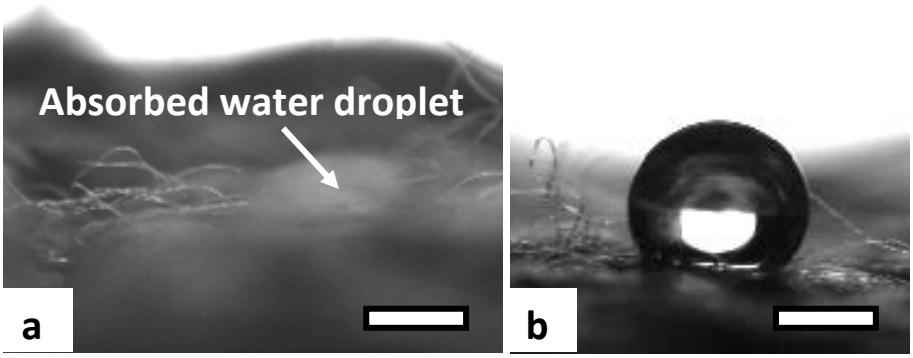

Figure 7.4. Photographs of water droplet (pH 6.7) deposited on the yarns constituting PET/PP two component fabric (presented in Figure 7.3b) modified with PGMA layer. (a) Absorbed droplet deposited on the PET yarns. (b) Droplet deposited on the PP yarns. Scale bar for (a, b) - 1 mm.

7.3.3. Modification of PET yarns in textile chip with polymer grafting

Alkali and PGMA modification did not affect the PP parts of the fabric, leaving them hydrophobic and nonreactive, thus resulting in generic reactive stripes constituted from PET yarns. To affect the wetting behavior and functionality of the stripes, they were locally modified with polymers of dissimilar nature. The grafting was conducted using the "grafting to" technique, by which end-functionalized polymer molecules reacted with complementary functional groups located on the surface to form tethered chains.[33] For our experiments, we selected three different polymers possessing carboxyl groups capable of reacting with the epoxide groups of the PGMA: PAA, P2VP-COOH, and carboxyl-terminated PEG. The polymers were selected based on pH sensitivity of their surface energies and water sorption characteristics. Surface energy and water sorption differences established by the treatments were used to control the movement of the aqueous liquid along the PET stripes.

Among the polymers selected, PEG is soluble in most liquid media, including water of different pH and ionic strength, ethanol, toluene, hexane, and many others. PAA chains (pK=4.5–4.7) demonstrate significant variations in the interaction with water as a function of pH:[45] (a) At low pH values, they are practically not swollen in water; (b) at high pH values, PAA macromolecules are significantly swollen in an aqueous environment. P2VP chains are not soluble in water at pH > 4 due to a hydrophobic backbone. P2VP macromolecules, however, can be protonated and dissolved in an acidic aqueous solution. In general, P2VP demonstrates the properties of a weak polyelectrolyte. The polymer is soluble at pH < 4 due to the protonated charged pyridine nitrogen when

electrostatic repulsion overcomes the short-range hydrophobic attraction in the backbone of the polymer chain. Conformation of the P2VP chain is sensitive to the pH and ionic strength of aqueous solutions.[46, 47]

Initially, we grafted the polymers to the model substrate, PGMA-modified PET film deposited on a silicon wafer. This reference experiment was conducted to estimate the thickness of the polymer layer that can be attached to the surface of PET fibers in the fabric structure, as well as to measure the wettability of the fibers. Since parameters of grafted polymer layer on film (thickness and morphology) are reported in **Chapter 4**, here only wettability of the film for water with different pH is covered.

The modification with polymer grafting significantly changed the wettability of the PET film surface with water of different pH values **(Figure 7.5)**. PAA-grafted layers demonstrated high wettability at pH 6.7 and 9. At pH 2, where the majority of the carboxyl groups are protonated, the contact angle increased to ~30 ° from ~17° (pH 6.7). The P2VP grafted layers showed even more significant changes in wettability as a function of pH. At pH 2, the P2VP chains are protonated and water soluble. This explains the low water contact angle of ~14° that was observed for the PET surface modified with P2VP grafting. Higher contact angles (~46° for pH 6.7 and ~57° for pH 9) were observed for the P2VP layers. The wettability of PEG-grafted layers was not significantly affected by changes in pH.

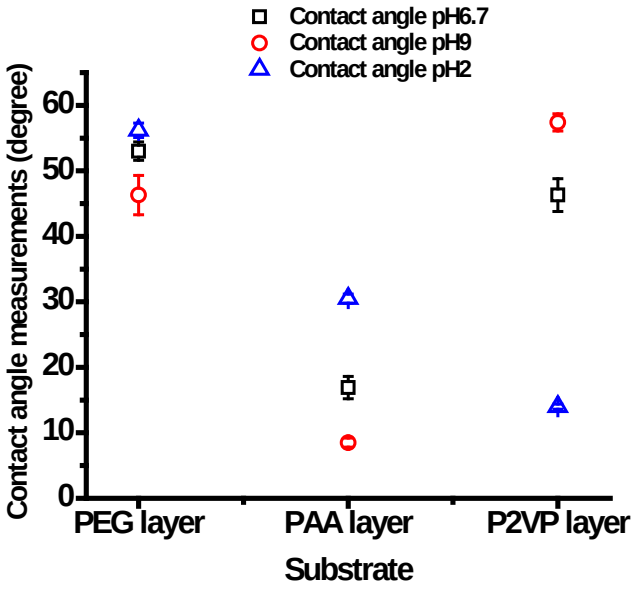

Figure 7.5. Contact angle of substrates for water with different pHs.

The wettability measurements for the grafted films indicated that by grafting PAA and P2VP to the different parts of the textile chip, it should be possible to regulate the transport of water based on the pH value of the aqueous system. Therefore, we modified two adjacent sections B of the PET rich stripes **(Figure 7.2)** in the textile structure with P2VP and PAA grafting conducted at the same conditions as were used for the model PET films. The part A connecting the modified fragments was grafted with PEG **(Figure 7.6)**. By grafting PEG, we obtained a pH-insensitive port for the deposition of a water droplet possessing the pH of interest. We tested wettability of the grafted area with water of pH2, pH6.7, and pH9 and found that the grafted areas were wetted by water of different pHs and, therefore, are capable to transport an aqueous liquid. Wettability of PP rich part of the chip was not altered during the grafting procedures as shown in **Figure**

7.6c by water drop placed on PP rich part and does not penetrate in to fabric proving that PP part remains hydrophobic.

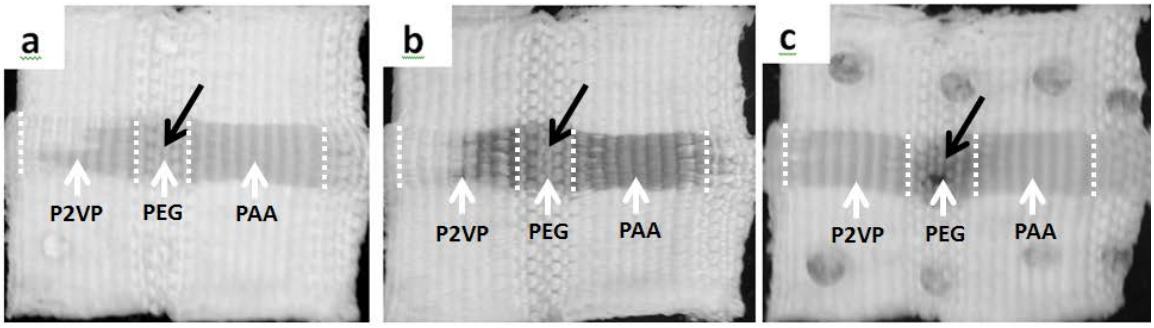

Figure 7.6. Movement of water in the microfluidic textile chips: (a) pH9, (b) pH 6.7, and (c) pH 2. Black arrow shows the place where droplet of water was deposited. White arrows and dashed lines indicating the part of the PET rich stripe modified with different polymers. (a) and (c) shows droplets of the aqueous solution placed on the PP rich parts of the textile chip.

7.3.4. Transport of water in the model textile chip

The fluid wicking kinetics can be described as a first approximation by the Lucas-Washburn equation:[48, 49]

$$\boldsymbol{L = \sqrt{\frac{2kP_c}{\mu\varepsilon}}\mathrm{t}.} \qquad \textbf{E.7.1}$$

where L is the length of wet part of the fabric as a function of time t, k is the fabric permeability, ε is its porosity, and μ is the viscosity. Modeling the fibrous material as a bundle of capillaries, the capillary pressure can be estimated as $P_c \sim 4\gamma cos\theta/D$,[50] where γ is the interfacial tension of the liquid/air pair; D is the characteristic pore diameter; and θ is the contact angle that the liquid meniscus forms with the pore wall. Using this scaling

relation, one can see that the dependence of the wicking kinetics on the contact angle is as follows $L \propto (\cos\theta\, t)^{1/2}$.

According to **E.7.1** the movement of a liquid in the textile structure is proportional to the square root of $\cos\theta$. The square root values of $\cos\theta$ with the values of θ from **Figure 7.5** are as follows; $\sqrt{\cos\theta}$ = 0.99 (PAA, pH 9), 0.985 (P2VP, pH 2), 0.97 (PAA, pH 7), and 0.93 (PAA, pH 2), respectively, and the square root values of $\cos\theta$ for P2VP at pH 7 and P2VP at pH 9 are $\sqrt{\cos\theta}$ = 0.83 and 0.73, respectively (**Figure 7.7**). Having these materials with different contact angles (**Figure 7.5**) and different wicking kinetics with water of different pH (**Figure 7.7**), we investigated whether these small differences in the materials wettability is sufficient to direct the transport of an aqueous solutions in a certain direction.

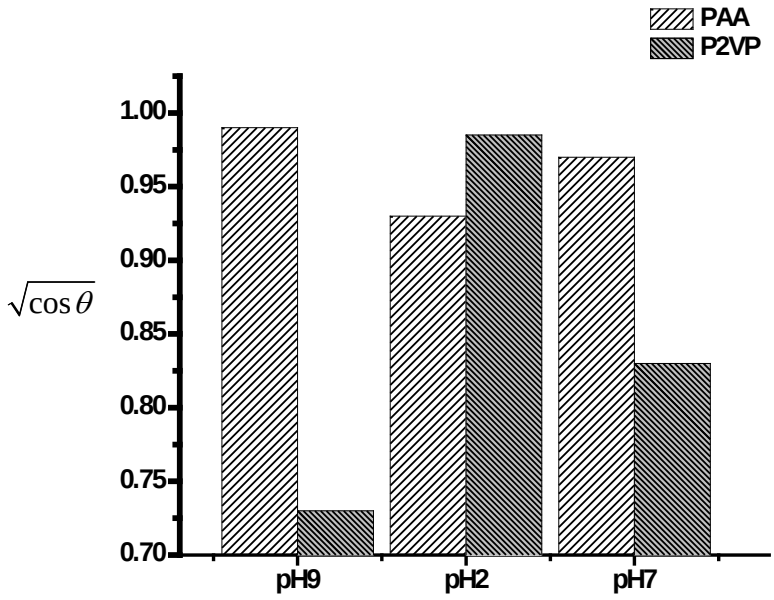

Figure 7.7. The square root values of $\cos\theta$ with the values of contact angles (θ) measured on model film surface with water drop of different pH values.

The first experiments were conducted with water of pH 9. At this pH the difference between wettability of the sections A modified with P2VP and PAA is the largest **(Figure 7.5)**. In the experiment 5μl droplets were placed in a sequential manner on the section A of the textile chip modified with PEG grafted layer **(Figure 7.6)**. The water from the first drop readily filled the section A and started movement into the section B of the chip modified with PAA grafting. The liquid practically did not penetrate into the PP rich part of the chip and section modified with P2VP grafted chains. As more droplets were added, the liquid continues to move into the PAA section until the section is full. After that the liquid started to penetrate into the P2VP section of the chip (**Figure 7.6a** and **Figure 7.8**). When the experiment was conducted for the water of pH 6.7 the same results as for pH 9 were obtained (**Figure 7.6b**). For liquid with pH 2, however, when the droplets were deposited on the PEG port, the liquid moved into both P2VP and PAA directions (**Figure 7.6c**).

Therefore, fabric sections modified with P2VP and PAA demonstrate significantly different kinetics of fluid penetration for water with higher pH values. In essence, the grafted P2VP layers serve as a pH sensitive element which allows the directed movement of micro amounts of water into prescribed direction. It is important that in all cases the liquid deposited on the PEG port was confined within the PET-rich stripes and was not transported into PP-rich parts of the fabric structure. The obtained results demonstrate that with pointed surface modification, it is possible to regulate the transport of micro-amounts water through the textile chip.

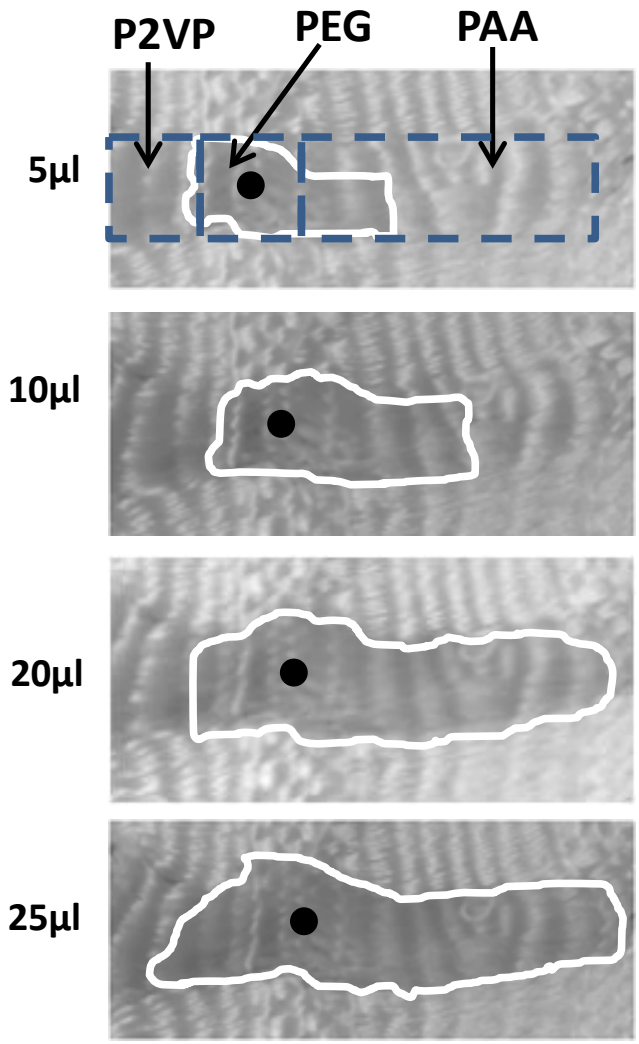

Figure 7.8. Movement of water (pH9) in the textile chip as a function of water amount placed on the section (A) grafted with PEG. Black dot shows the location of the droplet placement. White line indicates border of the water propagation.

7.4. Conclusions

In conclusion, an effective method for pointed surface modification of a PET/PP textile material to produce yarn-based channels having different functionalities in the fabric was developed. Specifically, the PET yarns were selectively modified with an

epoxide-containing polymer to obtain generic reactive channels. The modification did not affect the PP parts of the fabric, leaving them hydrophobic and nonreactive. To affect the wetting behavior and the functionality of the channels, they can be further locally modified with different pH-sensitive polymers. The dimensions of the modified area (patterns) can be adjusted by controlling the volume and placement of the droplet of a reactive polymer solution on the fabric. Stimuli-responsive properties of the channel coatings are used to regulate pH-triggered transport of liquids in the textile. We foresee that the textile with stimuli-responsive channels could find a number of intriguing applications for lab-on-chip analytical devices including devices built into apparel with smart functions. We expect that the developed method can be easily scaled- up and employed for the mass production of the yarn-based microfluidic devices.

7.5. References

1. McDonald, J. C.; Whitesides, G. M., Poly(dimethylsiloxane) as a material for fabricating microfluidic devices. *Accounts of Chemical Research* **2002,** *35* (7), 491-499.

2. Klank, H.; Kutter, J. P.; Geschke, O., CO_2-laser micromachining and back-end processing for rapid production of PMMA-based microfluidic systems. *Lab on a Chip* **2002,** *2* (4), 242-246.

3. Becker, H.; Locascio, L. E., Polymer microfluidic devices. *Talanta* **2002,** *56* (2), 267-287.

4. Hansen, C. L.; Skordalakes, E.; Berger, J. M.; Quake, S. R., A robust and scalable microfluidic metering method that allows protein crystal growth by free interface diffusion. *Proceedings of the National Academy of Sciences* **2002,** *99* (26), 16531-16536.

5. Tarn, M. D.; Pamme, N., Microfluidic platforms for performing surface-based clinical assays. *Expert Review of Molecular Diagnostics* **2011,** *11* (7), 711-720.

6. Trietsch, S. J.; Hankemeier, T.; van der Linden, H. J., Lab-on-a-chip technologies for massive parallel data generation in the life sciences: A review. *Chemometrics and Intelligent Laboratory Systems* **2011,** *108* (1), 64-75.

7. Tentori, A. M.; Herr, A. E., Photopatterned materials in bioanalytical microfluidic technology. *Journal of Micromechanics and Microengineering* **2011,** *21* (5), 054001.

8. Becker, H.; Gärtner, C., Polymer microfabrication technologies for microfluidic systems. *Anal Bioanal Chem* **2008,** *390* (1), 89-111.

9. Beebe, D. J.; Mensing, G. A.; Walker, G. M., Physics and applications of microfluidics in biology. *Annual Review of Biomedical Engineering* **2002,** *4* (1), 261-286.

10. McDonald, J. C.; Duffy, D. C.; Anderson, J. R.; Chiu, D. T.; Wu, H.; Schueller, O. J. A.; Whitesides, G. M., Fabrication of microfluidic systems in poly(dimethylsiloxane). *ELECTROPHORESIS* **2000,** *21* (1), 27-40.

11. Bhandari, P.; Narahari, T.; Dendukuri, D., 'Fab-Chips': a versatile, fabric-based platform for low-cost, rapid and multiplexed diagnostics. *Lab on a Chip* **2011,** *11* (15), 2493-2499.

12. Ionov, L.; Houbenov, N.; Sidorenko, A.; Stamm, M.; Minko, S., Smart microfluidic channels. *Advanced Functional Materials* **2006,** *16* (9), 1153-1160.

13. Owens, T. L.; Leisen, J.; Beckham, H. W.; Breedveld, V., Control of microfluidic flow in amphiphilic fabrics. *ACS Applied Materials & Interfaces* **2011,** *3* (10), 3796-3803.

14. Reches, M.; Mirica, K. A.; Dasgupta, R.; Dickey, M. D.; Butte, M. J.; Whitesides, G. M., Thread as a matrix for biomedical assays. *ACS Applied Materials & Interfaces* **2010,** *2* (6), 1722-1728.

15. Safavieh, R.; Zhou, G. Z.; Juncker, D., Microfluidics made of yarns and knots: from fundamental properties to simple networks and operations. *Lab on a Chip* **2011,** *11* (15), 2618-2624.

16. Li, X.; Tian, J.; Shen, W., Thread as a versatile material for low-cost microfluidic diagnostics. *ACS Applied Materials & Interfaces* **2009,** *2* (1), 1-6.

17. Tsai, C.-C.; Mikes, P.; Andrukh, T.; White, E.; Monaenkova, D.; Burtovyy, O.; Burtovyy, R.; Rubin, B.; Lukas, D.; Luzinov, I.; Owens, J. R.; Kornev, K. G., Nanoporous artificial proboscis for probing minute amount of liquids. *Nanoscale* **2011,** *3* (11), 4685-4695.

18. Abe, K.; Suzuki, K.; Citterio, D., Inkjet-printed microfluidic multianalyte chemical sensing paper. *Analytical Chemistry* **2008,** *80* (18), 6928-6934.

19. Callegari, G.; Tyomkin, I.; Kornev, K. G.; Neimark, A. V.; Hsieh, Y.-L., Absorption and transport properties of ultra-fine cellulose webs. *Journal of Colloid and Interface Science* **2011,** *353* (1), 290-293.

20. Khan, M. S.; Thouas, G.; Shen, W.; Whyte, G.; Garnier, G., Paper diagnostic for instantaneous blood typing. *Analytical Chemistry* **2010,** *82* (10), 4158-4164.

21. Li, X.; Tian, J.; Nguyen, T.; Shen, W., Paper-based microfluidic devices by plasma treatment. *Analytical Chemistry* **2008,** *80* (23), 9131-9134.

22. Martinez, A. W.; Phillips, S. T.; Butte, M. J.; Whitesides, G. M., Patterned paper as a platform for inexpensive, low-volume, portable bioassays. *Angewandte Chemie International Edition* **2007,** *46* (8), 1318-1320.

23. Martinez, A. W.; Phillips, S. T.; Whitesides, G. M., Three-dimensional microfluidic devices fabricated in layered paper and tape. *Proceedings of the National Academy of Sciences* **2008,** *105* (50), 19606-19611.

24. Martinez, A. W.; Phillips, S. T.; Wiley, B. J.; Gupta, M.; Whitesides, G. M., FLASH: A rapid method for prototyping paper-based microfluidic devices. *Lab on a Chip* **2008,** *8* (12), 2146-2150.

25. Monaenkova, D.; Andrukh, T.; Kornev, K. G., Wicking of liquids into sagged fabrics. *Soft Matter* **2012,** *8* (17), 4725-4730.

26. Martinez, A. W.; Phillips, S. T.; Whitesides, G. M.; Carrilho, E., Diagnostics for the developing world: Microfluidic paper-based analytical devices. *Analytical Chemistry* **2009,** *82* (1), 3-10.

27. Bruzewicz, D. A.; Reches, M.; Whitesides, G. M., Low-cost printing of poly(dimethylsiloxane) barriers to define microchannels in paper. *Analytical Chemistry* **2008,** *80* (9), 3387-3392.

28. Minko, S.; Luzinov, I.; Motornov, M.; Sheparovych, R.; Lupitskyy, R.; Liu, Y.; Klep, V., Coatings via self-assembly of smart nanoparticles. In *Smart Coatings II*, American Chemical Society: 2009; Vol. 1002, pp 145-157.

29. Fang, X.; Chen, H.; Jiang, X.; Kong, J., Microfluidic devices constructed by a marker pen on a silica gel plate for multiplex assays. *Analytical Chemistry* **2011,** *83* (9), 3596-3599.

30. Safavieh R, M. M., Qasaimeh MA, Juncker D. Proceedings of MicroTAS 2009,the 13th international conference on miniaturized systems for chemistry and life sciences, Jeju, South Korea, 2009.

31. Ballerini, D. R.; Li, X.; Shen, W., Flow control concepts for thread-based microfluidic devices. *Biomicrofluidics* **2011,** *5*, 014105.

32. Nilghaz, A.; Wicaksono, D. H. B.; Gustiono, D.; Abdul Majid, F. A.; Supriyanto, E.; Abdul Kadir, M. R., Flexible microfluidic cloth-based analytical devices using a low-cost wax patterning technique. *Lab on a Chip* **2012,** *12* (1), 209-218.

33. Zdyrko, B.; Luzinov, I., Polymer brushes by the “grafting to” method. *Macromolecular Rapid Communications* **2011,** *32* (12), 859-869.

34. Liu, Y.; Klep, V.; Zdyrko, B.; Luzinov, I., Synthesis of high-density grafted polymer layers with thickness and grafting density gradients. *Langmuir* **2005,** *21* (25), 11806-11813.

35. Ramaratnam, K.; Tsyalkovsky, V.; Klep, V.; Luzinov, I., Ultrahydrophobic textile surface via decorating fibers with monolayer of reactive nanoparticles and non-fluorinated polymer. *Chemical Communications* **2007,** (43), 4510-4512.

36. Samadi, A.; Husson, S. M.; Liu, Y.; Luzinov, I.; Michael Kilbey, S., Low-temperature growth of thick polystyrene brushes via ATRP. *Macromolecular Rapid Communications* **2005,** *26* (23), 1829-1834.

37. Tsyalkovsky, V.; Klep, V.; Ramaratnam, K.; Lupitskyy, R.; Minko, S.; Luzinov, I., Fluorescent reactive core–shell composite nanoparticles with a high surface concentration of epoxy functionalities. *Chemistry of Materials* **2007,** *20* (1), 317-325.

38. Burtovyy, O.; Klep, V.; Chen, H. C.; Hu, R. K.; Lin, C. C.; Luzinov, I., Hydrophobic modification of polymer surfaces via "grafting to" approach. *Journal of Macromolecular Science, Part B* **2007,** *46* (1), 137-154.

39. Luzinov, I., *Nanofabrication of thin polymer films. In Nanofibers and nanotechnology in textiles; Brown, P. J.; Stevens, K, Eds.; Woodhead Publishing, Ltd.: Boca Raton, FL,* . 2007.

40. Pittman, J. J.; Klep, V.; Luzinov, I.; Marcus, R. K., Extraction of metals from aqueous systems employing capillary-channeled polymer (C-CP) fibers modified with poly(acrylic acid) (PAA). *Analytical Methods* **2010,** *2* (5), 461-469.

41. Ramaratnam, K. I., K. S.; Kinnan, M. K.; Chumanov, G.; Brown, P. J.; Luzinov, I., Ultrahydrophobic textiles: Lotus approach. *AATCC Review* **2008,** *8*, 42-48.

42. Reukov, V.; Vertegel, A.; Burtovyy, O.; Kornev, K.; Luzinov, I.; Miller, P., Fabrication of nanocoated fibers for self-diagnosis of bacterial vaginosis. *Materials Science and Engineering: C* **2009,** *29* (3), 669-673.

43. Köthe, M.; Müller, M.; Simon, F.; Komber, H.; Jacobasch, H. J.; Adler, H. J., Examination of poly(butadiene epoxide)-coatings on inorganic surfaces. *Colloids and Surfaces A: Physicochemical and Engineering Aspects* **1999,** *154* (1–2), 75-85.

44. Hsieh, Y.-L.; Miller, A.; Thompson, J., Wetting, pore structure, and liquid retention of hydrolyzed polyester fabrics. *Textile Research Journal* **1996,** *66* (1), 1-10.

45. Currie, E. P. K.; Sieval, A. B.; Fleer, G. J.; Stuart, M. A. C., Polyacrylic acid brushes: Surface pressure and salt-induced swelling. *Langmuir* **2000,** *16* (22), 8324-8333.

46. Roiter, Y.; Minko, S., Afm single molecule experiments at the solid−liquid interface: In situ conformation of adsorbed flexible polyelectrolyte chains. *Journal of the American Chemical Society* **2005,** *127* (45), 15688-15689.

47. Roiter, Y.; Trotsenko, O.; Tokarev, V.; Minko, S., Single molecule experiments visualizing adsorbed polyelectrolyte molecules in the full range of mono- and divalent counterion concentrations. *Journal of the American Chemical Society* **2010,** *132* (39), 13660-13662.

48. Lucas, R., Ueber das Zeitgesetz des kapillaren Aufstiegs von Flüssigkeiten. *Kolloid-Zeitschrift* **1918,** *23* (1), 15-22.

49. Washburn, E. W., The dynamics of capillary flow. *Physical Review* **1921,** *17* (3), 273-283.

50. Scheidegger, A. E., *The physics of flow through porous media*. 1974.

CHAPTER EIGHT

SUMMARY

The broad basis of this dissertation is the idea that polymer coatings on fabric can be designed to control the direction of a fluid. Thus, the goal of this thesis was to perform fundamental experimental studies to evaluate the behavior of polymer layers, to develop a methodology for fabric surface modification, and show the feasibility of using polymer grafted fabric for controlled fluid transport for one way directional control as well as selective directional control. The conclusions from the investigations in the current research are categorized according to the perspective chapters.

8.1. Modification of thin PET film with polymer layer via the "grafting to" approach

Before grafting on the fabric surface, a model PET surface was fabricated. The grafting of polymers was studied on the model surface to optimize the grafting condition. The thin PET film was deposited on a silicon wafer successfully, and crystals were formed in the PET layer after annealing. It has been shown that a reactive layer can be formed on the PET surface by plasma and hydroxide treatments. A PGMA anchoring layer was formed on the surface by a reaction between the epoxy functionality with the active groups of the surface: carboxyl and hydroxyl. Different polymers were grafted to the PET surfaces through the epoxy containing anchoring layer, and the water contact angle and thickness studies proved that the polymer grafting was successful. The "grafting to" technique was used for all polymer graftings.

8.2. Modification of textile substrate: Influence of polymer grafting on the wettability of PET fabric

The wetting behavior of the model PET film changed after polymer grafting. This indicated that the surface interaction with the fluid was changed. Thus, a polymer coating can alter the fluid movement when such coating is applied to the textile surface.

The methodology used for the polymer grafting on the PET film was successfully applied to graft various polymers to the PET fabric surface, and the wettability of the surface after polymer grafting was altered, as detected by the water contact angle measurements.

Fluid movement in textile materials is related to wicking; therefore, this chapter focused on how a surface coating altered the wicking in polymer-coated fabrics. The porosity and permeability did not change significantly after surface modification, while the water wicking rate was changed, which indicates that the polymer coating was the main factor of change in the wicking rate.

8.3. PET surface with a wettability gradient

In the **Chapter 5**, it was shown that the wicking property of the fabric could be altered by polymer grafting. Next, we formed a wettability gradient on the fabric surface in order to obtain wicking in a controlled direction on the fabric, calling it “one way directional control.” This was achieved by first grafting a hydrophobic polymer on the PGMA anchoring layer in a gradient manner; then, reacting free epoxy groups with the hydrophilic polymer. Thus, the grafting thickness of the hydrophobic polymer was

increased in one direction while hydrophilic polymer's grafting thickness was increased in the opposite direction. Such dual polymer grafting generated a surface with a gradient in the wetting property (on model film and fabric).

Model studies were done on the PET film. Single component polymer graftings were done to obtain the grafting kinetics of the polymers. A mixed polymer brush layer was used to evaluate the relationship between the polymer thickness ratios and surface wetting behavior. The polymer coatings using the dynamic annealing mode were accomplished by an oven-dip coater assembly. Both studies, dynamic grafting and the mixed polymer brush, indicated that the wetting behavior of the surface was directly related to the grafted polymer ratios. The wettability gradient on the fabric was also successfully obtained by the oven-dip coater assembly, and the coated fabrics were tested on the surface differential scanning calorimeter (SDSC) to measure the effects of the polymer coatings on the cooling efficiency of the PET fabric. Enhanced cooling effect was measured with the fabric that has a gradual change in the wetting properties.

8.4. Toward fabric-based flexible microfluidic devices: Pointed surface modification for pH sensitive aqueous liquid transport

This section focused on the fabrication of active channels on fabric surfaces for the selective and directional control of fluid movement. Fabrics from PET, PP, and PP/PET yarns were manufactured. The blended fabric containing both PET/PP yarns was designed to have channels of PET yarns in a matrix of PP yarns. The fabrics were first exposed to an alkali environment, and then a PGMA layer was deposited to create

generic reactive channels from the PET fibers. As shown in the previous chapters, the wicking rate of the fluid in the fabric can be altered by polymer grafting; therefore, the PET channels in the hydrophobic PP matrix were locally modified with different pH sensitive polymers to obtain different wicking kinetics of a liquid in the PET channels, leading to selective directional fluid movement and control. Changes in the wettability of the model PET film with liquids of different pHs were reported.

In conclusion, an effective method for pointed surface modification of a textile material to produce yarn based active channels, and pH triggered selective transport of liquids in the textile material was reported.

8.5. Publications and presentations

Vatansever, F, et al. "Toward fabric-based flexible microfluidic devices: Pointed surface modification for pH sensitive liquid transport." *ACS Appl. Mater. Interfaces*, 2012, 4 (9), 4541–4548

Sharma, S.; Vatansever, F.; Hodges, J. N.; Luzinov, I., Blends and composites from proteins produced by Animal Co–Products Industry. In cellulose based composites : new green nanomaterials, Hinestroza, J.; Netravali, A. N., Eds. Wiley-VCH Weinheim; Chichester, 2012

F. Vatansever, et. al., ``Surface modification of fibrous structure to design wettability gradient`` American Chemical Society National Meeting, Pennsylvania, 2012, poster presentation.

F. Vatansever, et. al., “Selectively functionalized fabric for control of fluid movement.” American Chemical Society National Meeting, Colorado, 2011, oral presentation.

F. Vatansever, et. al., “Fabrication and characterization of polymer films containing albumin protein.” American Chemical Society National Meeting, Anaheim, CA, 2011, oral presentation.

F. Vatansever, et. al., “Biodegradable plastics from meat and bone meal.” American Chemical Society National Meeting, Anaheim, CA, 2011, poster presentation.

F. Vatansever, et. al., `` Pointed surface modification of fibrous structure for development of fiber based microfluidic devices`` The Fiber Society Spring 2010 Conference, Bursa, Turkey, May 2010,oral presentation.

F. Vatansever, et. al., “ Development of fiber based micro fluidic devices.” American Chemical Society National Meeting, Boston, 2010, poster presentation.

F. Vatansever, et. al., “Coating from human albumin plastic on titanium orthopedic implants.” American Chemical Society National Meeting, Boston, 2010, poster presentation.

F. Vatansever, et. al., `` Towards pointed surface modification of fibrous structures.`` The Fiber Society 2009 Fall Meeting and Technical Conference , Athens, Georgia, USA, October 2009,poster presentation.

F. Vatansever, et. al., ``Biodegradable polymer blends and composites from proteins produced by animal co-product industry`` Clemson, SC,2008